

8-14-2015

Investigations of the Stability of Pyrolysis Oil during High Temperature Treatment

Laibao Zhang

Follow this and additional works at: <https://scholarsjunction.msstate.edu/td>

Recommended Citation

Zhang, Laibao, "Investigations of the Stability of Pyrolysis Oil during High Temperature Treatment" (2015). *Theses and Dissertations*. 2871.
<https://scholarsjunction.msstate.edu/td/2871>

This Graduate Thesis - Open Access is brought to you for free and open access by the Theses and Dissertations at Scholars Junction. It has been accepted for inclusion in Theses and Dissertations by an authorized administrator of Scholars Junction. For more information, please contact scholcomm@msstate.libanswers.com.

Investigations of the stability of pyrolysis oil during high temperature treatment

By

Laibao Zhang

A Thesis
Submitted to the Faculty of
Mississippi State University
in Partial Fulfillment of the Requirements
for the Degree of Master of Science
in Chemical Engineering
in the Swalm School of Chemical Engineering

Mississippi State, Mississippi

August 2015

Copyright by

Laibao Zhang

08/2015

Investigations of the stability of pyrolysis oil during high temperature treatment

By

Laibao Zhang

Approved:

Keisha B. Walters
(Major Professor)

Priscilla J. Hill
(Committee Member)

Santanu Kundu
(Committee Member)

W. Todd French
(Graduate Coordinator)

Jason M. Keith
Dean
Bagley College of Engineering

Name: Laibao Zhang

Date of Degree: August 14, 2015

Institution: Mississippi State University

Major Field: Chemical Engineering

Major Professor: Dr. Keisha B. Walters

Title of Study: Investigations on the stability of pyrolysis oil during high temperature treatment

Pages in Study: 139

Candidate for Degree of Master Science

Pyrolysis oil is produced from biomass when a feedstock is rapidly heated in a non-oxidizing environment during a short residence time. While pyrolysis oil is inexpensive, major issues prevent the facile use of this oil product ‘as produced’. Principally, since the rapid condensation results in a product not in thermodynamic equilibrium, the oil components continue to react until equilibrium is reached. Understanding how and why these reactions—including polymerization—occur in pyrolysis oil is important in designing treatments to stabilize or transform pyrolysis oil before further upgrading. Physical and chemical changes in pyrolysis oils are investigated as a function of temperature and time to simulate the aging process during storage. The effects of alcohol addition on pyrolysis oil stability during high temperature treatment are investigated. The pretreatment of pyrolysis oil with low-cost alcohols is promising prior to hydrotreating or catalytic cracking.

DEDICATION

I would like to dedicate this thesis to my wife, Peng Zhou, who has always supported me to achieve my utmost potential, to my daughter, Doreen, who has brought so much pleasure to my family, and to my parents and parents-in-law, for all of their love and support throughout this writing process.

ACKNOWLEDGEMENTS

I would like to thank my wonderful advisor and mentor Dr. Keisha B. Walters. I would like to thank everyone who assisted my research efforts within the past two and half years. I would also like to thank Dr. Mark Bricka for the usage of rheometer and Yan Luo for assistance with GC-MS. I'd also like to thank the members of my committee, Dr. Santanu Kundu and Dr. Priscilla Hill for their time and input regarding my research project and thesis. This project was funded by KiOR, Inc. I would thank undergraduate researchers Andres Chaparro Sosa and Evan Prehn for collecting some of the data.

TABLE OF CONTENTS

DEDICATION	ii
ACKNOWLEDGEMENTS	iii
LIST OF TABLES	vii
LIST OF FIGURES	viii
CHAPTER	
I. INTRODUCTION	1
1.1 Drive for sustainable energy	1
1.2 Pyrolysis oil from biomass	3
1.3 Fast pyrolysis considerations	6
1.3.1 Feedstocks	7
1.3.2 Reactors	8
1.3.3 Vapor cleaning and quenching	10
1.3.4 Pyrolysis characteristics	11
1.3.5 Pyrolysis oil stability	12
1.3.5.1 Pyrolysis oil composition	12
1.3.5.2 Organic Compounds	13
1.3.5.3 Inorganic Compounds	14
1.3.5.4 Accelerated aging	15
1.3.5.5 Additives to stabilize pyrolysis oil	19
1.3.6 Pyrolysis oil upgrading	20
1.3.6.1 Filtration	20
1.3.6.2 Hydrotreating	21
1.4 Objective	24
1.5 References	25
II. CHARACTERIZATION OF KIOR'S RENEWABLE RECRUDE OIL	32
2.1 Introduction	32
2.2 Experiment	34
2.2.1 Solvent extraction	34
2.2.2 Water content	34
2.2.3 Thermogravimetric analysis	35
2.2.4 Differential Scanning Calorimetry	35

2.2.5	GC-MS.....	35
2.2.6	ATR-FTIR.....	36
2.3	Results and Discussion	36
2.3.1	Water content.....	36
2.3.2	Solids content.....	37
2.3.3	HMM lignin content	38
2.3.4	Ash content	39
2.3.5	TGA	40
2.3.6	DSC.....	46
2.3.7	ATR-FTIR.....	47
2.3.8	GC-MS.....	48
2.3.9	Comparison of LMM lignin and HMM lignin.....	52
2.4	Conclusion	56
2.5	References.....	57
III.	IMPACTS OF THERMAL PROCESSING ON THE PHYSICAL AND CHEMICAL PROPERTIES OF PYROLYSIS OIL	60
3.1	Introduction.....	60
3.2	Experimental.....	62
3.2.1	Heat treatment of the oil	63
3.2.2	Viscosity	63
3.3	Results and discussion	63
3.3.1	Water content for aged oils.....	63
3.3.2	HMM lignin content	64
3.3.3	Viscosity	66
3.3.4	TGA	67
3.3.5	DSC.....	71
3.3.6	FTIR.....	74
3.3.7	GPC.....	77
3.3.8	GC-MS.....	80
3.4	Conclusion	82
3.5	References.....	84
IV.	ALCOHOL STABILIZATION OF PYROLYSIS OIL DURING HIGH TEMPERATURE TREATMENT	89
4.1	Introduction.....	89
4.2	Materials and Methods.....	92
4.2.1	Pyrolysis oil/alcohol mixture preparation.....	92
4.2.2	Pyrolysis oil/alcohol aging.....	92
4.2.3	Characterization	92
4.3	Results and discussion	93
4.3.1	Effect of alcohol on chemical composition of pyrolysis oil	93
4.3.2	Effect of alcohol on viscosity of pyrolysis oil	98
4.3.3	Effect of alcohol on thermal properties of pyrolysis oil	100

4.3.3.1	TGA	100
4.3.3.2	DSC	109
4.3.4	Effect of alcohol on properties of pyrolysis oil after high temperature treatment	111
4.3.4.1	Water content	111
4.3.4.2	HMM lignin content	112
4.3.4.3	Rheology	113
4.3.4.4	GPC	115
4.3.4.5	ATR-FTIR Spectroscopy	120
4.3.4.6	GC-MS	123
4.4	Conclusions	128
4.5	References	130
V.	CONCLUSIONS AND FUTURE WORK	133
5.1	Conclusion	133
5.2	Future work	134
APPENDIX		
A.	CHROMATOGRAM FOR PYROLYSIS OIL/ALCOHOL MIXTURES	136

LIST OF TABLES

1.1	Catalysts used in hydropressing pyrolysis oil (Elliott 2007)	22
2.1	Solids content of renewable crude oil in different solvent	38
2.2	Composition of the ReCrude oil tested in ethyl acetate.....	49
2.3	Composition of the ReCrude oil tested in CH ₂ Cl ₂	51
3.1	Calculated M_n , M_w and PDI for fresh and aged pyrolysis oils.....	79
4.1	Percent band height change due to the introduction of alcohols.	97
4.2	Herschel-Bulkley rheology model fit results for pyrolysis oil and pyrolysis oil/alcohol mixtures.....	100
4.3	Kinetics parameters for pyrolysis oil and pyrolysis oil/alcohol mixtures.....	105
4.4	Herschel-Bulkley rheology model fit results for pyrolysis oil and pyrolysis oil/alcohol mixtures.....	115
4.5	Molecular weight and molecular weight distributions for pyrolysis oil and pyrolysis oil/alcohol mixtures.....	119
4.6	Esters detected in aged pyrolysis oil/alcohol mixtures.	124

LIST OF FIGURES

1.1	Total energy use by fuel type from 1980 to 2040 (EIA 2014).....	3
1.2	Strategies for the production of fuels from biomass (Huber, Iborra et al. 2006).	5
1.3	Fast pyrolysis process principles (Bridgwater and Peacocke 2000).	10
1.4	Reactivity scale of oxygenated groups found in pyrolysis oil under hydrotreatment conditions (Elliott 2007).....	23
2.1	Reactors used in fluid catalytic cracking process (Bartek, Cordle et al. 2012)	33
2.2	The solubility of crude oils in different solvents at ambient temperature	37
2.3	Plot of HMM lignin content vs $V_{CH_2Cl_2}/V_{oil}$	39
2.4	TGA and DTG plots for the ReCrude oil at different ramp rate in N_2 atmosphere	41
2.5	TGA and DTG plots for the ReCrude oil in air atmosphere.....	42
2.6	TG curves in nitrogen and air atmosphere.....	43
2.7	Activation energy versus fractional conversion for the pyrolysis of the ReCrude oil in nitrogen atmosphere	45
2.8	MDSC plots for the ReCrude oil	47
2.9	FTIR spectrum for the ReCrude oil	48
2.10	GC-MS chromatogram for the ReCrude oil tested in ethyl acetate	49
2.11	GC-MS chromatogram for the ReCrude oil in CH_2Cl_2	50
2.12	FTIR spectra for the LMM fraction and the HMM lignin	52
2.13	GPC plots for the ReCrude oil, LMM fraction and HMM lignin.....	53

2.14	DSC plots for the LMM fraction and the HMM lignin	53
2.15	TGA and DTG plots for the LMM lignin and the HMM lignin in air atmosphere	55
2.16	TGA and DTG plots for the HMM lignin in nitrogen atmosphere.....	55
3.1	Water content vs aging time plots for pyrolysis oils aged at different temperatures.....	64
3.2	A typical structure of pyrolytic lignin (Bayerbach and Meier 2009).....	65
3.3	HMM lignin content vs aging time plots for pyrolysis oils aged at different temperatures.....	66
3.4	Viscosity plots for pyrolysis oils aged at different temperatures.....	67
3.5	TG and DTG plots for pyrolysis oils aged at different temperatures.....	69
3.6	DSC plots for pyrolysis oils aged at different temperatures.....	72
3.7	Isothermal DSC plots for pyrolysis oils aged at different temperatures.....	73
3.8	Evolution of FTIR band height ratio for pyrolysis oils aged at different temperatures.....	76
3.9	GPC curves for pyrolysis oils aged at different temperatures.....	78
3.10	Peak area ratios for the CH ₂ Cl ₂ soluble fraction of fresh and aged oils.....	81
3.11	Proposed reaction mechanism during aging.....	82
4.1	Normalized peak area ratio for the ReCrude oil and pyrolysis oil/alcohol mixtures.....	95
4.2	FTIR spectra for the ReCrude oil and pyrolysis oil/alcohol mixtures.....	96
4.3	Reaction mechanism for pyrolysis oil/alcohol mixtures.....	98
4.4	Logarithmic plots of apparent viscosity vs. shear rate for pyrolysis oil and pyrolysis oil/alcohol mixtures.....	99
4.5	Residual weight and derived weight temperature vs. temperature plots for pyrolysis oil and pyrolysis oil/alcohol mixtures in N ₂ atmosphere.....	101
4.6	Heat flow and derivative heat flow vs. temperature plots for pyrolysis oil and pyrolysis oil/alcohol mixtures in N ₂ atmosphere.....	102

4.7	Decomposition kinetics plots for pyrolysis oil/alcohol mixtures (n=1.5 except for oil/2-propanol, n=2).....	104
4.8	Residual weight and derived weight temperature plots for pyrolysis oil and pyrolysis oil/alcohol mixtures during combustion in air.....	107
4.9	Heat flow and derivative heat flow vs. temperature plots for pyrolysis oil and pyrolysis oil/alcohol mixtures in air atmosphere.....	107
4.10	TG curves in nitrogen and air atmosphere for ignition temperature determination.	109
4.11	DSC plots for pyrolysis oil/alcohol mixtures.....	110
4.12	Isothermal DSC plots for pyrolysis oil and pyrolysis oil/alcohol.....	111
4.13	Water content vs aging time plots for pyrolysis oil and pyrolysis oil/alcohol mixtures aged at 200 °C.....	112
4.14	HMM lignin content vs aging time plots for pyrolysis oil and pyrolysis oil/alcohol mixtures aged at 200 °C.....	113
4.15	Logarithmic plots of apparent viscosity vs. shear rate for pyrolysis oil and pyrolysis oil/alcohol mixtures.....	114
4.16	GPC plots for pyrolysis oils/alcohol mixtures aged for 6 hours.....	116
4.17	GPC curves for the ReCrude oil and pyrolysis oil/alcohol mixtures.....	117
4.18	FTIR spectra and peak intensities change with aging time for the ReCrude oil aged at 200 °C.	120
4.19	FTIR spectra for control and aged pyrolysis oil/alcohol mixtures.	122
4.20	Peak area ratio for major compounds evident in control and aged pyrolysis oil/alcohol mixtures.....	126
A.1	Chromatogram for pyrolysis oil/methanol.....	137
A.2	Chromatogram for pyrolysis oil/ethanol.....	137
A.3	Chromatogram for pyrolysis oil/1-propanol.....	138
A.4	Chromatogram for pyrolysis oil/2-propanol.....	138
A.5	Chromatogram for pyrolysis oil/1-octanol.....	139

CHAPTER I

INTRODUCTION

1.1 Drive for sustainable energy

The United Nations Human Development Index (HDI) is a comprehensive measure of wealth, health, education. HDI rapidly increases with per capita power consumption and then levels off above about 4kW per capita (Martínez and Ebenhack 2008, Dale and Ong 2014). World wealth and other societal improvements have traditionally strongly correlated with energy consumption. In modern times, countries that consume energy at high rates also have high rates of wealth production (Martínez and Ebenhack 2008).

Fossil fuels have, and continue to be, the dominant source of world energy. After the Industrial Revolution, global wealth growth has largely depended on utilizing fossil fuels to power internal combustion engines. Global energy is obtained from six primary sources: 44% petroleum, 26% natural gas, 25% coal, 2.5% hydroelectric power, 2.4% nuclear power, and 0.2% nonhydro renewable energy (RFF). Therefore, approximately 95% of energy world-wide comes from fossil fuels (EIA 2003). The American Petroleum Institute estimated in 1999 that world's oil supply would be depleted between 2062 and 2094 (Wessner 1999). Even with an increase in drilling capabilities, world oil demand and utilization have increased more than its discoveries. A more recent estimation lowered the depletion year to 2057 (Appenzeller 2004).

The rapid consumption of fossil fuels and their non-renewability have been the major incentives for the development of alternative energy sources. Environmental concerns related to fossil, hydroelectric, and nuclear energy consumption also increase the attraction for alternative sources. For example, emission of CO₂ resulted from fossil fuels combustion, has increase by ~10.80% from 2005 to 2009 (EIA 2011). Continued high rates of greenhouse emissions in the transportation and industrial sectors will eventually negatively impede the economy. Government regulations on environmental standards, fuel and emission taxes, and subsidies for renewable energy production increasingly mandate diversified energy portfolios. In U.S. and Europe, policies have been successfully implemented to reduce air pollution and acid rain (Chow, Kopp et al. 2003). Figure 1.1 shows the history and projections of energy usage in the US from 1980 to 2040. As determined by the U.S. Energy Information Administration (EIA), the fossil fuel share of total energy will decrease 5% by 2040, while renewable energy will grow from 9% to 12% (EIA 2014).

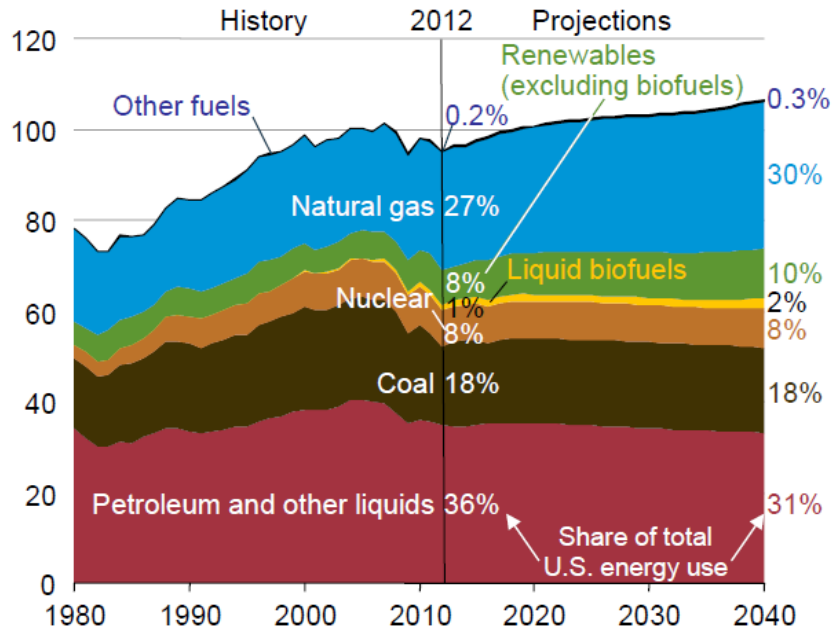


Figure 1.1 Total energy use by fuel type from 1980 to 2040 (EIA 2014).

Biomass accounts for over 50% of the total renewable energy. Biomass has no net impact on the CO₂ content of the atmosphere based on the assumption that CO₂ consumed during plant growth is equal to or greater than that produced during combustion or that by replanting the CO₂ produces can be offset (Schobert 2014). In the past few decades, there have been a large number of publications on biomass-based oil. EIA predicted that biomass to liquid production (excluding ethanol and biodiesel) will increase by 32,200 barrel oil per day (bbl/d) from 2012 to 2040 (EIA 2014).

1.2 Pyrolysis oil from biomass

Biomass is defined as any biological material that was taken or derived from living organisms and can be divided into five categories (Edenhofer, Pichs-Madruga et al. 2011): (1) woody feedstock such as bark, heartwood, leaves, etc.; (2) energy crops; (3)

agriculture residues; (4) food waste; (5) industrial waste and co-product material from manufacturing and industrial processes.

Biomass can be used as an energy source by many different processes.

Combustion is well-established commercial technology and now its development is focused on resolving environmental problems (Nussbaumer 2003). Fig. 1.2 summarizes the three strategies available for converting biomass to a more useful energy form – gasification, pyrolysis, and hydrolysis (Huber, Iborra et al. 2006). Gasification has been practiced for decades. In the gasification process, biomass feedstock is converted into syngas by the partial oxidation at high temperature. The main product components are CO, H₂, CO₂, CH₄ and H₂O (Goyal, Seal et al. 2008). And the concentration of NO_x is heavily dependent on process conditions (Hindsgaul, Schramm et al. 2000). While demonstrations and pre-commercial activities are reported, few are proved to be successful. Liquid oils from wet biomass can be produced with higher yields through hydrothermal liquefaction. However, the cost in scale up makes the technology less promising. Fast pyrolysis is the thermal decomposition of biomass occurring in non-oxidizing atmosphere. The process temperature and residence time for gas and biomass particles are key factors in determining the content of gas, charcoal and liquid oil.

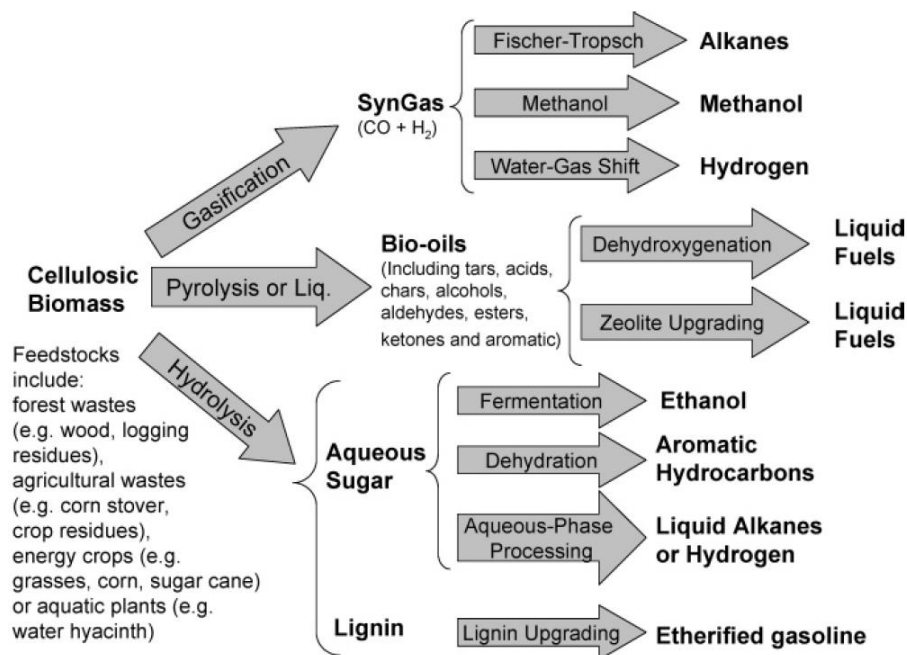


Figure 1.2 Strategies for the production of fuels from biomass (Huber, Iborra et al. 2006).

Pyrolysis oil is promising for its economy, sustainability and causing no greenhouse gas emission. Crude pyrolysis oil is a complex mixture of a large number of compounds that can be broadly classified into volatile organic compounds (hydroxyacetaldehyde, formic acid, acetic acid), furanic compounds, monophenols, sugars (fermentable and cross-linked), lignin oligomers and water (Ed and Thomas 1988, Piskorz, Scott et al. 1988, García-Pérez, Chaala et al. 2005). The raw pyrolysis oil is characterized by a number of deleterious properties such as high water content, high ash/solids content and immiscible with hydrocarbon liquids. The major issue with pyrolysis oil, since it is not a product of thermodynamical and chemical equilibrium as a result of rapid quench, the components will react until equilibrium is reached (Lu, Yang

et al. 2008). All these negatives make a substantially physical and chemical improvement necessary before it can be used as a transportation fuel.

1.3 Fast pyrolysis considerations

Pyrolysis of biomass under conditions of rapid heating and short gas residence times can produce a pyrolysis oil with yields higher than 70 wt%. The early study in fast pyrolysis became popular in the 1970's. Garrett and Mallan (Garrett and Mallan 1979) disclosed a process for the recovery of chemicals and fuel values from waste solids such as trash, rubber, and natural raw materials etc., which were intermixed with char and carrier gas and passed through a pyrolysis zone under turbulent conditions at a temperature ranging from 300-2000 °F, with residence time of under 10 s. Char was used as the heat source and was superior than using hot carrier gas alone for its higher heat capacity. Char can be reused after degasification and desulfurization. Significant research in pyrolysis has been done in the past decades. A number of reviews have been presented on the development of pyrolysis oil (Bridgwater and Peacocke 2000, Huber, Iborra et al. 2006, Mohan, Pittman et al. 2006, Bridgwater 2012).

Many pyrolysis technologies have been commercialized for relatively low capital costs. Recently, fast pyrolysis technologies have been scaled-up to pilot scale: Ensyn Technologies (fluidized bed, 50 t/day); Dynamotive (fluidized bed, 10 t/day); BTG (rotary cone reactor, 5 t/day); Fortum (12 t/day pilot plant); Bioenergy Partners (15 t/day pilot plant); and KiOR (fluidized bed, 13 million gallon/year). Unfortunately, none of these facilities have delivered an economically competitive strategy for the production of an alternative biomass-based fuel.

On both lab and pilot plant scale, the feedstock is rapidly heated in a non-oxidizing atmosphere. Vapors are condensed in several steps resulting in dark brown pyrolysis liquid. More careful control of the design and operation of the pyrolysis reactor and condensers is needed in order to give high pyrolysis liquid yields. Key fast pyrolysis design parameters (Bridgwater and Peacocke 2000) include:

- (1) very high heating and heat transfer rates;
- (2) carefully controlled temperatures around 450-550 °C; and
- (3) short vapor residence times.

1.3.1 Feedstocks

Theoretically any form of biomass can be utilized for fast pyrolysis. Over 100 different biomass types have been tested, ranging from agricultural wastes to energy crops and solid wastes such as sewage sludge (Rosendahl 2013). Biomass feedstocks need to be dried and then ground into small pieces in order to increase the heat transfer rates. Grinding specifications for circulating beds, fluid beds and rotating cone reactors are less than 6 mm, 2 mm and 200 µm respectively (Bridgwater and Peacocke 2000). Size reduction becomes increasingly expensive as size reduces.

Minimizing the wood chip size and improving the contact surface of raw material with the reactor wall can enhance mass and heat transfer through the system. Putun et al. (Uzun, Pütün et al. 2007) used a stainless steel basket to improve the heat and mass transfer in order to get a higher volatile yields. The maximum liquid yield was achieved as 46.72% with particle sizes of 0.45-0.85 mm, heating rate of 500 °C/min, pyrolysis temperature of 500 °C, and sweeping gas flowrate of 400 cm³min⁻¹.

1.3.2 Reactors

A fast pyrolysis reactor must have very high heating and heat transfer rates, moderate and carefully controlled temperature. Moreover, the pyrolysis vapors need to be rapidly cooled or quenched (Diebold and Bridgwater 1997). Four main reactor technologies are currently available for commercialization: fluidized beds, circulating fluid beds, ablative pyrolyzer (cyclonic and plate type), and vacuum pyrolyzer. While a wide variety of reactors have been tested, fluidized beds and circulating fluidized beds are the most promising configurations for the ease of operation and better quality of products.

Vacuum pyrolyzers have an advantage in adjusting the residence time for volatiles because the biomass particle residence time is not coupled to that of the volatiles (Roy, Chaala et al. 1999, Garcia-Pérez, Chaala et al. 2007). The challenge is from the poor heat and mass transfer rates which makes equipment scale-up less technically feasible (Bridgwater and Peacocke 2000).

Ablative pyrolysis reactors have been investigated since the 1980s. An advantage of ablative reactor is that large whole tree chips can be used since reaction rates are not limited by heat transfer (Di Blasi 1996, Helleur, Popovic et al. 2001). The process is only limited by the rate of heat supply to the reactor. Unfortunately, large amounts of tar are produced in ablative reactors. The long residence time for the biomass particles is not easily achieved which makes a recycle of the partially reacted solid particles necessary. The cone types or plate types ablative pyrolysis reactor are mechanically complex as they require moving parts. Moreover, ablative pyrolysis suffers a high heat loss for the hot

surface is at a temperature substantially above the reaction temperature (Peacocke and Bridgwater 1994).

Circulating fluid beds are energetically self-sustainable and can be used for very high throughputs due to high gas velocities. Heat is supplied by recirculation of heated sand or catalysts. To improve the conversion of biomass, solid recycling of partially reacted feed and fine sands or catalysts are necessary (Aho, Kumar et al. 2007, Boateng, Daugaard et al. 2007, Zhang, Xiao et al. 2011). The char residence time is slightly higher than gas residence time and in situ filtration of vapor (Hoekstra, Hogendoorn et al. 2009) or post-treatment (Lee, Kang et al. 2005, Kang, Lee et al. 2006) of the pyrolysis oil is needed to reduce the char content caused by carryover. The disadvantage for circulating fluid beds is the low thermal efficiency for heat transfer depend primarily on gas-solid convective transfer.

Bubbling fluidized beds have great technical advantages in short residence times for vapors and larger gas-solid interface area. The scale-up of bubbling fluidized beds has been proved to be successful in the past decades (Rüdisüli, Schildhauer et al. 2012). A conceptual fluidized bed fast pyrolysis system is shown below.

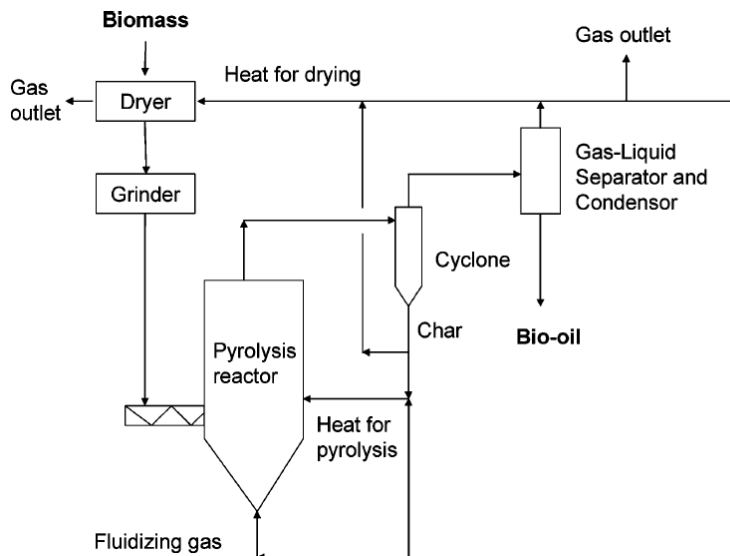


Figure 1.3 Fast pyrolysis process principles (Bridgwater and Peacocke 2000).

Bubbling fluidized beds has a good temperature control. Shallow bed depths and high gas flow rates favor the production higher quality pyrolysis oils. However, the bubbling fluidized bed suffer several disadvantages (Bridgwater and Peacocke 2000): (1) a low bed height-to-diameter ratio may cause transverse temperature and concentration gradients; (2) a high gas-to-biomass fed ratio leads to a low thermal efficiency; (3) grinding particles to less than 2-3 mm significantly increases the cost for feedstock processing.

1.3.3 Vapor cleaning and quenching

Char is inevitably carried over from cyclones after the pyrolysis. Rapid and complete char separation is difficult but desirable. Almost all of the ash in the biomass is retained in the char. The alkaline components of biomass ash are known to be cracking catalysts for the organic molecules in the vapor, with a consequent low yield of

condensed liquid. Even in the cooled liquid products char still contributes to the instability problems by accelerating the “aging” reactions. Char can be removed by a hot vapor filter or by liquid filtration using for example cartridge or rotary filters.

The collection of liquids has long been challenging due to the nature of the liquid which is mostly in the form of aerosols rather than a true vapor. A careful design and temperature control is necessary to avoid the blockage from differential condensation of heavy ends. The collected light ends could be used to reduce the liquid viscosity. Some research groups have used electrostatic precipitation to rapidly recover the aerosols (Daugaard, Jones et al. 2011). In fluidized bed type systems the vapor/aerosol concentration can be very low, further increasing the difficulty of product separation due to the low vapor pressure.

1.3.4 Pyrolysis characteristics

Pyrolysis characteristics of biomass can to some extent be predicted through the main components of the feedstock. Many groups have studied the pyrolysis of biomass on the basis of cellulose, hemicellulose, and lignin. Raveendran et al. (Raveendran, Ganesh et al. 1996) investigated the pyrolysis characteristics of biomass components in thermogravimetric analyzer (TGA) and a packed-bed pyrolyzer. Each kind of biomass had a characteristic pyrolysis behavior and no obvious interactions among the components during pyrolysis were observed. Yang et al. (Yang, Yan et al. 2006) used TGA to investigate the different roles of the three components in pyrolysis. A linear relationship was observed between the weight loss and proportion of hemicellulose/cellulose and residues at the specified temperature ranges. The pyrolysis results indicated negligible interaction existed among the components. Worasuwanarak et

al. (Worasuwannarak, Sonobe et al. 2007) studied the pyrolysis behavior of rice straw, rice husk and corncob by TG-MS technique. They found the difference in the composition of hemicellulose, cellulose and lignin caused the difference in the gas formation rates. Significant interactions between cellulose and lignin during pyrolysis were observed. They concluded the interactions between cellulose and lignin during pyrolysis contributed to a decrease in tar yields by an increase in char yields. Wang et al. (Wang, Li et al. 2008) performed pyrolysis of sawdust and its three components (cellulose, hemicellulose and lignin) in a TGA under syngas and hydrogen. They found hemicellulose was the easiest one to be pyrolyzed and then was cellulose, while lignin was the most difficult one. Both lignin and hemicellulose could affect the pyrolysis characteristic of cellulose while they could not affect each other substantially in the pyrolysis. Wang et al. (Wang, Guo et al. 2011) investigated the pyrolysis characteristics of biomass comprising of different amount hemicellulose, cellulose and lignin using both a TGA coupled with a FTIR and an experimental pyrolyzer. By investigating their pyrolysis products to predict the pyrolysis behavior of a certain lignocellulosic biomass feedstock is possible. The solid residue could be accurately predicted while inaccuracy occurred in predicting product yields.

1.3.5 Pyrolysis oil stability

1.3.5.1 Pyrolysis oil composition

Pyrolysis oils are usually a dark brown liquid that has a distinctive odor. During pyrolysis oil production, a large number of reactions—including hydrolysis, dehydration, isomerization, dehydrogenation, aromatization, retro-condensation, and coking occur due

to complexity in ingredients and high temperature. The exact composition of the pyrolysis oil is dependent on (Diebold 2000)

- (1) feedstock (including particle size, dirt, moisture, and protein content)
- (2) heat transfer rate
- (3) extent of vapor dilution, residence time and temperature of vapors in the reactor
- (4) efficiency of the condensation equipment
- (5) final char temperature during pyrolysis
- (6) efficiency of the char removal system
- (7) storage time and temperature
- (8) extent of contamination during pyrolysis and storage

1.3.5.2 Organic Compounds

Crude pyrolysis oil is a complex mixture that contain more than 400 different compounds, that can be broadly classified into volatile organic compounds (hydroxyacetaldehyde, formic acid, acetic acid), furanic compounds, monophenols, sugars (fermentable and cross-linked), lignin oligomers and water (Ed and Thomas 1988, Piskorz, Scott et al. 1988, Garcia-Pérez, Chaala et al. 2005).

The organic composition of pyrolysis oil is correlated with the biomass feedstocks. Milne (Milne 1997) and Diebold (Diebold 1997) made a comparison about the composition of fast pyrolysis oils derived from different feedstocks. The components were similar while their contents varied significantly. The liquid mixtures are derived primarily from decomposition/fragmentation reactions of the three major components of lignocellulose (Branca, Giudicianni et al. 2003): cellulose, hemicellulose, and lignin. The guaiacyl derivatives, coniferaldehyde and coniferyl alcohol are major products from

softwood lignins while guaiacyl and syringyl derivatives are derived from hardwood lignins. Grass lignins yield *p*-vinylphenol as a major compound (Saiz-Jimenez and De Leeuw 1986). Phenolic compounds in pyrolysis oils are mainly derived from pyrolysis of lignin. Bark has a tendency to contain highly reactive tannins. The miscellaneous oxygenates, sugars, and furans are from the decomposition of cellulose and hemicellulose. Levoglucosan is mainly produced from cellulose (Shafizadeh, Furneaux et al. 1979, Kawamoto, Murayama et al. 2003). The cellulose polymerization degree and crystallinity are relevant to the pyrolysis oil composition. The biomass having high protein contents, for example bark or grass would be expected to produce pyrolysis oils with higher nitrogen contents.

1.3.5.3 Inorganic Compounds

Inorganic compounds while their contents are very low play a key role in terms of the pyrolysis oil product selectivity. The inorganic or mineral content of biomass is found in aqueous phase, in organic phase and deposited solids. Initial feedstock composition has the most pronounced effect on alkali metal species and its content (Dayton 1997). The presence of alkali salts has a greater influence on the reaction mechanism. During pyrolysis, the inorganics, especially K and Ca, catalyze biomass decomposition (Agblevor and Besler 1996). The addition of minor amounts of alkalis to cellulose shifts the final product from levoglucosan to glycolaldehyde (Piskorz, Radlein et al. 1986, Evans and Milne 1987, Agblevor 1994). The counter ions in solution include oxalates, silicates, carbonates, phosphates, chlorides, and sulfates etc. (French and Milne 1994, Dayton 1997). The char and inorganic compounds are reported to catalyze

polymerization reactions during storage, resulting in increase in viscosity and average molecular weights (Agblevor 1994).

1.3.5.4 Accelerated aging

The storage properties of pyrolysis oil are critical to its usage as a transportation fuel. The raw pyrolysis oil is characterized by a number of deleterious properties such as high water content, low heating value, high viscosity, immiscibility with hydrocarbon liquids, and high solids content. Since pyrolysis oil is not a product of chemical and thermodynamic equilibrium as a result of rapid quench, the active ingredients continue to react until equilibrium is reached (Lu, Yang et al. 2008). All the reactions occur during storage produce hydrates, hemi-acetals, water, resins, oligomers, and esters etc. The pyrolysis oil will be oxidized if exposed to oxygen, forming more acids and peroxides that catalyze polymerization of unsaturated compounds. Because all these processes progress with time, it is called “aging” (Diebold and Czernik 1997). The aging reactions lead to increase in high molecular-mass lignin materials with a decrease in aldehydes, ketones, and lignin monomers. Etherification and esterification occurring between hydroxyl, carbonyl, and carboxyl groups are reported to be the main chemical reactions taking place in pyrolytic oils (Czernik, Johnson et al. 1994). Recently, aggregation of pyrolytic lignins is found to be the fundamental process in the aging processes (Fratini, Bonini et al. 2005). Char particles can also accelerate the aging reactions. Polarity of the pyrolysis oil may be changed by aging reactions.

It is necessary to evaluate the changes in the properties during storage and transportation to understand its chemical instability and develop stabilization strategies. The “accelerated aging method” has been used to short the investigation time. Heat was

reported to accelerate the aging reactions (Mohan, Pittman et al. 2006). Czernik (Czernik, Johnson et al. 1994) investigated the effects of storage conditions on physical and chemical properties of oak fast pyrolysis oils. Oil samples were stored at 37-90 °C in glass vessels. The water content, viscosity and molecular weight of the oil increased with aging time and temperature. First-order reaction kinetics were used to predict changes in molecular weight and viscosity during storage. FTIR results indicate that etherification or esterification are mechanisms for condensation of the oil during storage. Boucher et al. (Boucher, Chaala et al. 2000) investigated the stability of pyrolysis oil derived from softwood bark residue. The samples were sealed in Nalgene bottle and then kept at 40, 50 and 80 °C for up to 168 h and at room temperature for up to one year. The properties of the pyrolysis oil were dramatically altered when aged at 80 °C. The molecular weight increase after aging for one week at 80 °C was equivalent to storage for one year at room temperature. The addition of aqueous phase to the pyrolysis oil should be less than 15%, otherwise the oils' stability were lowered significantly. Oasmaa et al. (Oasmaa and Kuoppala 2003) investigated the physicochemical property change for pyrolysis liquid samples stored in firmly closed glass bottles in darkness at 9 °C or at room temperature under light. The average molecular mass, viscosity, water content, density and pour point of pyrolysis liquids increased with lengthened storage time. A clear correlation of the average molecular mass with the viscosity, water-insolubles, and the high-molecular-mass (HMM) fraction of water-insolubles was observed. The increase in lignin-derived HMM fraction of water-insoluble was caused by polymerization/condensation reactions of carbohydrate constituents, aldehydes, and ketones. Hilten and Das (Hilten and Das 2010) utilized three stability ranking methods to compare oxidative and thermal stability

of alcohol-stabilized and un-stabilized pyrolysis oil. Each method involved an accelerated aging procedure ranging from several minutes to 24 h. The C–O and C=O functional groups intensity increased after aging process. The methanol stabilized oils showed better average stability. Ortega et al. (Ortega, Renehan et al. 2011) studied the aging of the oils made from hardwood and softwood feedstocks at room temperature. The viscosity increased by approximately half of an order of magnitude over 5 months. However, this initial result was influenced by a ~4% decrease in water content due to evaporation. To explore aging characteristics in the absence of water loss, pyrolysis oils were aged in a water saturated environment at elevated temperatures (~ 65-85 °C). Fluid viscosity increased by less than an order of magnitude. The oils aged at 65 °C after 7 days showed increases in viscosity similar to the oils aged for 5 months at room temperature. The high water content and absence of char act to slow polymerization reactions.

To fully understand the fundamental chemistry of the aging process of pyrolysis oils, Ben and Ragauskas (Ben and Ragauskas 2012) investigated chemical structural changes during aging of loblolly pine residue pyrolysis oils at 80 °C for 60 h by in-situ NMR method. The content of aliphatic C-O bonds and aromatic C-H bonds decreased during the aging process while the contents of aliphatic C-C bonds, aromatic C-C, and C-O bonds increased. The HSQC NMR results indicated that the content of aromatic C-H bonds at ortho and para positions to hydroxyl groups decreased faster than that of aromatic C-H bonds at meta positions to hydroxyl groups. The content of levoglucosan decreased during aging. The condensation reaction to form aromatic C-O and C-C bonds could be initiated by the decomposition of the instable organic peroxides present in

pyrolysis oils. The crosslinking reaction between formaldehyde and aromatic C-H bonds could also form new aromatic C-C bonds and consume aromatic C-H bond and carbonyl groups. The condensation reactions also increase the molecular weight of the pyrolysis oils.

Hu et al. (Hu, Wang et al. 2013) investigated the roles of several typical compounds representing the sugars, sugar derivatives, and aromatics found in pyrolysis oil for their contribution to condensation reactions. Experiments were performed by increasing the temperature from 90 to 190 °C. The decomposition of glucose into volatile compounds with hydroxyl, carbonyl groups or conjugated C=C bonds played a key role for the polymerization. Furfural, hydroxyl aldehyde and hydroxyl acetone were also reactive toward polymerization. The carboxylic acids played the role of catalyst toward polymerization. The phenolic compounds promoted the acid catalyzed reactions. The adding of methanol significantly suppressed the decomposition of glucose and the polymerization of other compounds.

Alsbou et al. (Alsbou and Helleur 2014) described the evaluation of an accelerated aging process on the physical and chemical properties of pyrolysis oil from fast pyrolysis of ash and birch woods using two different pyrolyzers—a pilot scale auger reactor and lab scale tube furnace, respectively. The produced oils were aged at 80 °C over 1-7 days in sealed nitrogen-purged Nalgene vessels. The water content, viscosity, decomposition temperature and ash content levels increased as the aging period lengthened. GC/MS analysis of the pyrolysis oil indicated the amount of olefinic containing compounds significantly reduced. FTIR showed a reduction in aldehyde and

hydroxyl carbon signals indicating etherification and esterification occurred. TGA analysis showed increasing thermal degradation temperatures in oils with age.

1.3.5.5 Additives to stabilize pyrolysis oil

Various organics have been used to achieve stabilization of pyrolysis oil. Diebold et al. (Diebold and Czernik 1997) added methanol, ethanol, acetone, ethyl acetate, and methyl isobutyl ketone to improve the stability of pyrolysis oil. The oils were aged in sealed glass vials for 10-150 hours at 90 °C. The more severely aged samples has built up gas pressure and some leakage were observed. These additives significantly decreased the rate of aging, as measured by the rate of increase of oil viscosity with time, by factors of 7 to 18 times that observed with pyrolysis oil. The formation of hydrogen-bonding of pyrolysis oil with these additives and the chemical reactions between them caused the aging inhibition effect. Methanol was promising for its low cost and effectiveness to reduce aging rates.

Similar results were observed by other groups (Boucher, Chaala et al. 2000, Oasmaa, Kuoppala et al. 2004, Mante and Agblevor 2012). It is concluded the addition of alcohols improved the homogeneity while significantly lowered the rate of increase in viscosity and molecular mass. The reduction in the viscosity change was primarily due to a stabilizing effect of alcohols on the water-insoluble lignin-derived fraction. The formation of acetals due to reactions of alcohols with aldehydes, ketones, and anhydrosugars also slow down the aging reactions. A higher amount (> 10 wt%) of additive retarded the aging by almost a year.

Bakhshi et al. (Adjaye, Sharma et al. 1992) found the adding of tetralin improved the stability of pyrolysis oil. The properties of the pyrolysis oil mixture kept unchanged

with time. The free radicals existed in pyrolysis oil might be quenched by the donation of hydrogen from the tetralin. Meng et al.(Meng, Smirnova et al. 2014) observed free radicals were preferentially located in the pyrolysis oil lignin fraction, especially in the higher molecular weight lignin. The pyrolysis oil radicals were present in a stable state for radical scavengers showed negligible effects on the condensation of the pyrolytic lignin.

1.3.6 Pyrolysis oil upgrading

Pyrolysis oil has many drawbacks. The low heating value and chemical instability of pyrolysis oil need to be adjusted to make it an efficient fuel source. A number of physical and chemical pyrolysis oil upgrading technologies, such as filtration (Agblevor and Besler 1996), catalytic cracking (Vitolo, Seggiani et al. 1999, Zhang, Chang et al. 2006), hydrotreating (Elliott 2007), steam reforming (Chiaramonti, Bonini et al. 2003, Takanabe, Aika et al. 2004, Rioche, Kulkarni et al. 2005) etc. have been used. Catalytic hydrotreatment with heterogeneous catalysts at high temperature and pressure (eg. 500 °C, 300 bar) has been identified as a very promising way to improve the properties of pyrolysis liquids and make them suitable as a refinery feed (Elliott 2007, Venderbosch, Ardiyanti et al. 2010).

1.3.6.1 Filtration

The presence of char particles in the pyrolysis oil accelerates the aging reactions in storage and end-use. Also, the presence of high concentrations of submicron char particles in pyrolysis oils will potentially give out ash and alkali metals during

combustion when used as fuels for steam boilers, diesel engines, and turbine operations (Agblevor 1994).

Char is entrained with organic vapors and particles larger than about 10 μm in diameter could be efficiently separated from the vapors by cyclonic separation. Hot-gas filtration can efficiently remove the smaller char particles, but fine char passes through these filters as well. Agblevor et al. (Agblevor and Besler 1996) reported hot gas filtration can reduce the alkali metals content to less than 10 ppm while cold filtration of the oils dissolved in acetone was ineffective in reducing the alkali metals content to acceptable levels.

Microfiltration of the condensed pyrolysis oil can further remove the fine chars. Leaching studies conducted on the chars suspended in the oils showed no leaching of alkali metals (Agblevor 1994, Agblevor and Besler 1996). Javaid et al. (Javaid, Ryan et al. 2010) used tubular ceramic membranes to remove char particles less than 10 μm from pyrolysis oil. The process was conducted in a cross-flow mode at temperatures ranging from 38 to 45 $^{\circ}\text{C}$ and at three trans-membrane pressures varying from 1 to 3 bars. A significant reduction in overall ash content of the pyrolysis oil was observed while no significant changes in other properties occurred due to the microfiltration process. Nano-sized char particles are recently removed by nano-filtration. However, minerals solubilized by the acidic solution of pyrolysis oil cannot be removed by filtration.

1.3.6.2 Hydrotreating

Elliott (Elliott 2007) reviewed of the developments in the field of catalytic hydroprocessing of pyrolysis oil over the past decades. As shown in Table 1.1, both precious metal catalysts and conventional catalysts developed for petroleum

hydroprocessing have been tested. Adjustments to conventional hydroprocessing applied to petroleum feed stocks are needed for pyrolysis oil hydroprocessing.

Table 1.1 Catalysts used in hydroprocessing pyrolysis oil (Elliott 2007)

supplier	catalyst id	active metals	weight %	support	form ^a
Harshaw	Ni-1404	Ni	68	proprietary	1/8-in T
Harshaw	CoMo0402	CoO/MoO ₃	3/15	silica–alumina	1/8-in T
Harshaw	HT 400	CoO/MoO ₃	3/15	γ-Al ₂ O ₃	1/8-in E
Harshaw	HT 500	NiO/MoO ₃	3.5/15.5	γ-Al ₂ O ₃	1/8-in E
Harshaw	Ni-3266	Ni	50	silica–alumina	1/16-in E
Harshaw	Ni-4301	NiO/WO ₂	6/19	γ-Al ₂ O ₃	
Haldor Topsoe ^b	TK 710	CoO/MoO ₃	2/6	Al ₂ O ₃	3/16-in R
Haldor Topsoe ^b	TK 750	CoO/MoO ₃	2.3/10	Al ₂ O ₃	1/16-in E
Haldor Topsoe ^b	TK 770	CoO/MoO ₃	3.4/14	Al ₂ O ₃	1/16-in E
Haldor Topsoe	TK 751	NiO/MoO ₃	3/13	Al ₂ O ₃	1 mm E
Katalco	CoMo479	CoO/MoO ₃	4.4/19	Al ₂ O ₃	1/16-in E
Katalco	CoMo499	CoO/MoO ₃	4.4/19	γ-Al ₂ O ₃	1/16-in E
Katalco	KAT 4000	CoO/MoO ₃	3.5/14	γ-Al ₂ O ₃	1/32-in E
Shell	S411	NiO/MoO ₃	2.67/14.48	Al ₂ O ₃ ^c	1/20-in T
PNL/Linde	CoMo/Y	CoO/MoO ₃	3.5/13.9	Y-zeolite/ Al ₂ O ₃	1/16-in E
PNL/Grace	CoMo/SiAl	CoO/MoO ₃	3/13	13%Al ₂ O ₃ SiO ₂	3/16-in T
Amoco	NiMo/Y	NiO/MoO ₃	3.5/18	Y-zeolite/ Al ₂ O ₃ ^c	1/16-in E
BASF	K8–11	CoO/MoO ₃	4.3/11	MgO spinel/ Al ₂ O ₃	1 mm E
Akzo	KF-742	CoO/MoO ₃	4.4/15.0	γ-Al ₂ O ₃	1.3 mm Q
Akzo	KF-840	NiO/MoO ₃	3.9/19.6	Al ₂ O ₃ ^c	1.3 mm Q
Criterion	C-424	NiO/MoO ₃	4/19.5	Al ₂ O ₃ ^c	1.3 mm Q
Strem	78–166	Pt	5	γ-Al ₂ O ₃	P

^a E = extrudates; R = ring; T = tablet; Q = quadrilobe extrudates; P = powder; and the size given is the o.d. ^b All three catalysts were used in a layered bed. ^c Includes phosphorus oxide.

Hydroprocessing is normally carried out at temperatures 250–450 °C. It is crucial to have a catalyst able to withstand water at the extreme conditions of high temperature and pressure. Degrees of deoxygenation increased with increasing residence times. Thus large liquid phase residence times are required. In general liquid hourly space velocity (LHSV) should be in the order of 0.1–1.5 h⁻¹ (McCall and Brandvold 2009) for flow reactors. The favored residence time in batch reactors are 3–4 hours (Gagnon and Kaliaguine 1988, Gutierrez, Kaila et al. 2009).

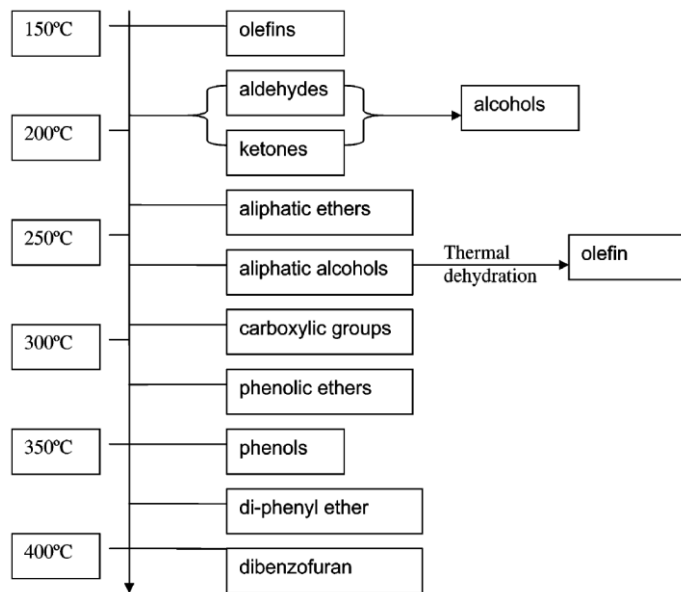


Figure 1.4 Reactivity scale of oxygenated groups found in pyrolysis oil under hydrotreatment conditions (Elliott 2007)

Figure 1.4 shows the reactivity scale of oxygenated groups found in pyrolysis oil during hydrotreatment. At low temperatures, olefins, aldehydes, and ketones are readily reduced by hydrogen. These reactions improve the stability for pyrolysis oil by removing the well-known reactive groups. Alcohols are reacted at 250-300 °C by catalytic hydrogenation. However, the thermal dehydration of alcohols form olefins which may further polymerize at hydrotreatment conditions. Carboxylic and phenolic ethers are also reduced at ~300 °C. Venderbosch et al. (Venderbosch, Ardiyanti et al. 2010) recently developed an integral processing route for the hydrotreatment of pyrolysis oil. It includes a lower operating temperature step of 175 to 250 °C in which reactive components (olefins, aldehydes, ketones and alcohols) are reacted, and subsequently, the stabilized product fraction can be further processed by hydrotreatment at high temperature.

1.4 Objective

Pyrolysis oil is a promising source for alternative fuel, but there are many issues to overcome before it can be used as transportation fuel. The biggest challenge is from its thermodynamical and chemical instability. The existing knowledge obtained by the accelerated aging method significantly broaden and deepen our understanding about the stability of pyrolysis oils. Unfortunately, almost all the processes were carried out in a low temperature range i.e., below 90 °C and the applicable temperature range for this method are still not decided. This study investigates the physical and chemical changes for oils aged in a broad temperature range, covering the conditions for low temperature hydrotreatment. Furthermore, the effect of addition of alcohols on the physicochemical properties of pyrolysis oil will be investigated. This research will contribute to develop practical solutions to eliminate or mitigate the aging of pyrolysis oil during storage or transportation.

1.5 References

- Adjaye, J. D., R. K. Sharma and N. N. Bakhshi (1992). "Characterization and stability analysis of wood-derived bio-oil." Fuel Processing Technology **31**(3): 241-256.
- Agblevor, F. A. and S. Besler (1996). "Inorganic Compounds in Biomass Feedstocks. 1. Effect on the Quality of Fast Pyrolysis Oils." Energy & Fuels **10**(2): 293-298.
- Agblevor, F. A. B., S.; and Evans, R.J. (1994). Inorganic Compounds in Biomass Feedstocks: Their Role in Char Formation and Effect on the Quality of Fast Pyrolysis Oils, National Renewable Energy Laboratory.
- Aho, A., N. Kumar, K. Eränen, T. Salmi, M. Hupa and D. Y. Murzin (2007). "Catalytic Pyrolysis of Biomass in a Fluidized Bed Reactor: Influence of the Acidity of H-Beta Zeolite." Process Safety and Environmental Protection **85**(5): 473-480.
- Alsbou, E. and B. Helleur (2014). "Accelerated Aging of Bio-oil from Fast Pyrolysis of Hardwood." Energy & Fuels **28**(5): 3224-3235.
- Appenzeller, T. (2004). "End of Cheap Oil." from <http://ngm.nationalgeographic.com/ngm/0406/feature5/fulltext.html>.
- Ben, H. and A. J. Ragauskas (2012). "In Situ NMR Characterization of Pyrolysis Oil during Accelerated Aging." ChemSusChem **5**(9): 1687-1693.
- Boateng, A. A., D. E. Dugaard, N. M. Goldberg and K. B. Hicks (2007). "Bench-Scale Fluidized-Bed Pyrolysis of Switchgrass for Bio-Oil Production†." Industrial & Engineering Chemistry Research **46**(7): 1891-1897.
- Boucher, M. E., A. Chaala, H. Pakdel and C. Roy (2000). "Bio-oils obtained by vacuum pyrolysis of softwood bark as a liquid fuel for gas turbines. Part II: Stability and ageing of bio-oil and its blends with methanol and a pyrolytic aqueous phase." Biomass and Bioenergy **19**(5): 351-361.
- Branca, C., P. Giudicianni and C. Di Blasi (2003). "GC/MS Characterization of Liquids Generated from Low-Temperature Pyrolysis of Wood." Industrial & Engineering Chemistry Research **42**(14): 3190-3202.
- Bridgwater, A. and G. Peacocke (2000). "Fast pyrolysis processes for biomass." Renewable and sustainable energy reviews **4**(1): 1-73.
- Bridgwater, A. V. (2012). "Review of fast pyrolysis of biomass and product upgrading." Biomass and Bioenergy **38**(0): 68-94.

- Chiaramonti, D., M. Bonini, E. Fratini, G. Tondi, K. Gartner, A. V. Bridgwater, H. P. Grimm, I. Soldaini, A. Webster and P. Baglioni (2003). "Development of emulsions from biomass pyrolysis liquid and diesel and their use in engines—Part 1 : emulsion production." Biomass and Bioenergy **25**(1): 85-99.
- Chow, J., R. J. Kopp and P. R. Portney (2003). "Energy Resources and Global Development." Science **302**(5650): 1528-1531.
- Czernik, S., D. K. Johnson and S. Black (1994). "Stability of wood fast pyrolysis oil." Biomass and Bioenergy **7**(1–6): 187-192.
- Dale, B. E. and R. G. Ong (2014). "Design, implementation, and evaluation of sustainable bioenergy production systems." Biofuels, Bioproducts and Biorefining **8**(4): 487-503.
- Daugaard, D., S. T. Jones, D. L. Dalluge and R. C. Brown (2011). Selective temperature quench and electrostatic recovery of bio-oil fractions, Google Patents.
- Dayton, D. (1997). The Fate of Alkali Metal during Biomass Thermochemical Conversion. Developments in Thermochemical Biomass Conversion. A. V. Bridgwater and D. G. B. Boocock, Springer Netherlands: 1263-1277.
- Di Blasi, C. (1996). "Heat transfer mechanisms and multi-step kinetics in the ablative pyrolysis of cellulose." Chemical Engineering Science **51**(10): 2211-2220.
- Diebold, J. P. (1997). A Review of the Toxicity of Biomass Pyrolysis Liquids Formed at Low Temperatures. NREL/TP-430-22739, National Renewable Energy Laboratory, Golden, CO: 35.
- Diebold, J. P. (2000). A Review of the Chemical and Physical Mechanisms of the Storage Stability of Fast Pyrolysis Bio-Oils, National Renewable Energy Laboratory.
- Diebold, J. P. and A. V. Bridgwater (1997). Overview of Fast Pyrolysis of Biomass for the Production of Liquid Fuels. Developments in Thermochemical Biomass Conversion. A. V. Bridgwater and D. G. B. Boocock, Springer Netherlands: 5-23.
- Diebold, J. P. and S. Czernik (1997). "Additives To Lower and Stabilize the Viscosity of Pyrolysis Oils during Storage." Energy & Fuels **11**(5): 1081-1091.
- Ed, J. S. and A. M. Thomas (1988). Pyrolysis Oils from Biomass, American Chemical Society.
- Edenhofer, O., R. Pichs-Madruga, Y. Sokona, K. Seyboth, S. Kadner, T. Zwickel, P. Eickemeier, G. Hansen, S. Schlömer and C. von Stechow (2011). Renewable Energy Sources and Climate Change Mitigation: Special Report of the Intergovernmental Panel on Climate Change, Cambridge University Press.

- EIA (2003). International Energy Annual 2001 Edition, U.S. Department of Energy.
- EIA (2011). Annual Energy Review 2010, Energy Information Administration.
- EIA (2014). Annual Energy Outlook 2014 with Projections to 2040, Energy Information Administration.
- Elliott, D. C. (2007). "Historical Developments in Hydroprocessing Bio-oils." Energy & Fuels **21**(3): 1792-1815.
- Evans, R. J. and T. A. Milne (1987). "Molecular characterization of the pyrolysis of biomass." Energy & Fuels **1**(2): 123-137.
- Fratini, E., M. Bonini, A. Oasmaa, Y. Solantausta, J. Teixeira and P. Baglioni (2005). "SANS Analysis of the Microstructural Evolution during the Aging of Pyrolysis Oils from Biomass." Langmuir **22**(1): 306-312.
- French, R. J. and T. A. Milne (1994). "Vapor phase release of alkali species in the combustion of biomass pyrolysis oils." Biomass and Bioenergy **7**(1-6): 315-325.
- Gagnon, J. and S. Kaliaguine (1988). "Catalytic hydrotreatment of vacuum pyrolysis oils from wood." Industrial & Engineering Chemistry Research **27**(10): 1783-1788.
- García-Pérez, M., A. Chaala, H. Pakdel, D. Kretschmer, D. Rodrigue and C. Roy (2005). "Multiphase Structure of Bio-oils." Energy & Fuels **20**(1): 364-375.
- García-Pérez, M., A. Chaala, H. Pakdel, D. Kretschmer and C. Roy (2007). "Vacuum pyrolysis of softwood and hardwood biomass: Comparison between product yields and bio-oil properties." Journal of Analytical and Applied Pyrolysis **78**(1): 104-116.
- Garrett, D. E. and G. M. Mallan (1979). Pyrolysis process for solid wastes, Google Patents.
- Goyal, H. B., D. Seal and R. C. Saxena (2008). "Bio-fuels from thermochemical conversion of renewable resources: A review." Renewable and Sustainable Energy Reviews **12**(2): 504-517.
- Gutierrez, A., R. K. Kaila, M. L. Honkela, R. Slioor and A. O. I. Krause (2009). "Hydrodeoxygenation of guaiacol on noble metal catalysts." Catalysis Today **147**(3-4): 239-246.
- Helleur, R., N. Popovic, M. Ikura, M. Stanculescu and D. Liu (2001). "Characterization and potential applications of pyrolytic char from ablative pyrolysis of used tires." Journal of Analytical and Applied Pyrolysis **58-59**(0): 813-824.

- Hilten, R. N. and K. C. Das (2010). "Comparison of three accelerated aging procedures to assess bio-oil stability." Fuel **89**(10): 2741-2749.
- Hindsgaul, C., J. Schramm, L. Gratz, U. Henriksen and J. Dall Bentzen (2000). "Physical and chemical characterization of particles in producer gas from wood chips." Bioresource Technology **73**(2): 147-155.
- Hoekstra, E., K. J. A. Hogendoorn, X. Wang, R. J. M. Westerhof, S. R. A. Kersten, W. P. M. van Swaaij and M. J. Groeneveld (2009). "Fast Pyrolysis of Biomass in a Fluidized Bed Reactor: In Situ Filtering of the Vapors." Industrial & Engineering Chemistry Research **48**(10): 4744-4756.
- Hu, X., Y. Wang, D. Mourant, R. Gunawan, C. Lievens, W. Chaiwat, M. Gholizadeh, L. Wu, X. Li and C.-Z. Li (2013). "Polymerization on heating up of bio-oil: A model compound study." AIChE Journal **59**(3): 888-900.
- Huber, G. W., S. Iborra and A. Corma (2006). "Synthesis of Transportation Fuels from Biomass: Chemistry, Catalysts, and Engineering." Chemical Reviews **106**(9): 4044-4098.
- Javaid, A., T. Ryan, G. Berg, X. Pan, T. Vispute, S. R. Bhatia, G. W. Huber and D. M. Ford (2010). "Removal of char particles from fast pyrolysis bio-oil by microfiltration." Journal of Membrane Science **363**(1-2): 120-127.
- Kang, B.-S., K. H. Lee, H. J. Park, Y.-K. Park and J.-S. Kim (2006). "Fast pyrolysis of radiata pine in a bench scale plant with a fluidized bed: Influence of a char separation system and reaction conditions on the production of bio-oil." Journal of Analytical and Applied Pyrolysis **76**(1-2): 32-37.
- Kawamoto, H., M. Murayama and S. Saka (2003). "Pyrolysis behavior of levoglucosan as an intermediate in cellulose pyrolysis: polymerization into polysaccharide as a key reaction to carbonized product formation." Journal of Wood Science **49**(5): 469-473.
- Lee, K.-H., B.-S. Kang, Y.-K. Park and J.-S. Kim (2005). "Influence of Reaction Temperature, Pretreatment, and a Char Removal System on the Production of Bio-oil from Rice Straw by Fast Pyrolysis, Using a Fluidized Bed." Energy & Fuels **19**(5): 2179-2184.
- Lu, Q., X.-l. Yang and X.-f. Zhu (2008). "Analysis on chemical and physical properties of bio-oil pyrolyzed from rice husk." Journal of Analytical and Applied Pyrolysis **82**(2): 191-198.
- Mante, O. D. and F. A. Agblevor (2012). "Storage stability of biocrude oils from fast pyrolysis of poultry litter." Waste Management **32**(1): 67-76.

- Martínez, D. M. and B. W. Ebenhack (2008). "Understanding the role of energy consumption in human development through the use of saturation phenomena." Energy Policy **36**(4): 1430-1435.
- McCall, M. J. and T. A. Brandvold (2009). Fuel and Fuel Blending Components from Biomass Derived Pyrolysis Oil, Google Patents.
- Meng, J., T. I. Smirnova, X. Song, A. Moore, X. Ren, S. Kelley, S. Park and D. Tilotta (2014). "Identification of free radicals in pyrolysis oil and their impact on bio-oil stability." RSC Advances **4**(56): 29840-29846.
- Milne, T. A. A., F.; Davis, M.; Deutch, S.; and Johnson, D (1997). A Review of the Chemical Composition of Fast Pyrolysis Oils, in Developments in Thermal Biomass Conversion. London, Blackie Academic and Professional.
- Mohan, D., C. U. Pittman and P. H. Steele (2006). "Pyrolysis of Wood/Biomass for Bio-oil: A Critical Review." Energy & Fuels **20**(3): 848-889.
- Nussbaumer, T. (2003). "Combustion and Co-combustion of Biomass: Fundamentals, Technologies, and Primary Measures for Emission Reduction†." Energy & Fuels **17**(6): 1510-1521.
- Oasmaa, A. and E. Kuoppala (2003). "Fast Pyrolysis of Forestry Residue. 3. Storage Stability of Liquid Fuel." Energy & Fuels **17**(4): 1075-1084.
- Oasmaa, A., E. Kuoppala, J.-F. Selin, S. Gust and Y. Solantausta (2004). "Fast Pyrolysis of Forestry Residue and Pine. 4. Improvement of the Product Quality by Solvent Addition." Energy & Fuels **18**(5): 1578-1583.
- Ortega, J. V., A. M. Renehan, M. W. Liberatore and A. M. Herring (2011). "Physical and chemical characteristics of aging pyrolysis oils produced from hardwood and softwood feedstocks." Journal of Analytical and Applied Pyrolysis **91**(1): 190-198.
- Peacocke, G. V. C. and A. V. Bridgwater (1994). "Ablative plate pyrolysis of biomass for liquids." Biomass and Bioenergy **7**(1-6): 147-154.
- Piskorz, J., D. Radlein and D. S. Scott (1986). "On the mechanism of the rapid pyrolysis of cellulose." Journal of Analytical and Applied Pyrolysis **9**(2): 121-137.
- Piskorz, J., D. S. Scott and D. Radlein (1988). Composition of Oils Obtained by Fast Pyrolysis of Different Woods. Pyrolysis Oils from Biomass, American Chemical Society. **376**: 167-178.
- R.J. French, D. C. D., T.A. Milne (1994). The Direct Observation of Alkali Vapor Species in Biomass Combustion and Gasification. Golden, Colorado 80401-3393 National Renewable Energy Laboratory/TP-430-5597.

- Raveendran, K., A. Ganesh and K. C. Khilar (1996). "Pyrolysis characteristics of biomass and biomass components." Fuel **75**(8): 987-998.
- RFF. "Global Energy Resources: an overview." from http://www.rff.org/rff/News/Features/upload/10687_1.pdf.
- Rioche, C., S. Kulkarni, F. C. Meunier, J. P. Breen and R. Burch (2005). "Steam reforming of model compounds and fast pyrolysis bio-oil on supported noble metal catalysts." Applied Catalysis B: Environmental **61**(1-2): 130-139.
- Rosendahl, L. (2013). Biomass Combustion Science, Technology and Engineering, Elsevier Science.
- Roy, C., A. Chaala and H. Darmstadt (1999). "The vacuum pyrolysis of used tires: End-uses for oil and carbon black products." Journal of Analytical and Applied Pyrolysis **51**(1-2): 201-221.
- Rüdisüli, M., T. J. Schildhauer, S. M. A. Biollaz and J. R. van Ommen (2012). "Scale-up of bubbling fluidized bed reactors — A review." Powder Technology **217**(0): 21-38.
- Saiz-Jimenez, C. and J. W. De Leeuw (1986). "Lignin pyrolysis products: Their structures and their significance as biomarkers." Organic Geochemistry **10**(4-6): 869-876.
- Schobert, H. H. (2014). Energy and Society: An Introduction, Second Edition, CRC Press.
- Shafizadeh, F., R. H. Furneaux, T. G. Cochran, J. P. Scholl and Y. Sakai (1979). "Production of levoglucosan and glucose from pyrolysis of cellulosic materials." Journal of Applied Polymer Science **23**(12): 3525-3539.
- Takanabe, K., K.-i. Aika, K. Seshan and L. Lefferts (2004). "Sustainable hydrogen from bio-oil—Steam reforming of acetic acid as a model oxygenate." Journal of Catalysis **227**(1): 101-108.
- Uzun, B. B., A. E. Pütün and E. Pütün (2007). "Rapid Pyrolysis of Olive Residue. 1. Effect of Heat and Mass Transfer Limitations on Product Yields and Bio-oil Compositions." Energy & Fuels **21**(3): 1768-1776.
- Venderbosch, R. H., A. R. Ardiyanti, J. Wildschut, A. Oasmaa and H. J. Heeres (2010). "Stabilization of biomass-derived pyrolysis oils." Journal of Chemical Technology & Biotechnology **85**(5): 674-686.
- Vitolo, S., M. Seggiani, P. Frediani, G. Ambrosini and L. Politi (1999). "Catalytic upgrading of pyrolytic oils to fuel over different zeolites." Fuel **78**(10): 1147-1159.

- Wang, G., W. Li, B. Li and H. Chen (2008). "TG study on pyrolysis of biomass and its three components under syngas." Fuel **87**(4–5): 552-558.
- Wang, S., X. Guo, K. Wang and Z. Luo (2011). "Influence of the interaction of components on the pyrolysis behavior of biomass." Journal of Analytical and Applied Pyrolysis **91**(1): 183-189.
- Wessner, C. (1999). "What Is the Best Guess as to When the World's Oil Reserves Will Run Out?" Popular Science **February**
- Worasuwannarak, N., T. Sonobe and W. Tanthapanichakoon (2007). "Pyrolysis behaviors of rice straw, rice husk, and corncob by TG-MS technique." Journal of Analytical and Applied Pyrolysis **78**(2): 265-271.
- Yang, H., R. Yan, H. Chen, C. Zheng, D. H. Lee and D. T. Liang (2006). "In-Depth Investigation of Biomass Pyrolysis Based on Three Major Components: Hemicellulose, Cellulose and Lignin." Energy & Fuels **20**(1): 388-393.
- Zhang, H., R. Xiao, D. Wang, G. He, S. Shao, J. Zhang and Z. Zhong (2011). "Biomass fast pyrolysis in a fluidized bed reactor under N₂, CO₂, CO, CH₄ and H₂ atmospheres." Bioresource Technology **102**(5): 4258-4264.
- Zhang, Q., J. Chang, Wang and Y. Xu (2006). "Upgrading Bio-oil over Different Solid Catalysts." Energy & Fuels **20**(6): 2717-2720.

CHAPTER II

CHARACTERIZATION OF KIOR'S RENEWABLE RECRUDE OIL

2.1 Introduction

KiOR Inc. has developed a proprietary technology platform to convert non-food feedstock, such as wood and forestry residuals into a hydrocarbon-based renewable crude oil (Bartek, Brady et al. 2011). The first step was to torrefy wood chips at a temperature between 80 and 300 °C. Then the biomass particles were mixed with a liquid to form a suspension. The suspension was fed into a hydrolysis reactor. A large portion of the biomass can be converted into fuel by this process.

The company's recent technology platform combined a newly-designed catalyst (Adkins, Stamires et al. 2013) with a modified pyrolysis process (Bartek, Cordle et al. 2012) based on the existing fluid catalytic cracking (FCC) technology. The catalyst (Adkins, Stamires et al. 2013) was composed of a phosphorous-promoted ZSM-5 and a silica-containing binder. The catalyst attained high pyrolysis oil yields and lower coke than conventional catalysts. Another advantage was the conventional FCC technology was used for pyrolysis oil production after modification. Fig 2.1 a) shows a typical conventional reactor system wherein biomass is added to a hot heat carrier material/catalyst stream fluidized by lift gas. Premature heating of biomass was sometimes observed which may lead to plugging and over cracking of the biomass. Fig

2.1 b) and c) show the optimized process—the hot heat carrier material/catalyst is added to the biomass stream fluidized by the lift gas. Also, the angle for the introduction of the hot heat carrier material was specially designed to induce a counter-current flow of the heat carrier material/catalyst to the flow path of the fluidized biomass. This design increased the mixing and heat transfer between the hot heat carrier material/catalyst and biomass. This biomass fluid catalytic cracking (BFCC) process showed a significant cost advantages, including lower capital and operating costs, versus traditional biofuels production methods.

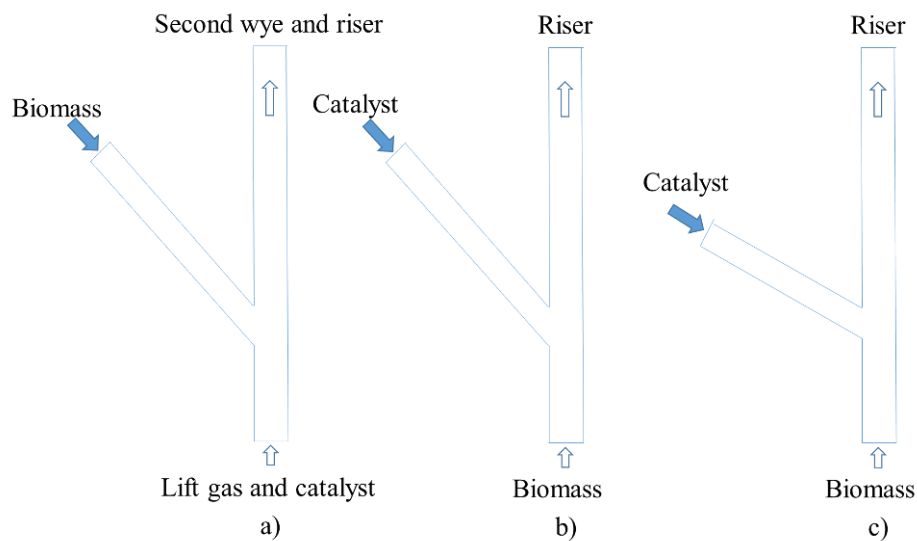


Figure 2.1 Reactors used in fluid catalytic cracking process (Bartek, Cordle et al. 2012)

Biomass pyrolysis liquids differ a great deal based on the feedstock and the pyrolysis process. Pyrolysis liquids characterization is very difficult for the presence of high molecular mass lignin and components with a wide distribution of molecular weights, polarity, acidity and boiling points. The standard fuel oil test methods developed

for mineral oils are not appropriate for pyrolysis liquids due to the significant difference in physical and chemical properties (Peacocke, Russell et al. 1994). The reliability of analytical methods is important (Oasmaa, Peacocke et al. 2005) and some round-robin tests have been carried out to validate methods (Oasmaa and Meier 2005, Elliott, Oasmaa et al. 2012). A detailed physicochemical analysis of pyrolysis oil requires multiple analytical techniques. In this research, the physical properties of the ReCrude oil, such as water content, ash content, viscosity and high molecular mass lignin content were measured. The thermal properties were analyzed by TGA (thermogravimetric analysis) and DSC (differential scanning calorimetry). The chemical composition of pyrolysis oil was analyzed by FTIR (Fourier transform infrared) spectroscopy and GC-MS (gas chromatography-mass spectroscopy).

2.2 Experiment

2.2.1 Solvent extraction

The high molecular mass (HMM) lignin (CH_2Cl_2 insoluble part) was separated from the pyrolysis liquid oil with CH_2Cl_2 . The mixture was shaken for 10 min at room temperature and left to equilibrate for 3 hours, forming distinct bottom and CH_2Cl_2 phases. The LMM lignin fraction was preferentially extracted into the organic phase and separated by decantation from the bottom phase. Excess CH_2Cl_2 was removed from the organic phase by evaporation at room temperature.

2.2.2 Water content

Water content was measured by Karl Fisher titration following ASTM method E-203-01 with Hydranal titrant and Hydranal solvent. The oil samples were first dissolved

into CM solvent. Then the water contents were measured for both CM and mixed solution.

2.2.3 Thermogravimetric analysis

Thermogravimetric analysis (TGA) was performed on a TA Instruments SDT Q600 under a nitrogen or air atmosphere with a flowrate of 50 mL/min. Dynamic ramps were performed on both heat-treated and untreated samples at a rate of 5 °C/min.

2.2.4 Differential Scanning Calorimetry

DSC measurements were collected with a TA DSC Q2000 instrument. A total of ~2 mg of each material was placed in a sealed aluminum pan and ramps of 5 °C/min were performed from -60 to 290 °C under a nitrogen atmosphere. The unheated ReCrude oils were analyzed by isothermal runs at 80, 150 and 200 °C with a N₂ flow rate of 50 mL/min.

2.2.5 GC-MS

The GC-MS were performed on a Hewlett Packard 5890 II gas chromatograph equipped with a Hewlett Packard 5971 mass spectrometer. A 30 m length × 0.32 mm internal diameter × 0.25 μm film thickness silica capillary column coated with 5% phenylmethylpolysiloxane was used. The injector temperature was 270 °C. The column was initially kept at 40 °C and then followed by heating at 5 °C/min to a final temperature of 280 °C and held for 15 min. The mass spectrometer employed a 70 eV electron impact ionization mode. The source temperature and interface temperature were 250 and 270 °C, respectively. Chlorobenzene was used as an internal standard for the semi-quantitative calibration.

2.2.6 ATR-FTIR

Attenuated total reflectance Fourier transform infrared (ATR-FTIR) spectra were collected using a Nicolet 6700 spectrometer (MCT-A* detector, 4 cm⁻¹ resolution) with a Pike Veemax accessory and ZnSe ATR crystal.

2.3 Results and Discussion

2.3.1 Water content

The water content is the most relevant features in pyrolysis oil composition with regard to combustion applications. A high water content of the pyrolysis oil leads to the oils' low energy density. Moreover, water content affects the adiabatic flame temperature, local combustion temperatures and combustion reaction rates. In addition, a high water content increases the ignition delay time by reducing the vaporization rate of the droplet due to its relatively high vaporization temperature and high specific heat. On the other hand, water can enhance the atomization of the pyrolysis oil by reducing its viscosity. Water can also reduce the NO_x emissions by lowering the flame temperatures inside the combustor. However, too high water content bring difficulties in the ignition and put at risk the flame stability and controllability of the combustion (Shihadeh and Hochgreb 2002).

The poor solubility of the ReCrude oil in Hydranal solvent made the determination of the titration end point a slow process. To accelerate response, the ReCrude oil was first dissolved into Hydranal solvent. The water contents for both the Hydranal and mixed solution were measured. The ReCrude oil water content was measured to be $4.77 \pm 0.27\%$.

2.3.2 Solids content

The inorganic solids content generally has negative effects on pyrolysis oil. The solid particles are reported as a catalyst for aging reactions and can agglomerate during storage and form a sludge layer on the bottom. Most of the alkali metals, such as K and Na that cause erosion in the pumps are concentrated in the solids. The presence of solids is not desirable considering the areas of pyrolysis oil storage, stability, and combustion behavior.

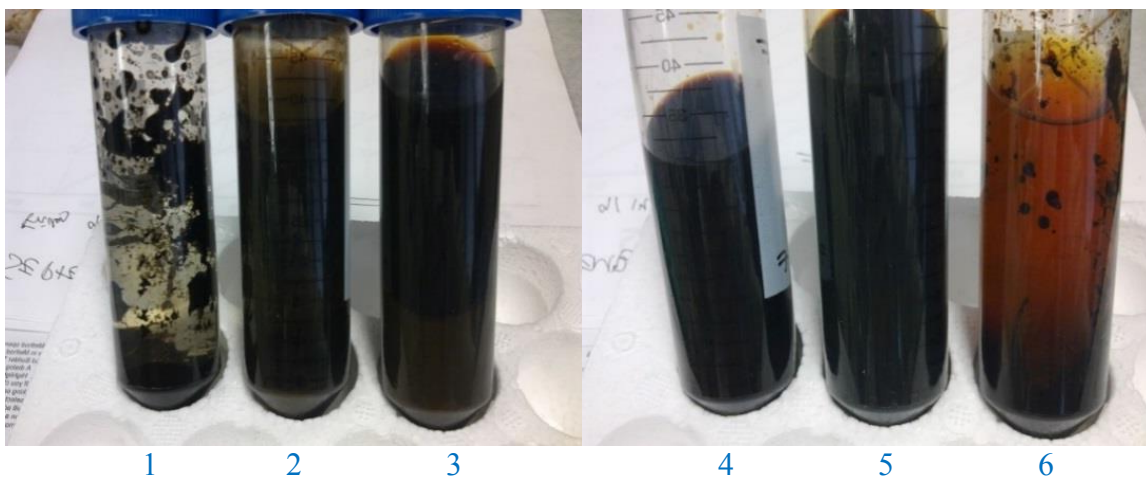


Figure 2.2 The solubility of crude oils in different solvents at ambient temperature

The ReCrude oil was water insoluble. It was immiscible with petroleum ether due to the high oxygen content of around 35-40 wt%, which was similar to that of biomass (French and Czernik 2010, Bridgwater 2012). As shown in Figure 2.2, phase separations were observed when the ReCrude oil was mixed methanol, ethanol, or isopropanol.

Table 2.1 Solids content of renewable crude oil in different solvent

No.	Solvent	Oil (g)	Solids (g)	Solvent (mL)	Solids content (wt%)
1	H ₂ O	3.031	----	30.3	----
2	Methanol	3.867	0.523	38.7	13.53
3	Ethanol	4.127	0.672	41.3	16.28
4	MeOH/DCM 50/50	3.307	0.110	33.1	3.323
5	MeOH/DCM 20/80	4.353	0.196	43.5	4.50
6	i-PrOH/H ₂ O 40/60	3.605	----	36.0	----

In some research, the solids content was determined as the ethanol insoluble part. Oasmaa and Meier (Oasmaa and Meier 2005) reported that the method was only accurate for oils produced from white wood liquids. A more polar solvent, like a mixture of methanol or ethanol and dichloromethane was required for the extractive-rich liquids. The solids content of 3.3% was obtained with a mixture of methanol and dichloromethane (50:50 v/v).

2.3.3 HMM lignin content

High molecular mass (HMM) Lignin has been reported to be a major reason for the instability of pyrolysis oil (Scholze and Meier 2001). Pyrolytic lignin has a peculiar structure compared to industrial lignin especially in its unsaturated structures. Lignin's structure is a complex with a great variety of functional groups and more than ten different types of linkages (Scholze and Meier 2001, Eide, Zahlse et al. 2006). The major part of HMM lignin is not distillable which makes it not suitable for combustion in gasoline engines. Moreover, the high molecular weight hinders its usage in spray combustors.

Oasmaa et al. (Oasmaa, Kuoppala et al. 2003) proposed a solvent fractionation method to separate pyrolysis oil into several parts for characterization. The water-insoluble fraction can be further divided into two parts by CH_2Cl_2 extraction. The CH_2Cl_2 insoluble part mainly contains HMM lignin. As shown in Figure 2.3, the HMM lignin content was ~33 wt%, slightly higher than the reported value 25–30 wt% (Czernik and Bridgwater 2004).

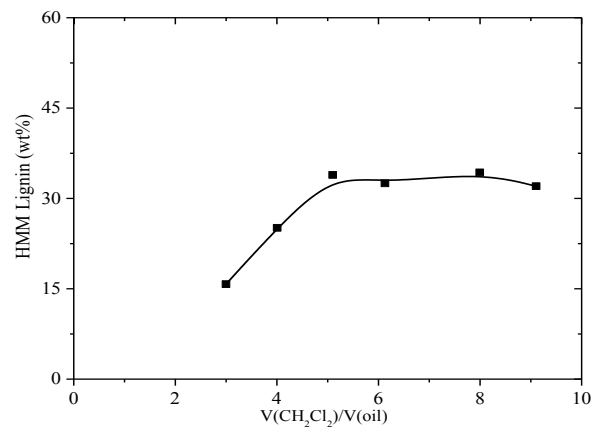


Figure 2.3 Plot of HMM lignin content vs $V\text{CH}_2\text{Cl}_2/V\text{oil}$

2.3.4 Ash content

The presence of ash in the pyrolysis oil can cause erosion, corrosion, and gumming problems in the engine valves. Problems associated with ash content become more serious when the ash content of the fuel is greater than 0.1 wt% (Peacocke, Russell et al. 1994). A certain amount of crude oil sample was put in a muffle furnace in the presence of air. The furnace was heated to 650 °C with a heating rate of 10 °C /min and then kept at 650 °C for 7 hours. The average ash content was 0.12 ± 0.02 wt%. The high ash content of the crude oil indicated a filtration process was necessary.

2.3.5 TGA

The thermal decomposition of organic polymers is commonly determined by thermogravimetric analysis (TGA) under nitrogen atmosphere. TG curves reveal the weight loss of substances in relation to the temperature of thermal degradation, while the first derivative thermogravimetric analysis (DTG) shows the corresponding rate of weight loss. The literature have used quite different heating rates for thermal analysis (5-20 °C/min) (Kang, Lee et al. 2006, Garcia-Perez, Wang et al. 2008, Jiang and Ellis 2010, Kim, Jung et al. 2010). The thermal conductivity (HLAVÁČ 2013) of pyrolysis oil was reported to be ~0.2-0.3 W/(m·K). Considering the low thermal conductivity, the effect of heating rate was investigated in a temperature range 2-10 °C/min. Figure 2.4 displays the TG and the corresponding DTG curves of crude oil at different heating rates in N₂ atmosphere. The sample remains ~20 wt% of the original weight after 700 °C. The higher heating rate shifted the plot to high temperature direction at the same weight loss. The DTG_{max} temperature also shifted to higher temperature with increasing ramp rate. A much higher DTG_{max} was observed at 10 °C/min indicating the change of sample temperature cannot catch up with the ramp rate.

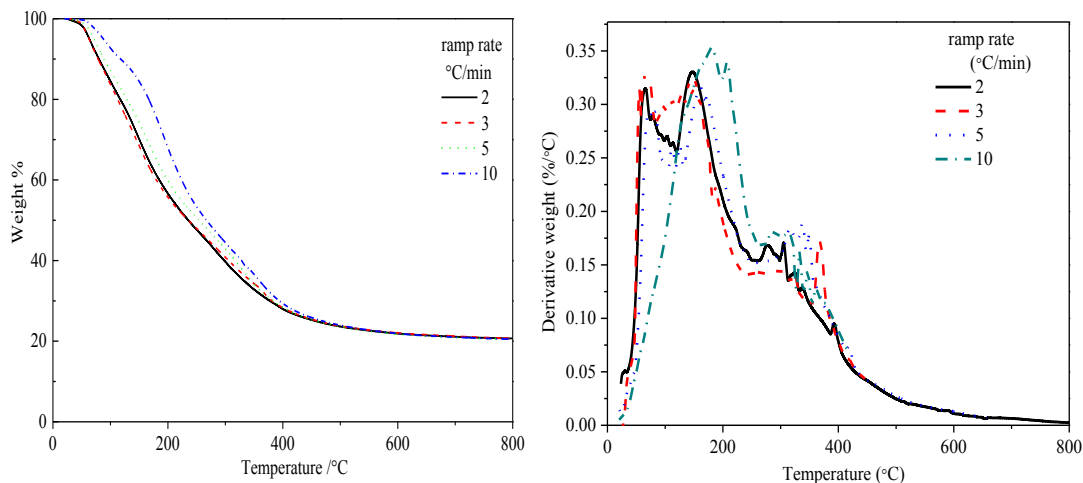


Figure 2.4 TGA and DTG plots for the ReCrude oil at different ramp rate in N₂ atmosphere

Three stages were observed in DTG plots. The first quick weight loss step included the removal of moisture and light hydrocarbons (aldehydes, carboxylic acid, and alcohols) in pyrolysis oil, with DTG_{max} shifting from 62 °C to 180 °C with increasing ramping rate. The quick weight loss at ~180 °C was due to the decomposition of thermally unstable compounds, for example glucose (Melligan, Dussan et al. 2012). The weight loss rate decreased significantly after 250 °C. In the second region broad peaks between 250 and 500 °C with DTG_{max} around 315 °C were found due to the breakup of inter-unit linkages of HMM lignin (Ba, Chaala et al. 2004) and evaporation of monomeric phenol units (Wörmeyer, Ingram et al. 2011). In the third stage, further heating to 800 °C only lead to 5 % weight loss.

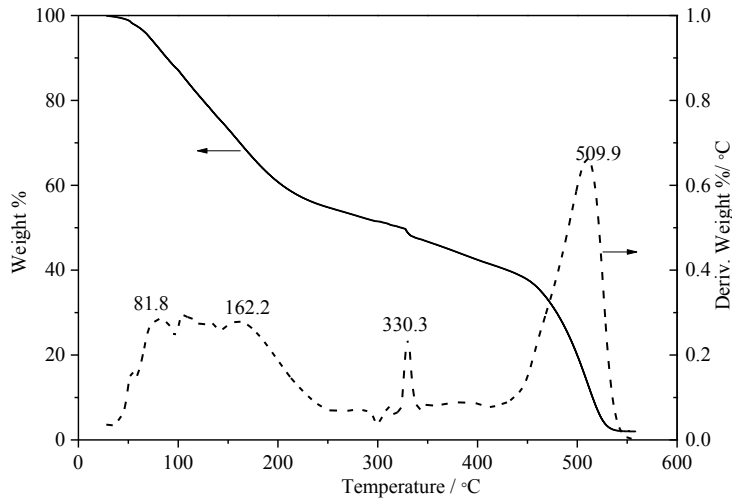


Figure 2.5 TGA and DTG plots for the ReCrude oil in air atmosphere.

As shown in Figure 2.5, three stages were also observed in TG and DTG plots for the combustion of the ReCrude oil in air atmosphere. In the first stage below 250 °C, similar weight loss behavior was observed as in nitrogen atmosphere. The second stage was from 250 °C to 450 °C during which combustion of HMM lignin and formation of carbon occurred. The combustion of carbon occurred at 510 °C and burned out at 540 °C. The ash content was 2 wt%.

The ignition temperature (Tognotti, Malotti et al. 1985, Crelling, Hippo et al. 1992) was an important parameter used to describe the combustion behavior of fuels. The air flowrate was kept 50 mL/min to avoid fluctuation in ignition and burnout performances caused by oxygen concentration. In this research, T_i was defined as the temperature at which TG curves in air and nitrogen diverge. From Figure 2.6, the T_i for the ReCrude oil was 175 °C.

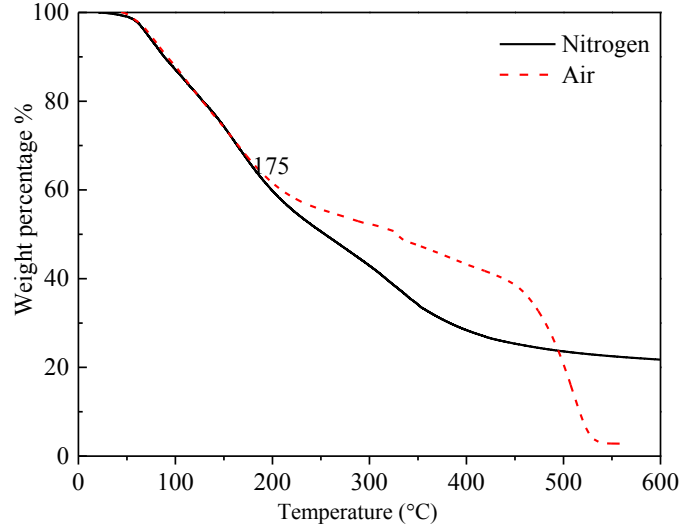


Figure 2.6 TG curves in nitrogen and air atmosphere

The decomposition kinetic parameters for the pyrolysis process can be measured by Coats-Redfern method (Coats and Redfern 1964). The kinetic equation can be described as

$$d\alpha / dt = K(T)f(\alpha) \quad (2.1)$$

$$K = A \exp\left(-\frac{E_a}{RT}\right) \quad (2.2)$$

$$\alpha = \frac{W_0 - W}{W_0 - W_\infty} \quad (2.3)$$

$$T = T_0 + \beta t \quad (2.4)$$

where α is the fraction of sample decomposed at time t . $f(\alpha)$ has many different forms according to the proposed reaction model (Vyazovkin and Wight 1997). W_0 and W_∞ represented the initial and final residual weight of the oil, respectively. K is the constant

of Arrhenius. E_a is the activation energy (J/mol). A is the frequency factor (s^{-1}). R is the universal constant of gas. T is the absolute temperature. β is the ramp rate.

$$\frac{d\alpha}{dT} = \frac{A}{\beta} \exp\left(-\frac{E_a}{RT}\right) f(\alpha) \quad (2.5)$$

Combining the above equations, rearranging and integrating, we get

$$\int_0^\alpha \frac{d\alpha}{f(\alpha)} = g(\alpha) = \frac{A}{\beta} \int_{T_0}^T e^{\left(-\frac{E_a}{RT}\right)} dT \quad (2.6)$$

For complex reactions, it takes risk in assuming the function $f(\alpha)$. The Model-Free Kinetics method (Vyazovkin and Wight 1999) applied an iso-conversion technique to calculate E_a as a function of α . Since for most values of E_a and for the general reaction temperature range the expression $\frac{E_a}{RT} \gg 1$ (Coats and Redfern 1964). Thus the

temperature integral on the right side can be approximated by

$$\frac{A}{\beta} \int_{T_0}^T e^{\left(-\frac{E_a}{RT}\right)} dT = \frac{A}{\beta} \cdot \frac{R}{E_a} T^2 e^{\left(-\frac{E_a}{RT}\right)} \quad (2.7)$$

Taking the natural logarithm operation, we can get

$$\ln\left(\frac{\beta}{T^2}\right) = \ln\left[\frac{AR}{g(\alpha)E_a}\right] - \frac{E_a}{RT} \quad (2.8)$$

The advantage of this equation is that $g(\alpha)$ is isolated into the linear coefficient. The activation energy E_a is a function of α and can be estimated even the function $f(\alpha)$ or $g(\alpha)$ are not given. Thus the plot of $\ln\left(\frac{\beta}{T^2}\right)$ against $1/T$ should result in a straight line

with slopes $-\frac{E_a}{R}$. The correlation coefficient was obtained by least-squares linear regression. Figure 2.7 displays the change of activation distribution with increasing fractional conversion. The value of E_a increased with the fractional conversion and a peak was observed at $\alpha = 0.7$. The final stage involved in decomposition of carbon which resulted in high values for E_a . An obvious increase was seen for $\alpha > 0.5$. The DTG plots indicated the increase in E_a was caused by the decomposition of HMM lignin. The increasing molecular weight resulted in an increase in E_a . Garcia et al. (Garcia-Perez, Wang et al. 2008) reported the E_a for the fraction of pyrolysis oil decomposed below 500 °C was in the range of 32.6-81.6 kJ/mol. The coherence of calculated results indicated the Model-Free Kinetics method can be used to estimate the E_a distribution of pyrolysis oil.

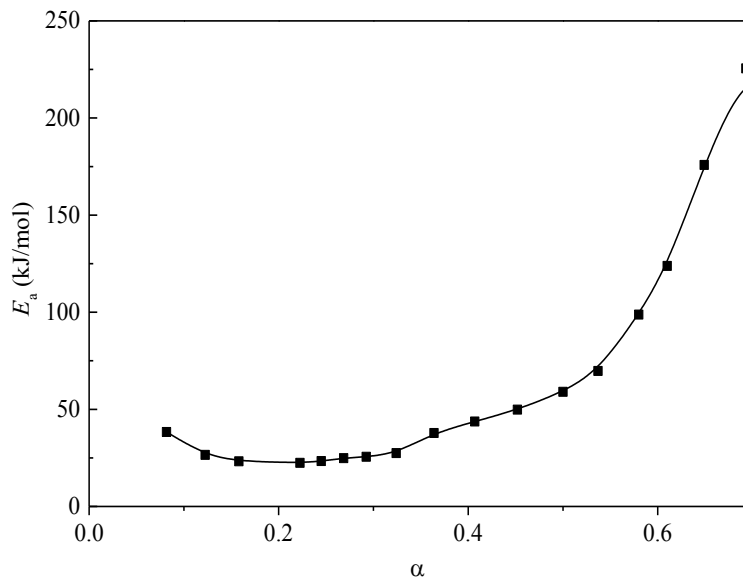


Figure 2.7 Activation energy versus fractional conversion for the pyrolysis of the ReCrude oil in nitrogen atmosphere

2.3.6 DSC

To better understand the effect of aging on the thermal behavior of aged oils, modulated DSC (MDSC) was performed on the crude oil. MDSC measures the difference in heat flow between a sample and a reference as both are subjected to a simultaneous linear and sinusoidal temperature program. MDSC offers all the benefits of conventional DSC while it simultaneously improves the sensitivity and resolution. Figure 2.8 shows the MDSC plots for the ReCrude oil. Two endothermic peaks were observed in the first heating process. No peaks were detected during the cooling process and the second heating-cooling loop. The two peaks were assigned to dehydration (Borde and Cesàro 2001, Yamaguchi, Sato et al. 2014) and decomposition of sugars in the pyrolysis oil (Wörmeyer, Ingram et al. 2011). MDSC can only separate signals which are truly reversible and the non-reversing signals which comes from an irreversible process. However, in this research, the non-reversing signal can also be the heat from the loss of water (dehydration), which is reversible in the sense that, with large-scale temperature changes, moisture can be reabsorbed. The glass transition was clearly observed from the reversible heat flow plot. The T_g for the HMM lignin was defined as the midpoint of the change and measured to be 110 °C which was in agreement with literature (Irvine 1985, Feldman, Banu et al. 2001).

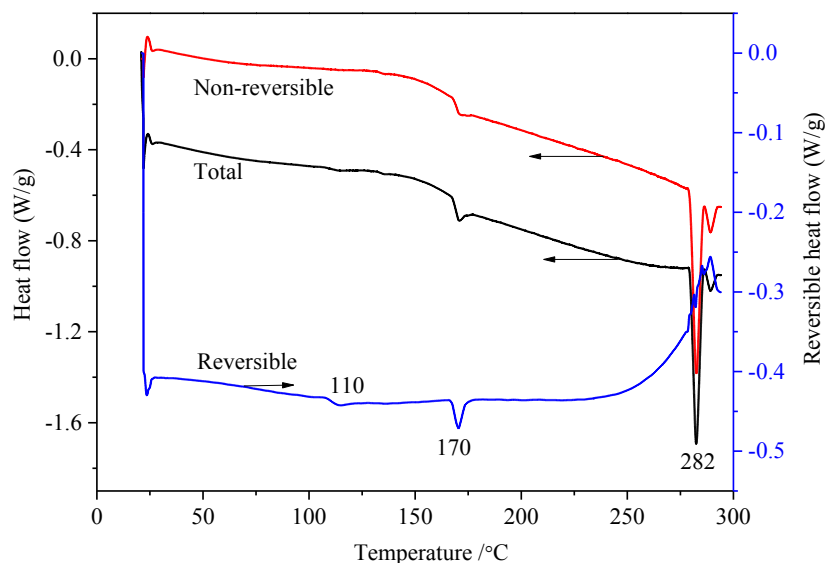


Figure 2.8 MDSC plots for the ReCrude oil

2.3.7 ATR-FTIR

The functional groups for the oil was identified by ATR-FTIR. Figure 2.9 shows the FTIR spectrum for the ReCrude oil. The broad band at $3000\text{-}3650\text{ cm}^{-1}$ assigned to hydroxyl groups indicated the presence of large amounts water, alcohols, phenols and acids. The bands at 2960, 2825 and 2860 were assigned to the C-H vibration of methyl and methylene groups. The adsorption bands from different components were superimposed heavily which made the interpretation of absorption bands in the fingerprint region below 1500 cm^{-1} difficult. The protonated carboxyl acid groups in solution were reported to absorb at $\sim 1740\text{ cm}^{-1}$ (Bociek and Welti 1975, Venyaminov and Kalnin 1990). It merged into the strong band at 1700 cm^{-1} caused by the carbonyl group in aldehydes, ketones, carboxylic acids, and esters (Scholze and Meier 2001). The conjugated C=O stretch was overlapped with the unconjugated C=O stretch. The

carboxylate groups absorbed at $\sim 1600\text{ cm}^{-1}$ and was overlapped with the aromatic skeletal vibration. The bands at 1600 , 1510 and 1440 cm^{-1} corresponding to aromatic ring vibrations. The strongest band at 1200 cm^{-1} was assigned to C-O stretch, C-C stretch and C=O stretch. The C=O bands can be used to monitor the esterification during oil storage.

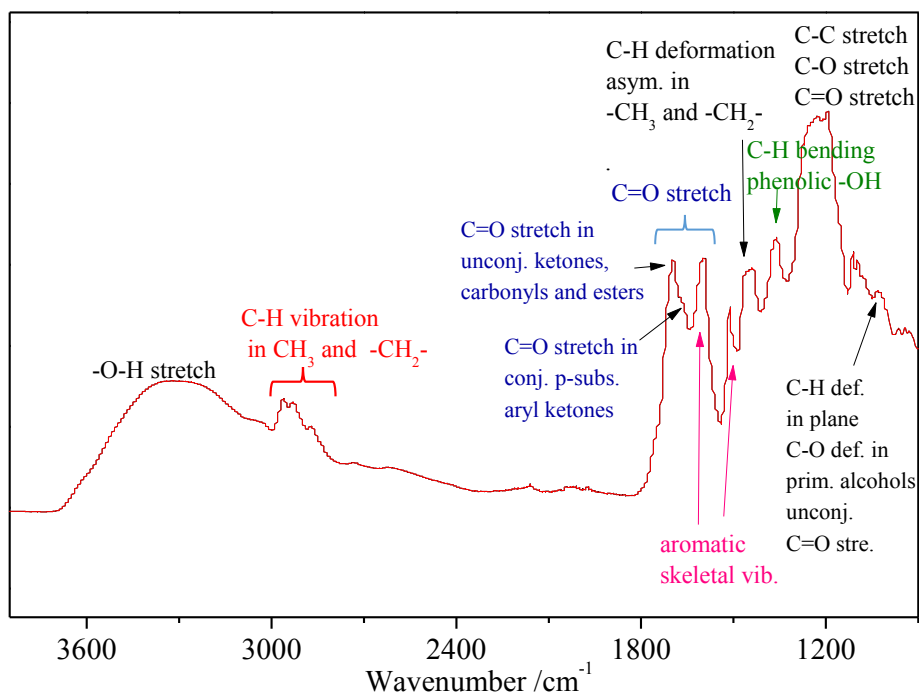


Figure 2.9 FTIR spectrum for the ReCrude oil

2.3.8 GC-MS

The chemical composition of the CH₂Cl₂ soluble fraction of the ReCrude oil was investigated by GC-MS. Due to the extreme complexity of pyrolysis oils, the GC analysis can only detect 40 wt% of the oil (Scholze and Meier 2001). Figure 2.10 showed the GC-MS chromatogram for the pyrolysis oil with ethyl acetate as the solvent. Peak

identification and area percentage were given in Table 2.2. The CH₂Cl₂ soluble fraction were mainly composed of phenols, benzenediols and their derivatives.

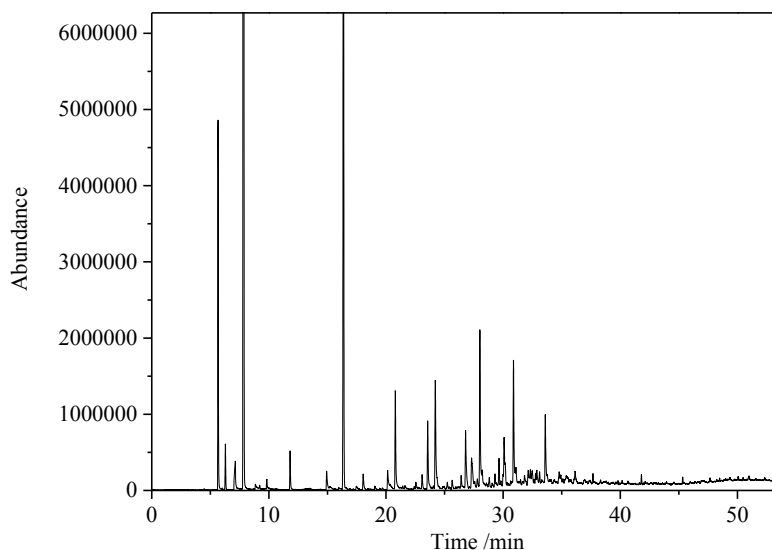


Figure 2.10 GC-MS chromatogram for the ReCrude oil tested in ethyl acetate

Table 2.2 Composition of the ReCrude oil tested in ethyl acetate

Time/min	Area%	Compound
6.2862	0.6674	methylene chloride
7.8183	68.7536	ethyl acetate
11.8127	0.629	methyl isobutyl ketone
16.362	16.3592	benzene, chloro-
20.7941	1.8566	phenol
23.5574	1.2383	phenol, 2-methyl-
24.21	2.5545	phenol, 4-methyl-
26.7974	1.4211	phenol, 2,4-dimethyl-
28.0168	2.7433	1,2-Benzenediol
30.0804	0.522	1,2-Benzenediol, 3-methyl-
30.8855	2.0263	1,2-Benzenediol, 4-methyl-
33.598	1.2287	1,3-Benzenediol, 4-ethyl-

While few compounds were identified with ethyl acetate due to its low solubility toward the oil, the more polar CH_2Cl_2 was used as the solvent. Figure 2.11 displays the GC-MS spectrum obtained in CH_2Cl_2 . Chlorobenzene was found at 10.58 min. Most of the peaks showed no obvious tailing. Table 2.3 shows the peak identification and area percentage for each compound. Phenols, benzenediols and their derivatives were the main compounds. Phenanthrene was found while it cannot be identified with ethyl acetate. The poor elution properties of acids resulted in a strong tailing. Sugar derivatives were not detected in the CH_2Cl_2 soluble fraction.

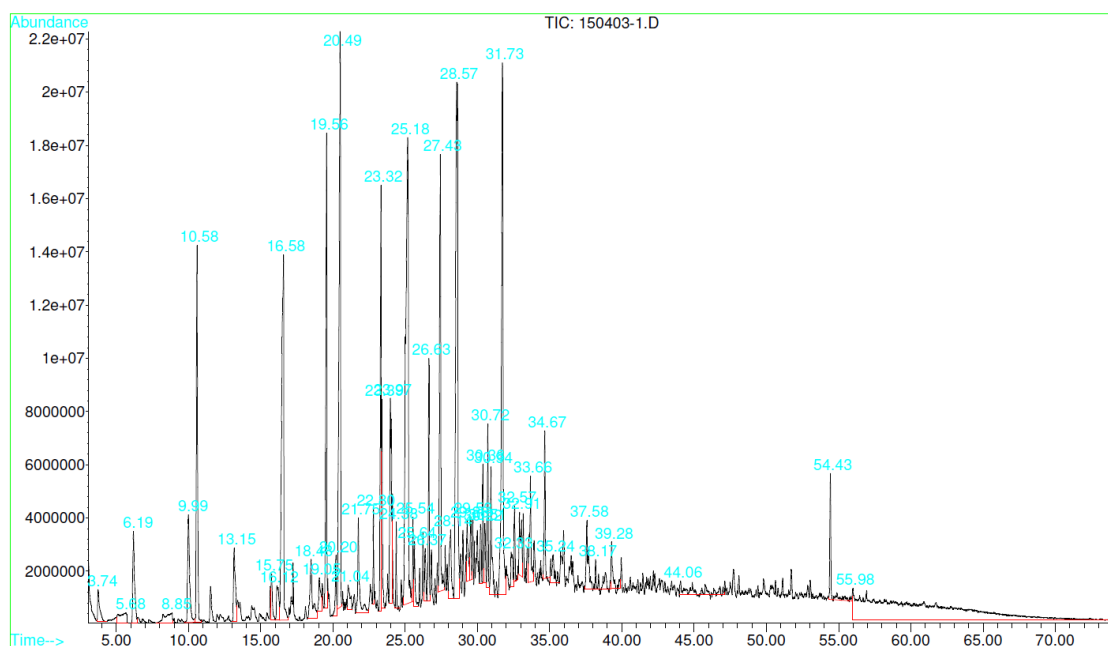


Figure 2.11 GC-MS chromatogram for the ReCrude oil in CH_2Cl_2

Table 2.3 Composition of the ReCrude oil tested in CH₂Cl₂

Time/min	Area %	Compound	Structure
3.74	0.5	2-propanone, 1-hydroxy-	
5.68	0.55	propanoic acid	
6.19	1.28	methyl isobutyl ketone	
8.75	0.57	butanoic acid	
9.99	1.65	furfural	
13.15	1.04	2-cyclopenten-1-one	
16.58	5.83	phenol	
18.48	1.15	2-cyclopenten-1-one, 2-hydroxy-3-methyl-	
19.56	3.66	phenol, 2-methyl-	
20.49	6.72	phenol, 4-methyl-	
21.75	1.16	phenol, 2,3-dimethyl-	
22.8	0.51	phenol, 2-ethyl-	
23.32	3.21	phenol, 3,5-dimethyl-	
23.39	1.03	phenol, 2,3-dimethyl-	
23.97	2.51	phenol, 4-ethyl-	
25.18	9.33	1,2-benzenediol	
26.63	1.58	phenol, 2-ethyl-5-methyl-	
27.43	4.06	1,2-benzenediol, 3-methyl-	
28.14	1.05	benzene, 1,4-dimethoxy-2-methyl-	
28.57	8.64	1,2-benzenediol, 4-methyl-	
29.28	0.69	2-methoxybenzyl alcohol	
30.72	1.16	1,3-benzenediol, 4,5-dimethyl-	
31.73	6.54	1,3-benzenediol, 4-ethyl-	
32.91	1.05	2-allyl-4-methylphenol	
33.66	1.24	phenol, 4-ethyl-2-methoxy-	
34.67	1.09	1,3-benzenediol, 4-propyl-	
37.58	1.13	benzamide, 2-(methylamino)-	
39.28	0.6	1-naphthalenol,2-methyl-	
54.43	1.16	phenanthrene,1-methyl-7-(1-methylethyl)-	

2.3.9 Comparison of LMM lignin and HMM lignin

Dichloromethane (DCM) was utilized to divide the oil (Oasmaa, Kuoppala et al. 2010) into a DCM soluble (low-molecular-mass, LMM lignin and other extractives, defined as LMM fraction) and DCM-insoluble (mainly high molecular mass lignin, defined as HMM lignin). Figure 2.12 showed the FTIR spectra for the LMM fraction and the HMM lignin, respectively. The band at 1700 assigned to the unconjugated C=O was much stronger for the LMM fraction indicating most of the aldehydes, ketones, carboxylic acids, and esters were contained in the LMM lignin. Gel permeation chromatography (GPC) plots in Figure 2.13 confirmed the LMM fraction mainly contained low molecular weight compounds. GPC plots also indicated the DCM extraction process cannot thoroughly separate the HMM lignin and the LMM fraction. CH₂Cl₂ is not powerful enough to break the hydrogen bonding between the low molecular weight polar compounds and lignin.

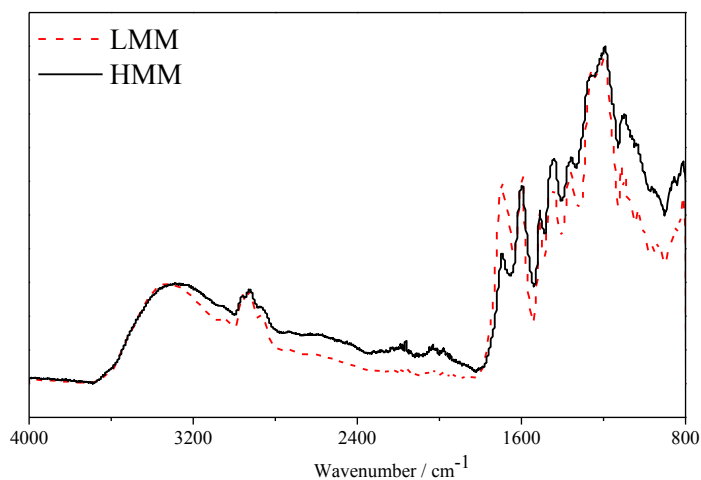


Figure 2.12 FTIR spectra for the LMM fraction and the HMM lignin

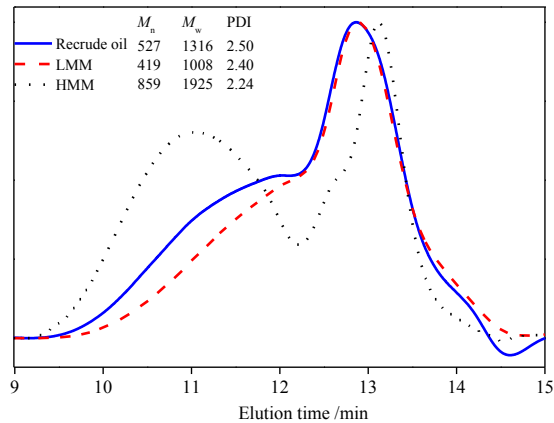


Figure 2.13 GPC plots for the ReCrude oil, LMM fraction and HMM lignin

The thermal behaviors were investigated by DSC and TGA. As shown in Figure 2.15, the DSC plots for both the LMM fraction and the HMM lignin exhibited two negative peaks which can only be detected in the first heating process. The two peaks were assigned to dehydration and decomposition of sugars, respectively. The lower concentration of sugars in the HMM lignin resulted in the lower dehydration temperature and decomposition temperature for the sugar compounds.

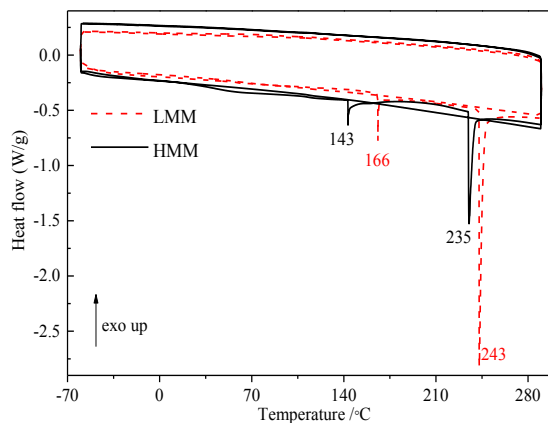


Figure 2.14 DSC plots for the LMM fraction and the HMM lignin

The combustion behavior for the LMM fraction and the HMM lignin were investigated by TG in air atmosphere. Figure 2.15 shows the TG and DTG plots for the LMM fraction and the HMM lignin. Both of them showed three stage combustion processes. The combustion behavior for the LMM fraction was similar to the ReCrude oil. However, new peaks at 436 °C and 447 °C were observed for the HMM lignin. These peaks were also found in the DTG plots (Figure 2.16) for the HMM lignin in nitrogen atmosphere. In the weight loss vs. temperature plot, it was evident that the event was accompanied by a sudden loss of a certain fraction of the sample at 422 °C. A very strong exothermic peak was also observed in the DTA. The peaks can only be assigned to combustion. When the pyrolysis oil was heated, numerous radicals were obtained as a result of thermal cleavage. These radicals can be stabilized by protons provided from low molecular weight compounds in pyrolysis oil, i.e., acids, phenols or alcohols (Saisu, Sato et al. 2003). However, when heated to 400 °C in the absence of these solvents, the HMM lignin began burn and rapidly released large amount of heat, resulting in a sharp increase in temperature.

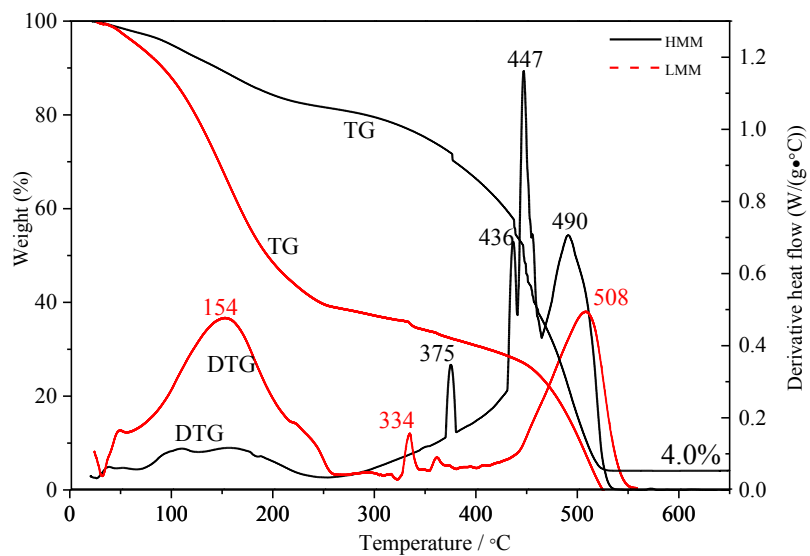


Figure 2.15 TGA and DTG plots for the LMM lignin and the HMM lignin in air atmosphere

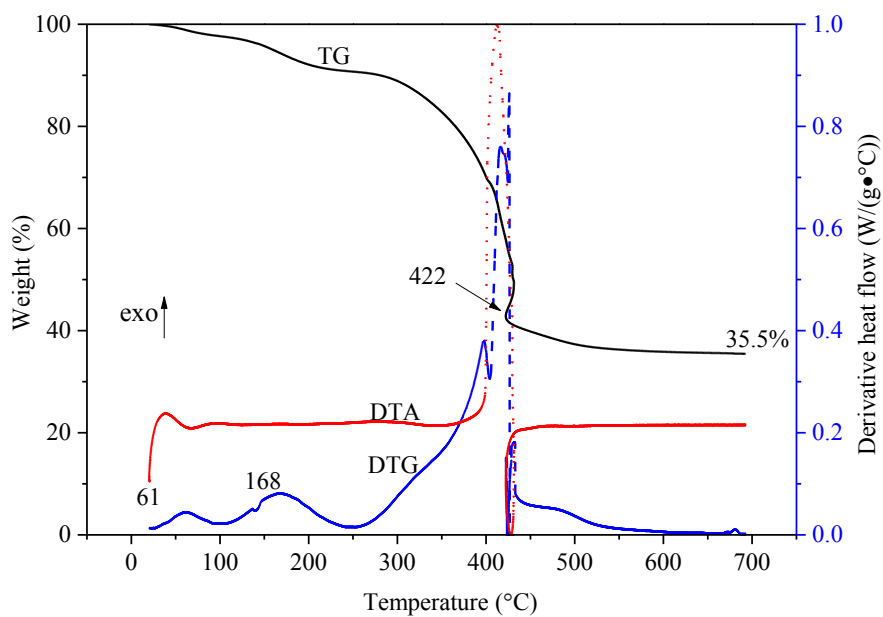


Figure 2.16 TGA and DTG plots for the HMM lignin in nitrogen atmosphere

2.4 Conclusion

The ReCrude oil was water insoluble. The water concentration was 4.77 wt%, significantly lower than those reported in literature for other pyrolysis oils. The solids content was measured to be 3.3 wt% using a mixture of methanol and dichloromethane (50:50 v/v) as the solvent. The HMM lignin content was 33 wt%, slightly higher than the reported value 25-30 wt%, and the ash content was 0.12 wt%. Three stages behavior were observed for both the pyrolysis in nitrogen and combustion in air. The ignition temperature T_i for the ReCrude oil was 175 °C. The T_g for the HMM lignin was 110 °C. The activation energy increased with increasing fractional conversion. The significant increase after $\alpha > 0.5$ was caused by the decomposition of HMM lignin. The increasing molecular weight resulted in an increase in E_a . The dehydration and decomposition of sugars were observed during the heating process.

The ReCrude oil was divided into two fraction by CH_2Cl_2 extraction. However, both GPC curves and TG plots indicated the process cannot thoroughly separate the HMM lignin and the LMM fraction. The LMM fraction mainly contained low molecular weight compounds, such as phenols, benzenediols and their derivatives. Phenanthrene was found while it cannot be identified with ethyl acetate. The HMM lignin showed a unique combustion behavior caused by radicals obtained by thermal cleavage of chains during heat treatment. Generally, the ReCrude oil was not thermodynamically and chemically stable. A further upgrading is required before it can be used as a transportation fuel.

2.5 References

- Adkins, B., D. Stamires, R. Bartek, M. Brady and J. Hackskaylo (2013). Catalyst for thermocatalytic conversion of biomass to liquid fuels and chemicals, Google Patents.
- Ba, T., A. Chaala, M. Garcia-Perez, D. Rodrigue and C. Roy (2004). "Colloidal Properties of Bio-oils Obtained by Vacuum Pyrolysis of Softwood Bark. Characterization of Water-Soluble and Water-Insoluble Fractions." Energy & Fuels **18**(3): 704-712.
- Bartek, R., M. Brady and D. Stamires (2011). Catalytic hydrolysis of organophilic biomass, Google Patents.
- Bartek, R., R. L. Cordle, S. Yanik and P. O'Connor (2012). Catalyst/biomass mixing in transport reactor, Google Patents.
- Bociek, S. M. and D. Welti (1975). "The quantitative analysis of uronic acid polymers by infrared spectroscopy." Carbohydrate Research **42**(2): 217-226.
- Borde, B. and A. Cesàro (2001). "A DSC Study of Hydrated Sugar Alcohols. Isomalt." Journal of Thermal Analysis and Calorimetry **66**(1): 179-195.
- Bridgwater, A. V. (2012). "Review of fast pyrolysis of biomass and product upgrading." Biomass and Bioenergy **38**(0): 68-94.
- Coats, A. W. and J. P. Redfern (1964). "Kinetic Parameters from Thermogravimetric Data." Nature **201**(4914): 68-69.
- Crelling, J. C., E. J. Hippo, B. A. Woerner and D. P. West Jr (1992). "Combustion characteristics of selected whole coals and macerals." Fuel **71**(2): 151-158.
- Czernik, S. and A. V. Bridgwater (2004). "Overview of Applications of Biomass Fast Pyrolysis Oil." Energy & Fuels **18**(2): 590-598.
- Eide, I., K. Zahlens, H. Kummernes and G. Neverdal (2006). "Identification and Quantification of Surfactants in Oil Using the Novel Method for Chemical Fingerprinting Based on Electrospray Mass Spectrometry and Chemometrics." Energy & Fuels **20**(3): 1161-1164.
- Elliott, D. C., A. Oasmaa, D. Meier, F. Preto and A. V. Bridgwater (2012). "Results of the IEA Round Robin on Viscosity and Aging of Fast Pyrolysis Bio-oils: Long-Term Tests and Repeatability." Energy & Fuels **26**(12): 7362-7366.

- Feldman, D., D. Banu, J. Campanelli and H. Zhu (2001). "Blends of vinylic copolymer with plasticized lignin: Thermal and mechanical properties." Journal of Applied Polymer Science **81**(4): 861-874.
- French, R. and S. Czernik (2010). "Catalytic pyrolysis of biomass for biofuels production." Fuel Processing Technology **91**(1): 25-32.
- Garcia-Perez, M., S. Wang, J. Shen, M. Rhodes, W. J. Lee and C.-Z. Li (2008). "Effects of Temperature on the Formation of Lignin-Derived Oligomers during the Fast Pyrolysis of Mallee Woody Biomass." Energy & Fuels **22**(3): 2022-2032.
- HLAVÁČ, M. B. a. P. (2013). "Thermophysical and rheologic properties of biooil samples." Journal of Central European Agriculture **14**(3): 1132-1143.
- Irvine, G. M. (1985). "The significance of the glass transition of lignin in thermomechanical pulping." Wood Science and Technology **19**(2): 139-149.
- Jiang, X. and N. Ellis (2010). "Upgrading Bio-oil through Emulsification with Biodiesel: Mixture Production." Energy & Fuels **24**(2): 1358-1364.
- Kang, B.-S., K. H. Lee, H. J. Park, Y.-K. Park and J.-S. Kim (2006). "Fast pyrolysis of radiata pine in a bench scale plant with a fluidized bed: Influence of a char separation system and reaction conditions on the production of bio-oil." Journal of Analytical and Applied Pyrolysis **76**(1-2): 32-37.
- Kim, S.-J., S.-H. Jung and J.-S. Kim (2010). "Fast pyrolysis of palm kernel shells: Influence of operation parameters on the bio-oil yield and the yield of phenol and phenolic compounds." Bioresource Technology **101**(23): 9294-9300.
- Melligan, F., K. Dussan, R. Aucaise, E. H. Novotny, J. J. Leahy, M. H. B. Hayes and W. Kwapinski (2012). "Characterisation of the products from pyrolysis of residues after acid hydrolysis of Miscanthus." Bioresource Technology **108**(0): 258-263.
- Oasmaa, A., E. Kuoppala, A. Ardiyanti, R. H. Venderbosch and H. J. Heeres (2010). "Characterization of Hydrotreated Fast Pyrolysis Liquids." Energy & Fuels **24**(9): 5264-5272.
- Oasmaa, A., E. Kuoppala and Y. Solantausta (2003). "Fast Pyrolysis of Forestry Residue. 2. Physicochemical Composition of Product Liquid." Energy & Fuels **17**(2): 433-443.
- Oasmaa, A. and D. Meier (2005). "Norms and standards for fast pyrolysis liquids: 1. Round robin test." Journal of Analytical and Applied Pyrolysis **73**(2): 323-334.
- Oasmaa, A., C. Peacocke, S. Gust, D. Meier and R. McLellan (2005). "Norms and Standards for Pyrolysis Liquids. End-User Requirements and Specifications." Energy & Fuels **19**(5): 2155-2163.

- Peacocke, G. V. C., P. A. Russell, J. D. Jenkins and A. V. Bridgwater (1994). "Physical properties of flash pyrolysis liquids." Biomass and Bioenergy **7**(1–6): 169-177.
- Saisu, M., T. Sato, M. Watanabe, T. Adschiri and K. Arai (2003). "Conversion of Lignin with Supercritical Water–Phenol Mixtures." Energy & Fuels **17**(4): 922-928.
- Scholze, B. and D. Meier (2001). "Characterization of the water-insoluble fraction from pyrolysis oil (pyrolytic lignin). Part I. PY–GC/MS, FTIR, and functional groups." Journal of Analytical and Applied Pyrolysis **60**(1): 41-54.
- Shihadeh, A. and S. Hochgreb (2002). "Impact of Biomass Pyrolysis Oil Process Conditions on Ignition Delay in Compression Ignition Engines." Energy & Fuels **16**(3): 552-561.
- Tognotti, L., A. Malotti, L. Petarca and S. Zanelli (1985). "Measurement of Ignition Temperature of Coal Particles Using a Thermogravimetric Technique." Combustion Science and Technology **44**(1-2): 15-28.
- Venyaminov, S. Y. and N. N. Kalnin (1990). "Quantitative IR spectrophotometry of peptide compounds in water (H₂O) solutions. I. Spectral parameters of amino acid residue absorption bands." Biopolymers **30**(13-14): 1243-1257.
- Vyazovkin, S. and C. A. Wight (1997). "KINETICS IN SOLIDS." Annual Review of Physical Chemistry **48**(1): 125-149.
- Vyazovkin, S. and C. A. Wight (1999). "Model-free and model-fitting approaches to kinetic analysis of isothermal and nonisothermal data." Thermochemica Acta **340–341**(0): 53-68.
- Wörmeyer, K., T. Ingram, B. Saake, G. Brunner and I. Smirnova (2011). "Comparison of different pretreatment methods for lignocellulosic materials. Part II: Influence of pretreatment on the properties of rye straw lignin." Bioresource Technology **102**(5): 4157-4164.
- Yamaguchi, A., O. Sato, N. Mimura and M. Shirai (2014). "Intramolecular dehydration of mannitol in high-temperature liquid water without acid catalysts." RSC Advances **4**(85): 45575-45578.

CHAPTER III
IMPACTS OF THERMAL PROCESSING ON THE PHYSICAL AND CHEMICAL
PROPERTIES OF PYROLYSIS OIL

3.1 Introduction

Fossil fuels have been playing a dominant role in the world energy consumption. However, the rapid consumption has been a challenge for its non-renewability and environmental issues. The development of renewable energy becomes of increasing importance. Pyrolysis oil, also known as bio-oil, is usually produced from fast pyrolysis of biomass feedstock when a sample is rapidly heated to 400-600 °C in a non-oxidizing environment during a short residence time. Pyrolysis oil is a promising alternative energy source, causing no greenhouse gas emission and is sustainable. In the past decades, there has been a large number of publications (Czernik and Bridgwater 2004, Mohan, Pittman et al. 2006, Elliott 2007, Mortensen, Grunwaldt et al. 2011, Bridgwater 2012, Zacher, Olarte et al. 2014) on biomass-based pyrolysis oil.

Crude pyrolysis oil is a complex mixture of a large number of compounds that can be broadly classified into volatile organic compounds (hydroxyacetaldehyde, formic acid, acetic acid), furanic compounds, monophenols, sugars (fermentable and cross-linked), lignin oligomers and water (Ed and Thomas 1988, Piskorz, Scott et al. 1988, Garcia-Pérez, Chaala et al. 2005). The raw pyrolysis oil suffer many deleterious properties such as high water content, high oxygen content, high viscosity, high ash/solids content and

immiscibility with hydrocarbon liquids. The major issue with pyrolysis oil, since it is not a product of thermodynamic equilibrium as a result of rapid quench, is that the components will react until equilibrium is reached (Lu, Yang et al. 2008). All these drawbacks indicate that a substantially physical and chemical improvement in pyrolysis oil quality is necessary before it can be used as a transportation fuel.

A number of physical and chemical pyrolysis oil upgrading technologies, such as filtration (Isahak et al., 2012; Hoekstra, 2009; Diebold, 2000), solvent addition (Oasmaa, 2004; Diebold, 1997), catalytic cracking (Vitolo, Seggiani et al. 1999, Zhang, Chang et al. 2006), hydrotreating (Elliott 2007, Xiu and Shahbazi, 2012; Nava et al., 2009), steam reforming (Chiaramonti, Bonini et al. 2003, Takanabe, Aika et al. 2004, Rioche, Kulkarni et al. 2005) etc. have been used. The chemically upgraded pyrolysis oils generally show better stabilities. Catalytic hydrotreatment with heterogeneous catalysts at high temperature and pressure (eg. 500 °C, 300 bars) has been identified as a very promising way to improve the properties of pyrolysis liquids and make them suitable as a refinery feed (Elliott 2007, Venderbosch, Ardiyanti et al. 2010). However, the decarboxylation and re-polymerization occur relatively faster than the hydrogenation at temperatures above 200 °C (Elliott 2007, De Miguel Mercader, Koehorst et al. 2011) which can cause blockage of the reactor and deactivation of the upgrading catalysts. Understanding how and why these reactions—including polymerization—occur in pyrolysis oil is important to design treatments to stabilize or transform pyrolysis oil before further upgrade.

Heat treatment has been applied to determine the exact chemical reactions and determine if a standard procedure can be used to mitigate or even prevent aging reactions. Heat-induced physical and chemical changes in pyrolysis oils are usually investigated in

studies using carefully sealed samples to simulate the aging process during storage. (Diebold and Czernik 1997, Boucher, Chaala et al. 2000, Ba, Chaala et al. 2004). Czernik et al. (Czernik, Johnson et al. 1994) concluded the reactions over the temperature range of 37-90 °C were quite similar—equivalent viscosities are obtained in oak pyrolysis oil after 3 months of aging at 37 °C, 4 days of aging at 60 °C, or 6 h of aging at 90 °C. It is advised to use a sealed sample of pyrolysis oil held at 80 °C (Oasmaa and Meier 2005, Elliott, Oasmaa et al. 2012) as a typical accelerated aging test.

These existing knowledge significantly broaden and deepen our understanding about the polymerization or stabilization of pyrolysis oils. However, the process was carried out in a low temperature range (below 90 °C). Moreover, even the low temperature hydrotreatment occurs at around 200 °C. To our knowledge, no report has investigated the applicable temperature range for this accelerated aging method. This study investigated the physical and chemical changes for oils aged in a broad temperature range (40-290 °C) in pressure reactors. The understanding of how and why the polymerization of pyrolysis oil occurs is important to plan for any possible measures to stabilize or transform pyrolysis oils before its further upgrading.

3.2 Experimental

The water content and high molecular mass (HMM) lignin content were measured by the same method used in Chapter 2. The parameters for TGA, DSC, ATR-FTIR and GC-MS characterization process were the same with those in Chapter 2.

3.2.1 Heat treatment of the oil

Pyrolysis oils were directly obtained from KiOR, Inc. Heat-treated oil samples were prepared by heating portions (~ 10 mL) in sealed stainless steel tubes for different time at 40, 60, 80, 150, 200 and 290 °C, respectively. A 1/2 inch stainless steel tube was used as a container for pyrolysis oil and was heated in an oven. A ~10% space was left in the upper part of the tube. The samples were then allowed to cool to room temperature, transferred to glass vials and stored at 2.5 °C until testing.

3.2.2 Viscosity

Viscosity tests were carried out on a Brookfield DV-I+ viscometer with 5 rpm at room temperature. The spindle #64 was used.

3.3 Results and discussion

3.3.1 Water content for aged oils

The fresh water insoluble pyrolysis oil is highly viscous black liquid. The ReCrude oil water content was $4.77 \pm 0.27\%$, significantly lower than that reported value in literature (Oasmaa and Czernik 1999, Oasmaa, Kuoppala et al. 2003, Oasmaa and Kuoppala 2008, Smets, Adriaensens et al. 2011). Figure 3.1 shows the water content change with increasing aging time at different temperatures. The water concentration in the oil increased with the length of storage. Slight increases were observed for oils stored below 80 °C even after extended storage time. Higher storage temperatures resulted in greater increases in water content. All aged oils are homogeneous indicating pyrolysis oils can tolerate the increase of water. The water content reached 11.8 wt% when stored for 150 minutes at 290 °C which was higher than those aged for tens of days at

temperatures below 200 °C. During “aging” process, several kinds of reactions occur—etherification, esterification, condensation or polymerization, decomposition of sugars (fermentable and cross-linked) yield water while hydration consumes water. The water content was a result of competition between the two kinds for reactions. The water content change indicated high temperature and short time favored the water formation reactions.

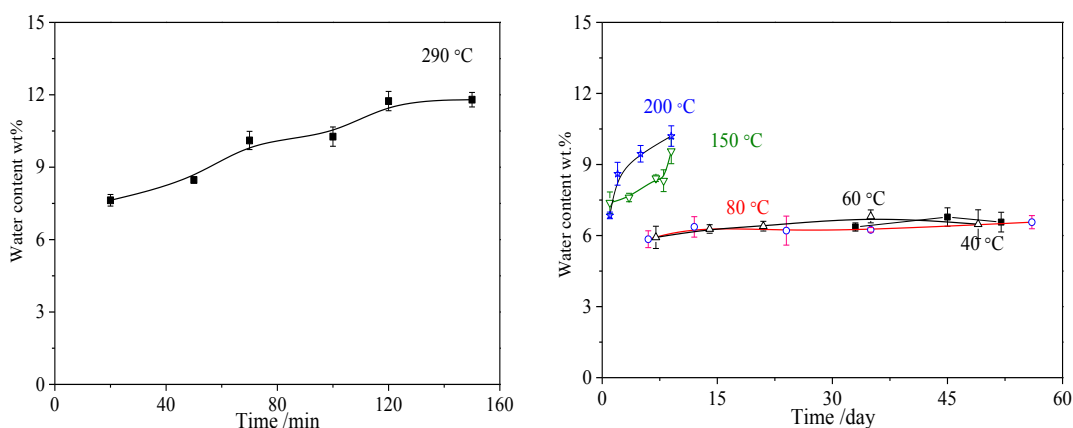


Figure 3.1 Water content vs aging time plots for pyrolysis oils aged at different temperatures.

3.3.2 HMM lignin content

HMM Lignin has been reported to be a major reason for the instability of pyrolysis oil (Scholze and Meier 2001). Most of the HMM lignin is not distillable which makes it not suitable for combustion in gasoline engines. The high molecular weight also hinders its usage in spray combustors. Lignin’s structure is a complex macromolecule with a great variety of functional groups and more than ten different types of linkages. Pyrolytic lignin has a peculiar structure compared to native and industrial lignin in its

unsaturated structure which often leads to apparent differences in properties (Scholze and Meier 2001, Eide, Zahlens et al. 2006). Figure 3.2 shows a typical structure of pyrolytic lignin (Bayerbach and Meier 2009). Polymerizations of low molecular weight component to the reactive sites, such as phenolic –OH, aliphatic –OH and double bonds could occur during aging process (Kim, Kim et al. 2012).

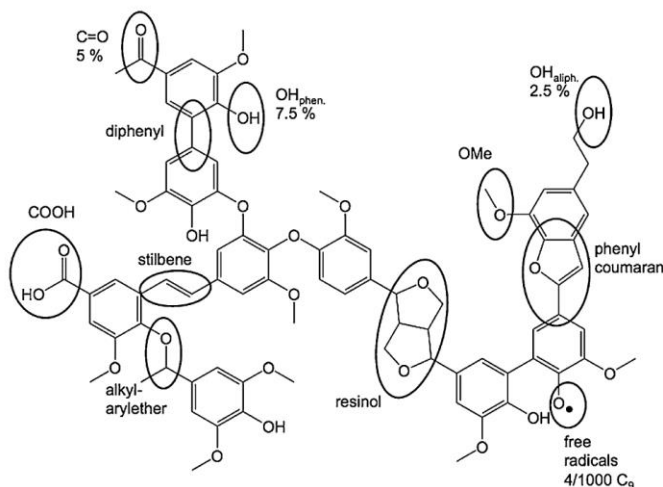


Figure 3.2 A typical structure of pyrolytic lignin (Bayerbach and Meier 2009).

As shown in Figure 3.3, obvious increases in HMM lignin content were observed for oils aged above 60 °C while very slight changes were observed for oils aged at 40 °C. Higher temperatures resulted in higher increase rates for HMM lignin content. The HMM lignin content was over 90 wt% for oils aged at 200 °C for 9 days and oils became solidified.

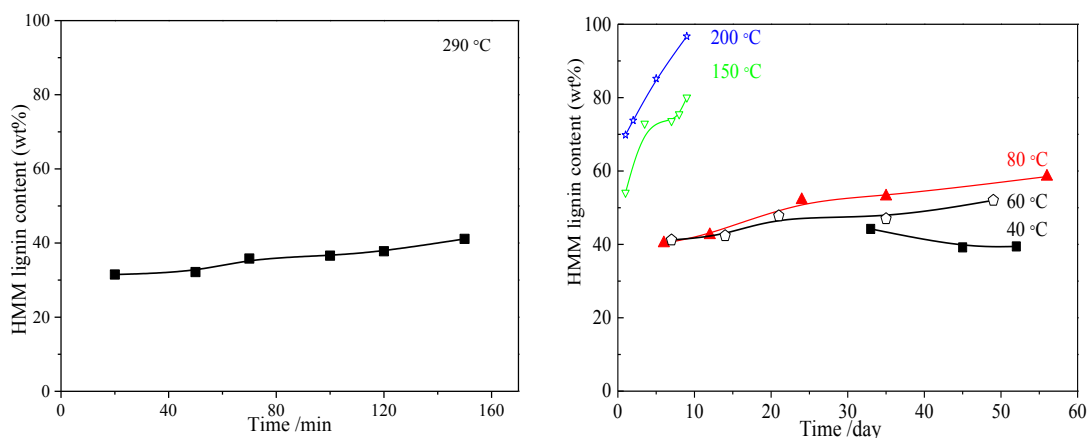


Figure 3.3 HMM lignin content vs aging time plots for pyrolysis oils aged at different temperatures.

3.3.3 Viscosity

The viscosity measurements for the fresh and aged samples are carried out at 40 °C. The reason for using a low temperature in viscosity tests was to avoid evaporation of volatile compounds. The reported viscosities for water soluble pyrolysis oils or the total oils were 200-300 cP at 40 °C (Oasmaa and Meier 2005, Oasmaa, Peacocke et al. 2005, Oasmaa, Kuoppala et al. 2010, Lehto, Oasmaa et al. 2014) while the viscosity for the water insoluble fraction of oak wood pyrolysis oil was reported as high as 50,000 cP (Vispute 2011). The high viscosity for the ReCrude oil can be explained by its high HMM lignin content and average molecular weight.

All oils aged above 150 °C were not tested because their viscosities were beyond the instrument limit. Figure 3.4 shows the relationship of viscosity and time for oils aged at 80, 60 and 40 °C, respectively. The high temperature led to a high increase in viscosity. Slight increase was observed for oils aged at 40 °C. Viscosities for oils aged at 60 and 80 °C showed tend to linearly increased within 49 and 35 days, respectively. An obvious deviation to high viscosity was observed for oils aged 80 °C after 35 days. The

existence of a network formed waxy materials (e.g., fatty acids, fatty alcohols, sterols, aliphatic hydrocarbons) and heavy compounds played an important role in the forming long-range network structures (García-Pérez, Chaala et al. 2005). The stronger interactions in the aged oils may lead to the significant increase in viscosity.

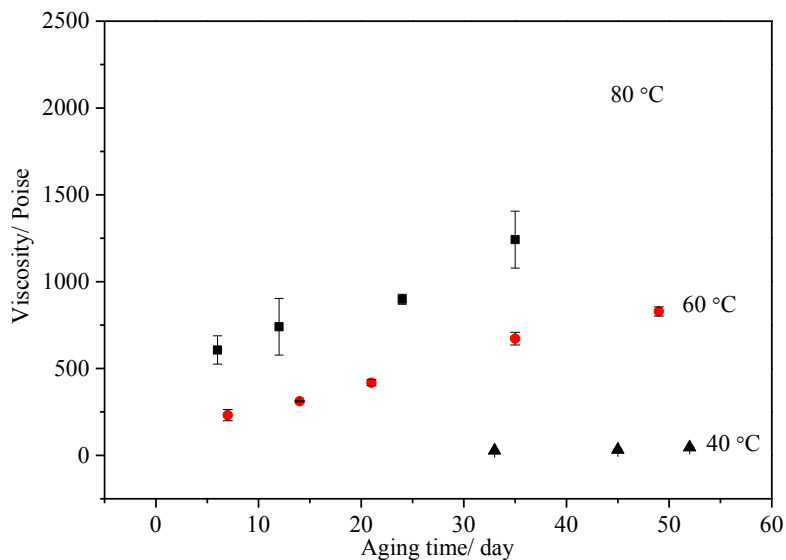


Figure 3.4 Viscosity plots for pyrolysis oils aged at different temperatures.

3.3.4 TGA

Thermogravimetric analysis was used to determine the oil thermal stability and its fraction of volatile components by monitoring the weight change that occurs as a specimen is heated. The maximum temperature was set to be 800 °C, so that the specimen weight was stable at the end of the test, implying that all chemical reactions were completed. Figure 3.5 shows the TG and DTG plots for fresh and aged oils at different temperatures. The maximum weight loss peak shifted to high temperatures with increases in aging time and temperature. The loss in mass of untreated oil began at a low

temperature, with mass maxima ~ 65 °C for the loss of easily volatile compounds. Most of light compounds and water were evaporated below 120 °C. These evaporations were clearly observed for oils aged below 80 °C and oils aged at 290 °C within 50 minutes. Dehydration of sugar compounds occurred at ~ 140 °C (Borde and Cesàro 2001, Yamaguchi, Sato et al. 2014). The decreasing intensity with time and temperature for peaks at 180-220 °C assigned to decomposition of sugar derivatives (Melligan, Dussan et al. 2012) indicating these compounds were unstable under the aging conditions. The pyrolytic lignin degradation in the temperature range 350-425 °C involves fragmentation of inter-unit linkages, releasing monomeric compounds such as phenols (Ba, Chaala et al. 2004, Tejado, Peña et al. 2007). In the temperature range above 500 °C the process was related to the decomposition of some aromatic rings (El-Saied and Nada 1993). The TGA curves suggest a significant increase in the pyrolysis oil thermal decomposition temperature after the heat treatment. The residues percentage increased with the aging time.

The peak of the DTG curve (DTG_{max}) can be used to compare thermal stability characteristics of oils. The DTG_{max} in low temperature range showed an obvious increase with the increase in aging time. Sun et al. (Sun, Tomkinson et al. 2000) reported that the thermal stability of the lignins increased with increasing molecular weight. This may reflect an increased degree of branching and condensation from oils aged for longer time. In addition, the non-volatile residue at 800 °C increased with increasing aging time, which may also be explained in terms of differences in degree of branching and condensation reactions.

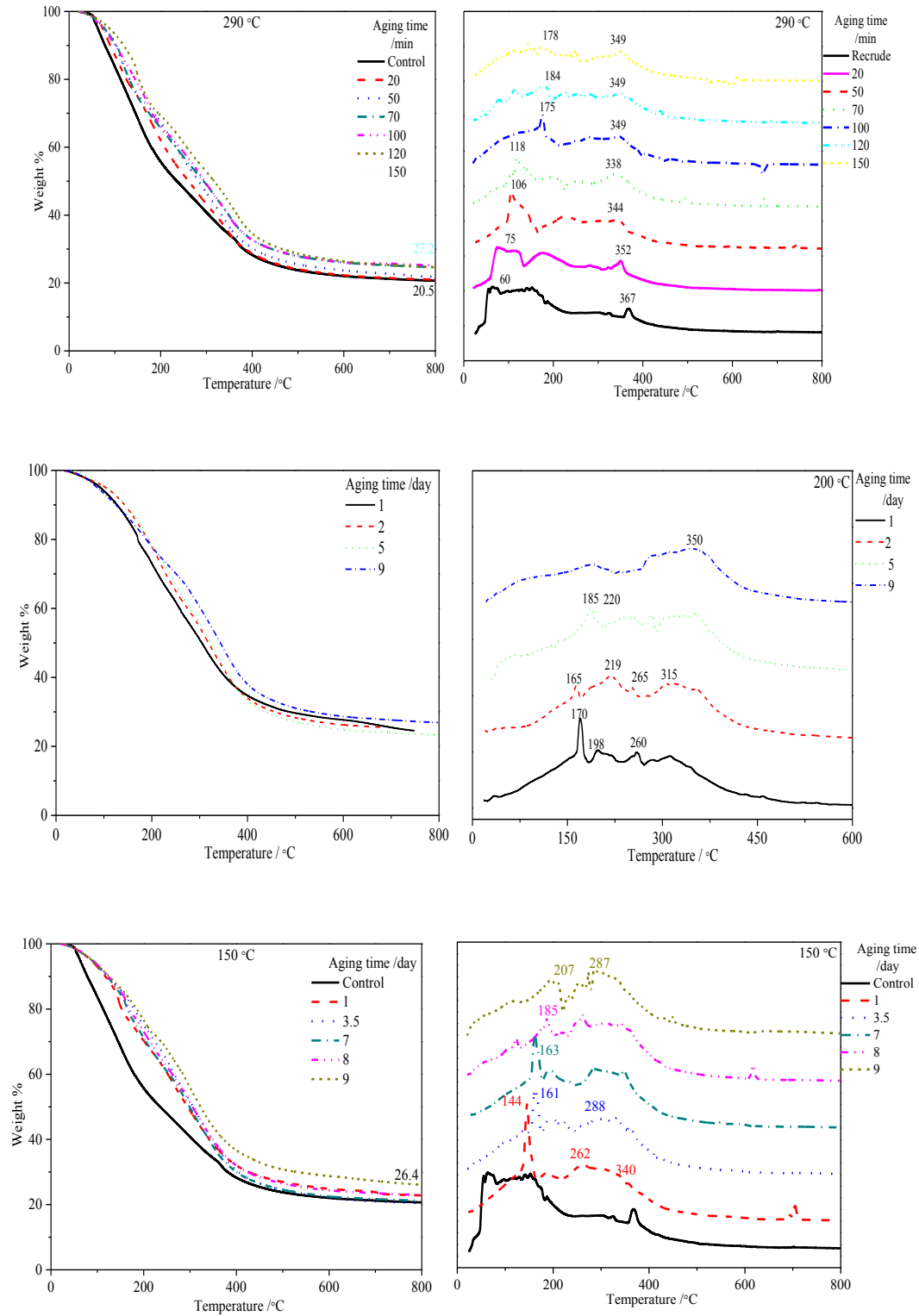


Figure 3.5 TG and DTG plots for pyrolysis oils aged at different temperatures.

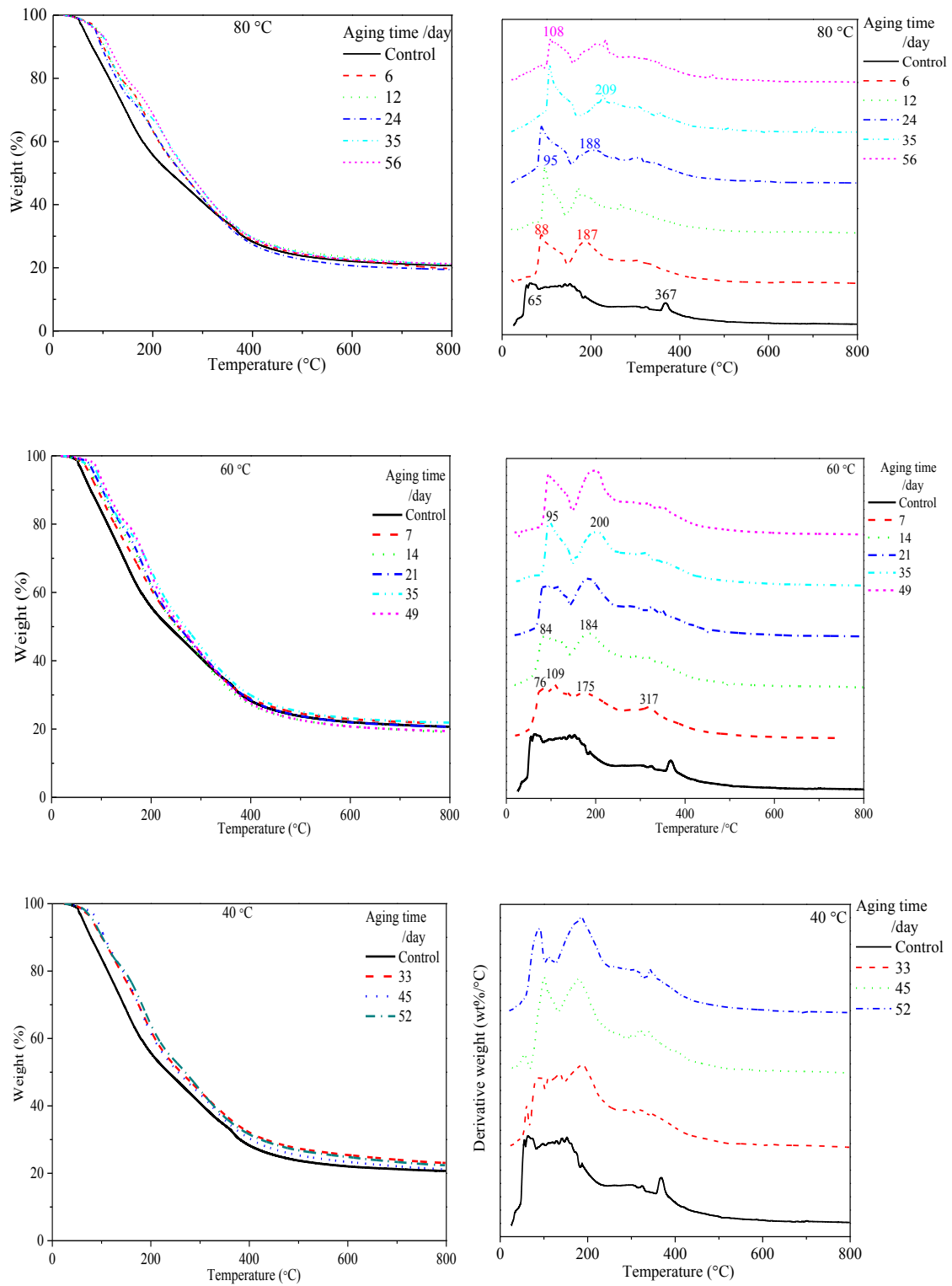


Figure 3.5 (Continued)

3.3.5 DSC

To better understand the effect of aging on the thermal behavior of aged oils, DSC was performed on the aged oils. Figure 3.6 shows the DSC plots for oils aged at different temperatures. For all the samples, two endothermic peaks were observed in the first heating process and no peaks were detected during the cooling process and the second heating-cooling loop. The two peaks were assigned to dehydration (Borde and Cesàro 2001, Yamaguchi, Sato et al. 2014) and decomposition of sugar derivatives (Wörmeyer, Ingram et al. 2011). No obvious trends were observed for both the dehydration and decomposition temperature.

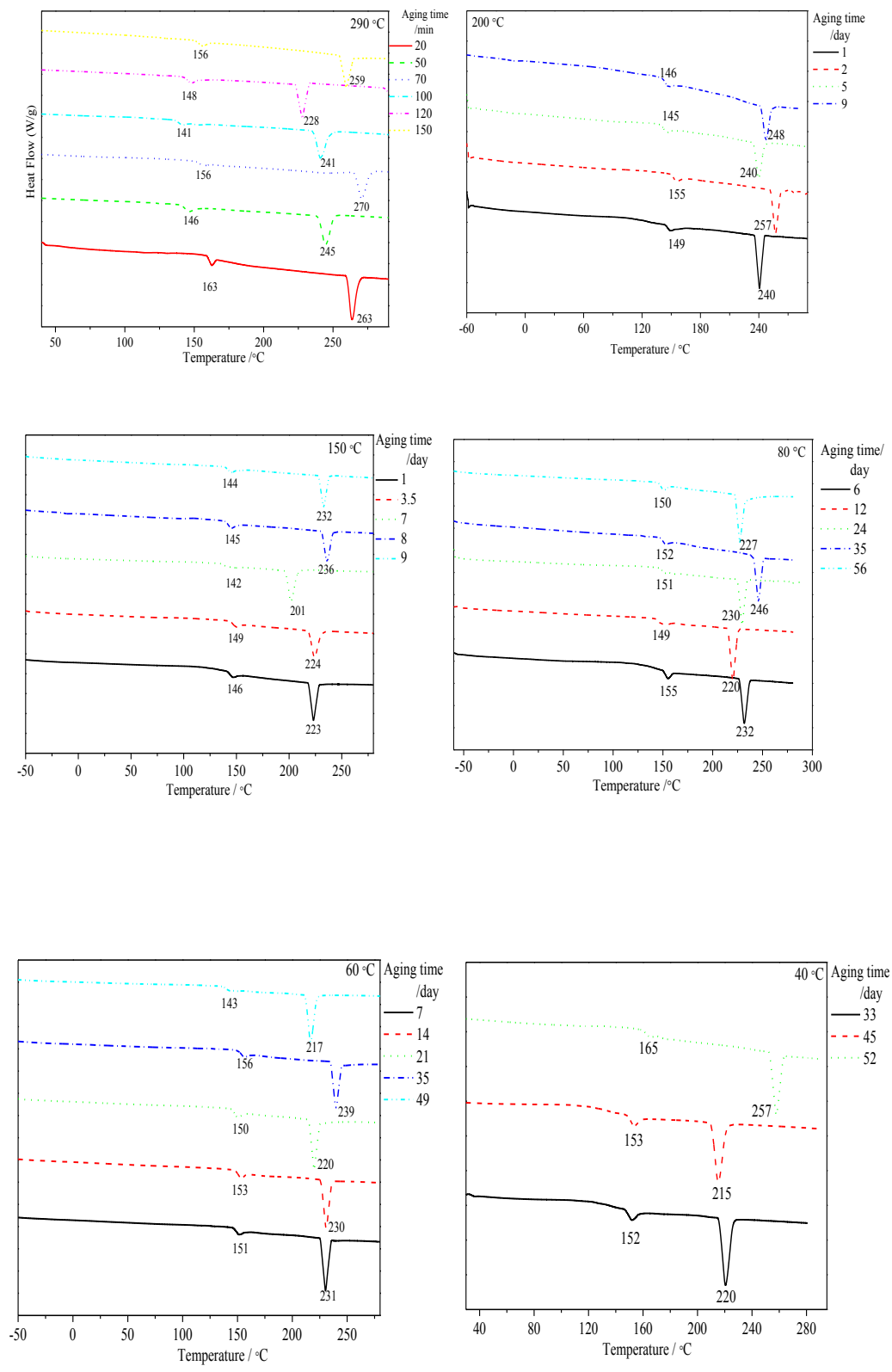


Figure 3.6 DSC plots for pyrolysis oils aged at different temperatures.

The aging reactions can also be classified as exothermic and endothermic according to whether energy released or absorbed via chemical reactions during the heating. The isothermal DSC technique can be used to monitor the net heat flows in and out of sample. Figure 3.7 shows the isothermal plots at 200, 150 and 80 °C, respectively. No obvious reactions occurred at 80 °C for no heat flow into or out of sample was found. Positive heat flows were observed when aging at 150 °C, indicating the net effect of all reactions gave out heat. However, negative heat flows were observed for isothermal processing at 200 °C indicating decomposition of sugar derivatives occurred. Hu et al. (Hu, Wang et al. 2013) found levoglucosan mainly underwent hydrolysis to glucose which was a key compound involved in polymer formation upon heating up. Glucose can further undergo dehydration or decomposition into various reactive compounds in return facilitate the decomposition of glucose and the condensation reactions.

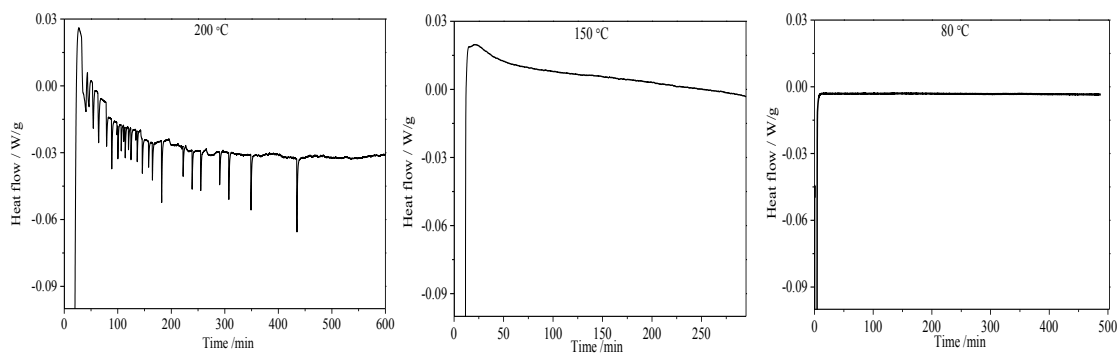


Figure 3.7 Isothermal DSC plots for pyrolysis oils aged at different temperatures.

3.3.6 FTIR

The change of specific functional groups among the aged samples was evaluated by ATR-FTIR. The percentage of transmittance intensities were normalized to the highest peak and can be used to represent the relative concentrations of selected functional groups. The adsorption bands from different components were superimposed heavily which makes the interpretation of absorption bands below 1500 cm^{-1} difficult. The broad band for hydroxyl groups ($3000\text{-}3650\text{ cm}^{-1}$) indicates the presence of large amounts water, alcohols, phenols and acids. The increase in O-H stretching absorbance is in agreement with higher water content of the stored oils measured by K-F titration. The carbonyl band ($1700\text{ and }1650\text{ cm}^{-1}$) indicates the presence of aldehydes, ketones, carboxylic acids, and esters (Scholze and Meier 2001). For all the samples, the bands at $1600\text{ and }1515\text{ cm}^{-1}$ correspond to aromatic skeletal vibrations did not show obvious change after aging indicating the ring formation reactions were not detectable. The intensities of the bands at $2860\text{-}2920$ assigned to $\text{-CH}_2\text{-}$ and -CH_3 increased with aging time. The higher the aging temperature lead to higher increasing rate. These changes can be assigned to the formation of new ester or ether groups during aging. The decreasing intensities of carbonyl bands (1700 cm^{-1}) can mostly be related to decarboxylation of esters or acids. Rennard et al. investigated the autothermal catalytic partial oxidation of pyrolysis oil model compounds (esters and acids). Thermal cracking of ethyl propionate could produce the intermediate, propionic acid, which could then undergo additional decomposition to ethylene (Rennard, Dauenhauer et al. 2008). For oils aged below $150\text{ }^\circ\text{C}$, the intensities of carbonyl bands increased with aging time which can be explained by the formation of carbonyl through oxidation reactions. Kim et al. (Kim, Kim et al. 2012)

also observed the intensity of the C=O band at 1710 cm^{-1} increased considerably during pyrolysis oil storage at $23\text{ }^{\circ}\text{C}$.

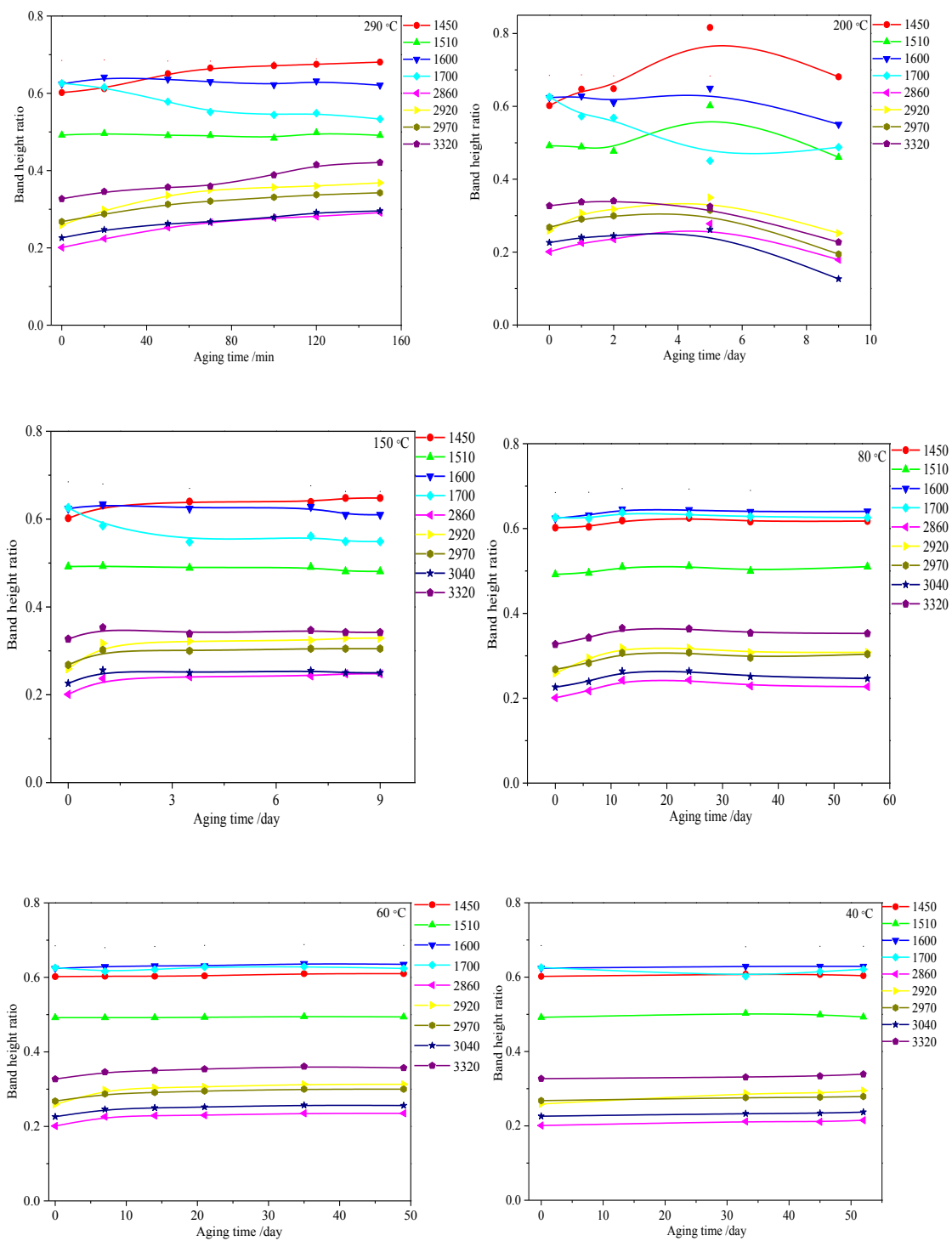


Figure 3.8 Evolution of FTIR band height ratio for pyrolysis oils aged at different temperatures.

3.3.7 GPC

The oils were investigated using GPC, by which the molecular weight and molecular weight distribution can be obtained. The retention time determined by GPC depends not only on the molecular size but also on the functional groups of samples. It is crucial to use standards which possess the same functional groups as the compounds to be tested for the calibration curves for GPC measurements. However, the pyrolysis oil is a mixture of various compounds and contains a large number of different functional groups, making all the known standards for GPC calibration not suitable. In this study, the polystyrene standards were used. All the oil samples exhibited multi-peaks. Table 3.1 listed the number-average molecular weight (M_n), weight-average molecular weight (M_w) and polydispersity index (PDI) for the fresh and aged oils. The M_n and M_w for the ReCrude oil were significantly higher than reported in literature (Chaala, Ba et al. 2004, Westerhof, Brilman et al. 2009, Nolte and Liberatore 2011). Both M_n and M_w generally increased with aging time while some fluctuations were observed. Czernik et al. (Czernik, Johnson et al. 1994) also observed a poor correlation between M_w with conversion the oil, where the conversion was defined as the ratio of the actual increase in M_w to the increase that would occur after infinite time of storage. The deviation was caused by the complexity of the reaction system—proportion of compounds with different molecular weight kept changing throughout the aging process.

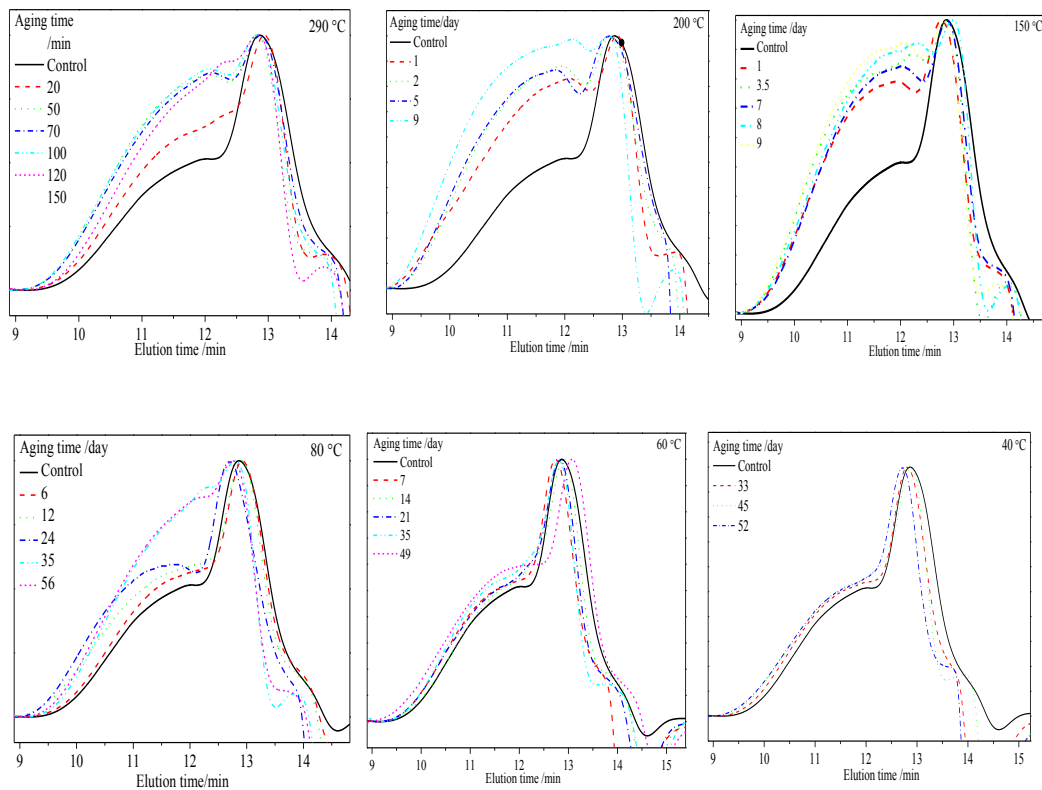


Figure 3.9 GPC curves for pyrolysis oils aged at different temperatures.

Figure 3.9 displays the GPC curves for fresh and aged oils. With the progress of storage, the proportion of high-molecular-weight fraction increased. This effect was more distinctive for the oils stored at higher temperatures and longer times. The increase in the amount of the high-molecular-weight fraction resulted in an increase in average molecular weight. Heating can result in cross-linking and polymerization reactions of lignin oligomers that lead to the increase in average molar masses (Czernik, Johnson et al. 1994, Boucher, Chaala et al. 2000). Considering average molecular weight discrepancy between M_w values is less than 1000, reactions between lignins were less practical. It could be inferred that CH_2Cl_2 soluble low molecular weight components could be involved in the chemical reactions with the pyrolytic lignin reactive sites, such

as phenolic -OH, aliphatic -OH, -OMe and double bonds, giving rise to increasing yields of pyrolytic lignins as well as their molecular weights (Diebold 2000, Bayerbach and Meier 2009).

Table 3.1 Calculated M_n , M_w and PDI for fresh and aged pyrolysis oils.

Temperature /°C	Time /day	M_n	M_w	PDI
290 ^{a)}	Control	506	1330	2.63
	20	600	1480	2.46
	50	721	1710	2.37
	70	688	1700	2.47
	100	718	1740	2.42
	120	678	1660	2.45
	150	715	1710	2.39
200	1	845	2303	2.72
	2	882	2248	2.55
	5	889	2532	2.85
	9	1100	2678	2.44
150	1	817	2033	2.49
	3.5	787	1954	2.48
	7	878	2085	2.37
	8	814	2063	2.53
	9	908	2153	2.37
80	6	578	1475	2.55
	12	702	2100	2.99
	24	780	2020	2.59
	35	679	1550	2.28
	56	711	1780	2.51
60	7	601	1430	2.38
	14	544	1459	2.68
	21	586	1480	2.52
	35	608	1460	2.40
	49	627	1870	2.99
40	33	597	1510	2.52
	45	641	1670	2.61
	52	675	1760	2.60

a) time unit is min

3.3.8 GC-MS

The composition for the ReCrude oil was investigated by GC-MS. The chromatogram for the CH₂Cl₂ soluble fraction and peak identification were presented in Chapter 2. Due to the injector temperature was set to be 270 °C, the GC analysis can only detect 45-50 wt.% of the oil which was in agreement with literature (Scholze and Meier 2001). Since the distinguishable changes occurred during pyrolysis oil storage were a decrease in the concentration of CH₂Cl₂ soluble chemical components and an increase in HMM lignin content, CH₂Cl₂ was used as solvent for GC-MS tests. The main composition for CH₂Cl₂ soluble are phenols and its derivatives. This was in agreement with that the phenolic compounds originating from lignin were mainly present in the water insoluble fraction of pyrolysis oil.

The major peaks after aging match those of un-aged pyrolysis oil qualitatively. However, peak size varies somewhat. By normalizing the spectrum based on the area of the internal standard, chlorobenzene, comparisons could be made regarding the relative concentration of compounds before and after aging. Figure 3.10 compared the normalized area for the major peaks in the GC spectra for fresh and aged pyrolysis oils at 290 and 80 °C. Concentrations of phenol and methyl/ethyl substituted phenols decreased during aging. The contents for furfural, 1,2-benzenediol and benzamide decreased rapidly when aged at 290 °C. Conversely, phenanthrene content increased with aging time.

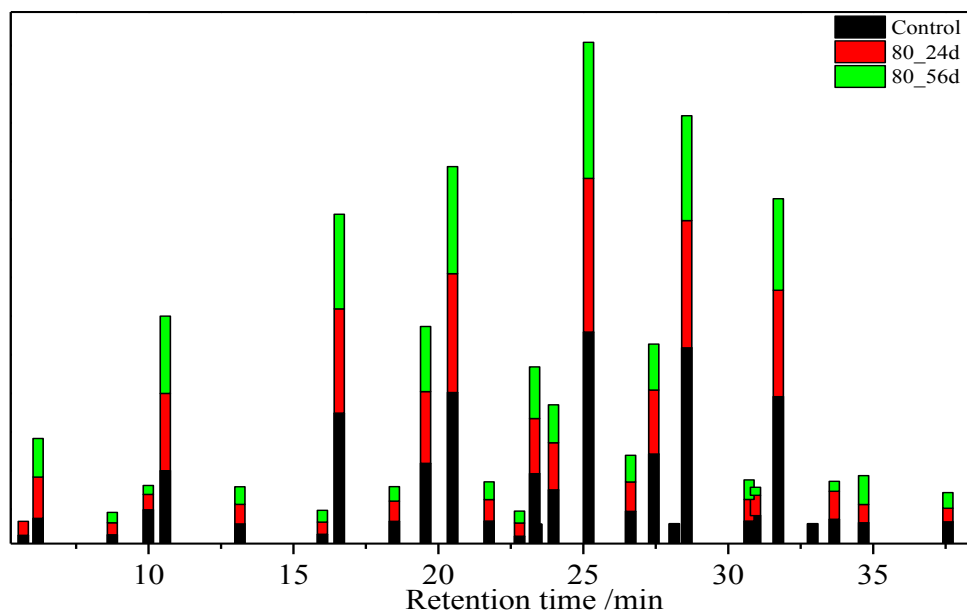
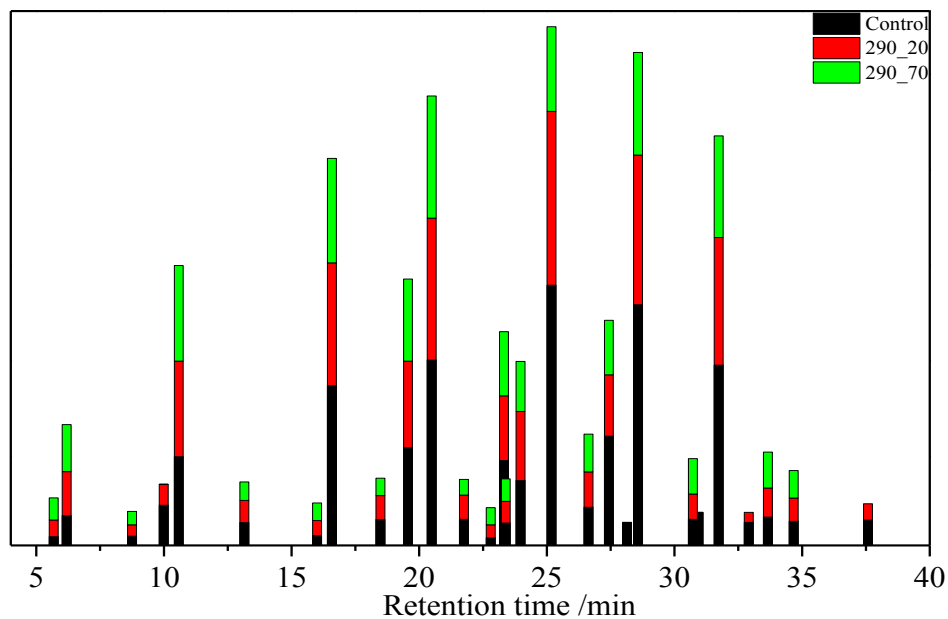


Figure 3.10 Peak area ratios for the CH₂Cl₂ soluble fraction of fresh and aged oils.

Based on the chemical composition change, the aging reaction mechanism can be proposed. Furfural can react with phenolic type compounds by a condensation reaction (Brown 1952). The phenolic -OH and -OMe in pyrolytic lignin (Erdtman 1972) were

reported to be very reactive during aging. The decreasing content of phenolic –OH was observed in this research. The proposed reaction mechanism during aging were shown in Figure 3.11.

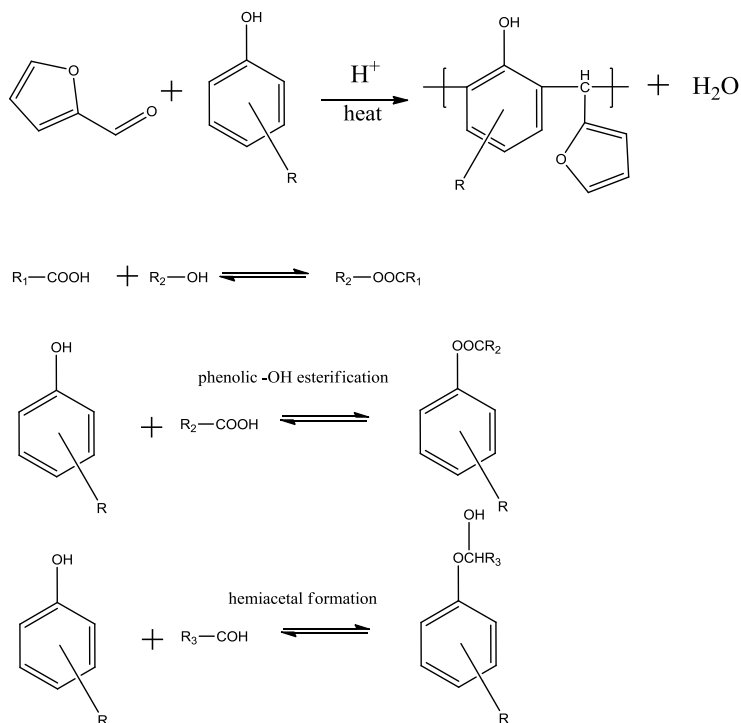


Figure 3.11 Proposed reaction mechanism during aging.

3.4 Conclusion

Major physicochemical changes of the ReCrude oil took place during storage at temperatures over 60 °C. No phase separation occurred during heat treatment. The water content, HMM lignin content and average molecular weight increase with increasing aging time and temperature. The higher temperature leads to higher increasing rate. The polymerization/condensation reactions of CH_2Cl_2 soluble compounds plays important role in the formation of HMM lignin. Decomposition of sugars for heat-treatment above

200 °C significantly affects the water content. Linear relationships between viscosity and aging time is observed for oils aged at 60 °C within 49 days and 80 °C within 28 days. FTIR results indicates the reactions mechanism were similar in the temperature range 40-150 °C. Concentrations of phenol and methyl/ethyl substituted phenols decreased while phenanthrene increased with aging time. The contents for furfural, 1,2-benzenediol and benzamide decreased more rapidly when aged at higher temperature. The applicable temperature range for the accelerated aging was below 150 °C.

3.5 References

- Aida, T. M., A. Ikarashi, Y. Saito, M. Watanabe, R. L. Smith Jr and K. Arai (2009). "Dehydration of lactic acid to acrylic acid in high temperature water at high pressures." The Journal of Supercritical Fluids **50**(3): 257-264.
- Ba, T., A. Chaala, M. Garcia-Perez, D. Rodrigue and C. Roy (2004). "Colloidal Properties of Bio-oils Obtained by Vacuum Pyrolysis of Softwood Bark. Characterization of Water-Soluble and Water-Insoluble Fractions." Energy & Fuels **18**(3): 704-712.
- Bayerbach, R. and D. Meier (2009). "Characterization of the water-insoluble fraction from fast pyrolysis liquids (pyrolytic lignin). Part IV: Structure elucidation of oligomeric molecules." Journal of Analytical and Applied Pyrolysis **85**(1–2): 98-107.
- Borde, B. and A. Cesàro (2001). "A DSC Study of Hydrated Sugar Alcohols. Isomalt." Journal of Thermal Analysis and Calorimetry **66**(1): 179-195.
- Boucher, M. E., A. Chaala, H. Pakdel and C. Roy (2000). "Bio-oils obtained by vacuum pyrolysis of softwood bark as a liquid fuel for gas turbines. Part II: Stability and ageing of bio-oil and its blends with methanol and a pyrolytic aqueous phase." Biomass and Bioenergy **19**(5): 351-361.
- Bridgwater, A. V. (2012). "Review of fast pyrolysis of biomass and product upgrading." Biomass and Bioenergy **38**(0): 68-94.
- Brown, L. H. (1952). "Resin Forming Reactions of Furfural and Phenol." Industrial & Engineering Chemistry **44**(11): 2673-2675.
- Chaala, A., T. Ba, M. Garcia-Perez and C. Roy (2004). "Colloidal Properties of Bio-oils Obtained by Vacuum Pyrolysis of Softwood Bark: Aging and Thermal Stability." Energy & Fuels **18**(5): 1535-1542.
- Chiaromonti, D., M. Bonini, E. Fratini, G. Tondi, K. Gartner, A. V. Bridgwater, H. P. Grimm, I. Soldaini, A. Webster and P. Baglioni (2003). "Development of emulsions from biomass pyrolysis liquid and diesel and their use in engines—Part 1 : emulsion production." Biomass and Bioenergy **25**(1): 85-99.
- Czernik, S. and A. V. Bridgwater (2004). "Overview of Applications of Biomass Fast Pyrolysis Oil." Energy & Fuels **18**(2): 590-598.
- Czernik, S., D. K. Johnson and S. Black (1994). "Stability of wood fast pyrolysis oil." Biomass and Bioenergy **7**(1–6): 187-192.

- De Miguel Mercader, F., P. J. J. Koehorst, H. J. Heeres, S. R. A. Kersten and J. A. Hogendoorn (2011). "Competition between hydrotreating and polymerization reactions during pyrolysis oil hydrodeoxygenation." *AIChE Journal* **57**(11): 3160-3170.
- Diebold, J. P. (2000). A Review of the Chemical and Physical Mechanisms of the Storage Stability of Fast Pyrolysis Bio-Oils, National Renewable Energy Laboratory.
- Diebold, J. P. and S. Czernik (1997). "Additives To Lower and Stabilize the Viscosity of Pyrolysis Oils during Storage." *Energy & Fuels* **11**(5): 1081-1091.
- Ed, J. S. and A. M. Thomas (1988). *Pyrolysis Oils from Biomass*, American Chemical Society.
- Eide, I., K. Zahlse, H. Kummernes and G. Neverdal (2006). "Identification and Quantification of Surfactants in Oil Using the Novel Method for Chemical Fingerprinting Based on Electrospray Mass Spectrometry and Chemometrics." *Energy & Fuels* **20**(3): 1161-1164.
- El-Saied, H. and A.-A. M. A. Nada (1993). "The thermal behaviour of lignins from wasted black pulping liquors." *Polymer Degradation and Stability* **40**(3): 417-421.
- Elliott, D. C. (2007). "Historical Developments in Hydroprocessing Bio-oils." *Energy & Fuels* **21**(3): 1792-1815.
- Elliott, D. C., A. Oasmaa, D. Meier, F. Preto and A. V. Bridgwater (2012). "Results of the IEA Round Robin on Viscosity and Aging of Fast Pyrolysis Bio-oils: Long-Term Tests and Repeatability." *Energy & Fuels* **26**(12): 7362-7366.
- Erdtman, H. (1972). "Lignins: Occurrence, formation, structure and reactions, K. V. Sarkanen and C. H. Ludwig, Eds., John Wiley & Sons, Inc., New York, 1971. 916 pp. \$35.00." *Journal of Polymer Science Part B: Polymer Letters* **10**(3): 228-230.
- García-Pérez, M., A. Chaala, H. Pakdel, D. Kretschmer, D. Rodrigue and C. Roy (2005). "Multiphase Structure of Bio-oils." *Energy & Fuels* **20**(1): 364-375.
- Hu, X., Y. Wang, D. Mourant, R. Gunawan, C. Lievens, W. Chaiwat, M. Gholizadeh, L. Wu, X. Li and C.-Z. Li (2013). "Polymerization on heating up of bio-oil: A model compound study." *AIChE Journal* **59**(3): 888-900.
- Kim, T.-S., J.-Y. Kim, K.-H. Kim, S. Lee, D. Choi, I.-G. Choi and J. W. Choi (2012). "The effect of storage duration on bio-oil properties." *Journal of Analytical and Applied Pyrolysis* **95**(0): 118-125.
- Lehto, J., A. Oasmaa, Y. Solantausta, M. Kytö and D. Chiaramonti (2014). "Review of fuel oil quality and combustion of fast pyrolysis bio-oils from lignocellulosic biomass." *Applied Energy* **116**(0): 178-190.

- Lu, Q., X.-l. Yang and X.-f. Zhu (2008). "Analysis on chemical and physical properties of bio-oil pyrolyzed from rice husk." Journal of Analytical and Applied Pyrolysis **82**(2): 191-198.
- Melligan, F., K. Dussan, R. Auccaise, E. H. Novotny, J. J. Leahy, M. H. B. Hayes and W. Kwapinski (2012). "Characterisation of the products from pyrolysis of residues after acid hydrolysis of Miscanthus." Bioresource Technology **108**(0): 258-263.
- Mohan, D., C. U. Pittman and P. H. Steele (2006). "Pyrolysis of Wood/Biomass for Bio-oil: A Critical Review." Energy & Fuels **20**(3): 848-889.
- Mortensen, P. M., J. D. Grunwaldt, P. A. Jensen, K. G. Knudsen and A. D. Jensen (2011). "A review of catalytic upgrading of bio-oil to engine fuels." Applied Catalysis A: General **407**(1-2): 1-19.
- Nolte, M. W. and M. W. Liberatore (2011). "Real-Time Viscosity Measurements during the Accelerated Aging of Biomass Pyrolysis Oil." Energy & Fuels **25**(7): 3314-3317.
- Oasmaa, A. and S. Czernik (1999). "Fuel Oil Quality of Biomass Pyrolysis Oils State of the Art for the End Users." Energy & Fuels **13**(4): 914-921.
- Oasmaa, A. and E. Kuoppala (2008). "Solvent Fractionation Method with Brix for Rapid Characterization of Wood Fast Pyrolysis Liquids." Energy & Fuels **22**(6): 4245-4248.
- Oasmaa, A., E. Kuoppala, A. Ardiyanti, R. H. Venderbosch and H. J. Heeres (2010). "Characterization of Hydrotreated Fast Pyrolysis Liquids." Energy & Fuels **24**(9): 5264-5272.
- Oasmaa, A., E. Kuoppala and Y. Solantausta (2003). "Fast Pyrolysis of Forestry Residue. 2. Physicochemical Composition of Product Liquid." Energy & Fuels **17**(2): 433-443.
- Oasmaa, A. and D. Meier (2005). "Norms and standards for fast pyrolysis liquids: 1. Round robin test." Journal of Analytical and Applied Pyrolysis **73**(2): 323-334.
- Oasmaa, A., C. Peacocke, S. Gust, D. Meier and R. McLellan (2005). "Norms and Standards for Pyrolysis Liquids. End-User Requirements and Specifications." Energy & Fuels **19**(5): 2155-2163.
- Piskorz, J., D. S. Scott and D. Radlein (1988). Composition of Oils Obtained by Fast Pyrolysis of Different Woods. Pyrolysis Oils from Biomass, American Chemical Society. **376**: 167-178.

- Rennard, D. C., P. J. Dauenhauer, S. A. Tupy and L. D. Schmidt (2008). "Autothermal Catalytic Partial Oxidation of Bio-Oil Functional Groups: Esters and Acids." Energy & Fuels **22**(2): 1318-1327.
- Rioche, C., S. Kulkarni, F. C. Meunier, J. P. Breen and R. Burch (2005). "Steam reforming of model compounds and fast pyrolysis bio-oil on supported noble metal catalysts." Applied Catalysis B: Environmental **61**(1-2): 130-139.
- Scholze, B. and D. Meier (2001). "Characterization of the water-insoluble fraction from pyrolysis oil (pyrolytic lignin). Part I. PY-GC/MS, FTIR, and functional groups." Journal of Analytical and Applied Pyrolysis **60**(1): 41-54.
- Smets, K., P. Adriaensens, J. Vandewijngaarden, M. Stals, T. Cornelissen, S. Schreurs, R. Carleer and J. Yperman (2011). "Water content of pyrolysis oil: Comparison between Karl Fischer titration, GC/MS-corrected azeotropic distillation and ¹H NMR spectroscopy." Journal of Analytical and Applied Pyrolysis **90**(2): 100-105.
- Sun, R., J. Tomkinson and G. Lloyd Jones (2000). "Fractional characterization of ash-AQ lignin by successive extraction with organic solvents from oil palm EFB fibre." Polymer Degradation and Stability **68**(1): 111-119.
- Takanabe, K., K.-i. Aika, K. Seshan and L. Lefferts (2004). "Sustainable hydrogen from bio-oil—Steam reforming of acetic acid as a model oxygenate." Journal of Catalysis **227**(1): 101-108.
- Tejado, A., C. Peña, J. Labidi, J. M. Echeverria and I. Mondragon (2007). "Physico-chemical characterization of lignins from different sources for use in phenol-formaldehyde resin synthesis." Bioresource Technology **98**(8): 1655-1663.
- Venderbosch, R. H., A. R. Ardiyanti, J. Wildschut, A. Oasmaa and H. J. Heeres (2010). "Stabilization of biomass-derived pyrolysis oils." Journal of Chemical Technology & Biotechnology **85**(5): 674-686.
- Vispute, T. P. (2011). Pyrolysis Oils: Characterization Stability Analysis, and Catalytic upgrading to fuels and chemicals.
- Vitolo, S., M. Seggiani, P. Frediani, G. Ambrosini and L. Politi (1999). "Catalytic upgrading of pyrolytic oils to fuel over different zeolites." Fuel **78**(10): 1147-1159.
- Westerhof, R. J. M., D. W. F. Brilman, W. P. M. van Swaaij and S. R. A. Kersten (2009). "Effect of Temperature in Fluidized Bed Fast Pyrolysis of Biomass: Oil Quality Assessment in Test Units." Industrial & Engineering Chemistry Research **49**(3): 1160-1168.

- Wörmeyer, K., T. Ingram, B. Saake, G. Brunner and I. Smirnova (2011). "Comparison of different pretreatment methods for lignocellulosic materials. Part II: Influence of pretreatment on the properties of rye straw lignin." Bioresource Technology **102**(5): 4157-4164.
- Yamaguchi, A., O. Sato, N. Mimura and M. Shirai (2014). "Intramolecular dehydration of mannitol in high-temperature liquid water without acid catalysts." RSC Advances **4**(85): 45575-45578.
- Zacher, A. H., M. V. Olarte, D. M. Santosa, D. C. Elliott and S. B. Jones (2014). "A review and perspective of recent bio-oil hydrotreating research." Green Chemistry **16**(2): 491-515.
- Zhang, Q., J. Chang, Wang and Y. Xu (2006). "Upgrading Bio-oil over Different Solid Catalysts." Energy & Fuels **20**(6): 2717-2720.

CHAPTER IV
ALCOHOL STABILIZATION OF PYROLYSIS OIL DURING HIGH
TEMPERATURE TREATMENT

4.1 Introduction

Pyrolysis oil, also known as bio-oil, is produced from fast pyrolysis of biomass using elevated temperature and oxygen-free conditions. The presence of large amounts of oxygenated and polar compounds—such as water, carboxylic acids, aldehydes and phenols—is the primary reason for the significantly different physical and chemical properties between fossil fuels and pyrolysis oils. The pyrolysis oil energy density (16-18 MJ/kg) is 50% less than conventional fossil fuel due to the high oxygen content while its acidity, viscosity and molecular weight are significantly higher. Pyrolysis oil is neither chemically nor thermally stable—water content, average molecular weight and viscosity increase, termed as aging, obstruct its further upgrading using conventional petroleum process. The acidity originates primarily from high concentrations of formic and acetic acid, while the cause of the chemical instability of pyrolysis oil is believed to be due to the presence of compounds containing reactive carbonyl, hydroxyl and aldehyde that can readily undergo esterification, acetalization, oxidization, dimerization, and condensation/polymerization to form compounds with higher molecular weights (Diebold 2000). These drawbacks make the reduction of oxygen content necessary to transform pyrolysis oil into a liquid transportation fuel.

Two effective routes for the deoxygenation of pyrolysis oil are hydrotreating and catalytic cracking. Some research has focused on processing pyrolysis oils in existing hydrotreatment and fluid catalytic cracking facilities which are routinely used in fossil oil industry. Hydrotreating (Elliott 2007) were performed at high temperatures (250-450 °C) and oxygen is eliminated in the form of water. Both precious metal catalysts and conventional catalysts developed for petroleum hydroprocessing have been tested. Adjustments to conventional hydroprocessing applied to petroleum feed stocks are needed for pyrolysis oil hydroprocessing. It is crucial to have a catalyst able to withstand water at the extreme conditions of high temperature and pressure. Another drawback of this method is a considerable consumption of hydrogen. A large amount of work has been published in catalytic cracking (Butler, Devlin et al. 2011, Mortensen, Grunwaldt et al. 2011, Al-Sabawi, Chen et al. 2012, Bridgwater 2012). Catalytic cracking occurring at a high temperature (e.g. 450-500 °C in the presence of HZSM-5) causes rejection of oxygen as H₂O, CO₂, and CO through simultaneous dehydration and decarboxylation processes (Aglebor, Mante et al. 2010). The resulting liquid product contains more aromatics and is generally more viscous than the original pyrolysis oils. The low hydrocarbon yield, catalyst deactivation, formation of undesirable products (coke, tar, char, etc.), and reactor plugging represents a significant barrier toward commercialization.

The heat treatment is well known for being able to accelerate the aging reactions. During catalytic upgrading process, severe aging reactions can occur when pyrolysis oil is heated to above 200 °C. An economic and efficient method to improve pyrolysis oil's properties is via the addition of chemicals to improve stability. Various organics have

been used to achieve stabilization of pyrolysis oil; methanol, ethanol, acetone, ethyl acetate, and methyl isobutyl ketone have previously been added to improve pyrolysis oil stability (Diebold and Czernik 1997). The oil/additive mixtures were aged in sealed glass vials from 10-150 hours at 90 °C. These additives were shown to significantly decrease the rate of aging, as measured by the rate of increase of oil viscosity with time. Reactive compounds in pyrolysis oil, for example aldehydes, can react with alcohols to form hemiacetals/acetals under acidic conditions to prevent homopolymerization. Alcohols can also act as a diluent to slow non-zero order reactions. It is concluded the addition of alcohols improved the homogeneity while significantly lowered the viscosity and molecular mass increasing rate. The reduction in the viscosity change was primarily due to a stabilizing effect of alcohols on the water-insoluble lignin-derived fraction. The formation of acetals due to reactions of alcohols with aldehydes, ketones, and anhydrosugars also slows down the aging reactions. Similar results were observed by other groups (Boucher, Chaala et al. 2000, Oasmaa, Kuoppala et al. 2004, Mante and Agblevor 2012).

The oil/additive strategy was mainly investigated on aqueous fraction of pyrolysis oil or the total pyrolysis oil with a high fraction of water. Very little research has been done on the stabilization of the water insoluble fraction of pyrolysis oil. This research investigated the stabilization effect of different alcohols on the stability of pyrolysis oil during high temperature treatment. Alcohols with different structures—methanol, ethanol, 1-propanol, 2-propanol and 1-octanol were introduced into the ReCrude oil at room temperature and then the pyrolysis oil/alcohol mixtures were aged at 200 °C. The

effect of alcohols on viscosity, molecular weight, thermal properties and chemical composition of fresh and aged pyrolysis oil/alcohol mixtures were investigated.

4.2 Materials and Methods

4.2.1 Pyrolysis oil/alcohol mixture preparation

Pyrolysis oil was mixed with different alcohols: methanol, ethanol, 1-propanol, 2-propanol, and 1-octanol. 10 mL (Weerachanchai, Tangsathikulchai et al. 2009) of alcohol was added to about 60 mL pyrolysis oil under mechanical stir at room temperature. The pyrolysis oil/alcohol mixtures were left at room temperature for 1 week.

4.2.2 Pyrolysis oil/alcohol aging

Approximately 10 mL of pyrolysis oil/alcohol mixtures were sealed in N₂ purged stainless steel tubes and then stored at 200 °C for specific time interval in an oven. The tubes were cooled to room temperature and weight loss after accelerated aging was under 0.1 %. The samples were then transferred to 50 mL vials and stored at 2.5 °C before the physicochemical properties and chemical composition were measured.

4.2.3 Characterization

The water content and high molecular mass (HMM) lignin content were measured by the same method used in Chapter 2. The parameters for TGA, DSC, ATR-FTIR and GC-MS characterization process were the same with those in chapter 2.

GPC. Gel Permeation Chromatography (GPC) characterization of the pyrolysis oil was carried out on a Waters 600 with an RI detector. Two columns (Waters Styragel[®] HR 5E and Agilent mesopore 300×7.5 mm) are connected in series for the separation of pyrolysis oil components. Tetrahydrofuran (THF) was used as the mobile phase flowing

at 2.0 mL/min. The pyrolysis oil/alcohol sample was dissolved into THF to approximately 2 wt. % and then filtered through a 0.45 μm PVDF filter. Polystyrene standards with molecular weight ranging from 162 to 174,000 were used to generate the calibration curve.

Rheology. Rheology test was performed on a TA Instruments AR 1500x rheometer with a 60 mm aluminum parallel plate accessory. Step-flow shear data were collected at 40 °C over the 0.1 to 100 s^{-1} shear rate range with 10 points per decade. The maximum limit for the rheometer is 15,000 cP.

4.3 Results and discussion

4.3.1 Effect of alcohol on chemical composition of pyrolysis oil

The etherification and esterification occurring between hydroxyl, carbonyl, and carboxyl group components are thermodynamically favored. Diebold and Czernik (Diebold and Czernik 1997) simulated the chemical equilibrium from stoichiometric amounts of methanol and acetic acid, formic acid and formaldehyde by the ASPEN PLUS program. The result indicated the reaction of methanol and formaldehyde to make dimethoxymethane and the reaction of methanol and acetic acid to make methyl acetate nearly went to completion at 25 °C. But these reactions were not as highly favored at higher temperatures. Moreover, the reaction rates are slow in the absence of catalysts.

Based on the above considerations, the pyrolysis oil/alcohol mixtures were mixed and left on a shaker at room temperature for one week to let the reactions reached equilibrium. These pyrolysis oil/alcohol mixtures without heat treatment were used as controls for samples aged at 200 °C. The chemical composition for the control samples were analyzed by GC-MS. The pyrolysis oil/alcohol controls were dissolved into CH_2Cl_2

and then filtrated with 0.45 PVDF membrane to remove the HMM lignin fraction. Chlorobenzene was used as the internal standard for the GC-MS test. The total ion chromatogram for pyrolysis oil/alcohol mixtures were listed in appendix. The peak assignment were listed in Chapter 2. Figure 4.1 shows the normalized peak area ratio for the ReCrude oil and pyrolysis oil/alcohol mixtures. Quantitative calculations were not performed on propanoic acid and butanoic acid for the peaks at 5.68 and 8.75 were broad and overlapped with the newly formed esters. The added alcohols were not detected in the pyrolysis oil/alcohol mixtures except for pyrolysis oil/1-octanol. Moreover, no obvious changes for peak areas of phenols were observed indicating no severe reactions between alcohols and phenols occurred. The added alcohols can be consumed by etherification. Unfortunately esters were not detected (except a small amount of acetic acid, octyl ester). This might because etherification was slow at room temperature. The existence of 1-octanol indicated the larger sterically hindered group of 1-octanol reduced its reaction rate with the carboxylic acids. Doerr (Doerr, Wasserman et al. 1966) reported an aging study of whole woodsmoke condensates at 25 °C. It was found that after 72 hours, the concentration of methyl formate reached 95% of its maximum value while methyl acetate reached 40% of the value reached after 26 days. The relatively slower rate to form methyl acetate compared to the smaller methyl formate indicated that larger esters would form at even slower rates.

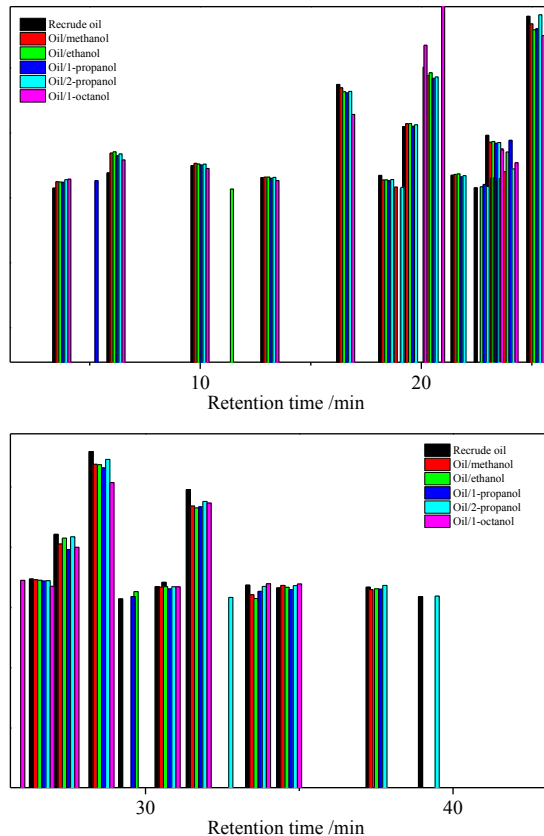


Figure 4.1 Normalized peak area ratio for the ReCrude oil and pyrolysis oil/alcohol mixtures.

Functional group change with treatment can be monitored using FTIR spectroscopy. Figure 4.2 shows the ATR-FTIR spectra collected for both the ReCrude oil and pyrolysis oil/alcohol controls. All samples showed large broad peaks at about 3300 cm^{-1} indicating the presence of -OH and COOH functional groups. The weak peaks at 3040 cm^{-1} were assigned to C-H stretch for aromatics. These peaks correspond with the peaks at 1513 cm^{-1} and 1465 cm^{-1} related to C-C stretch for aromatics and substituted aromatic ring skeletal vibrations. The three peaks in the range from 2950 cm^{-1} to 2850 cm^{-1} were assigned to C-H stretch of methyl and methylene for alkenes. The protonated

carboxyl acid groups at 1740 cm^{-1} (Bociek and Welti 1975, Venyaminov and Kalnin 1990) merged into the strong band at 1700 cm^{-1} assigned to carbonyl group in aldehydes, ketones, carboxylic acids, and esters (Scholze and Meier 2001). The conjugated C=O stretch at 1650 cm^{-1} was overlapped with the unconjugated C=O stretch at 1700 cm^{-1} . The carboxylate groups absorbed at $\sim 1600\text{ cm}^{-1}$ and was overlapped with the aromatic skeletal vibration.

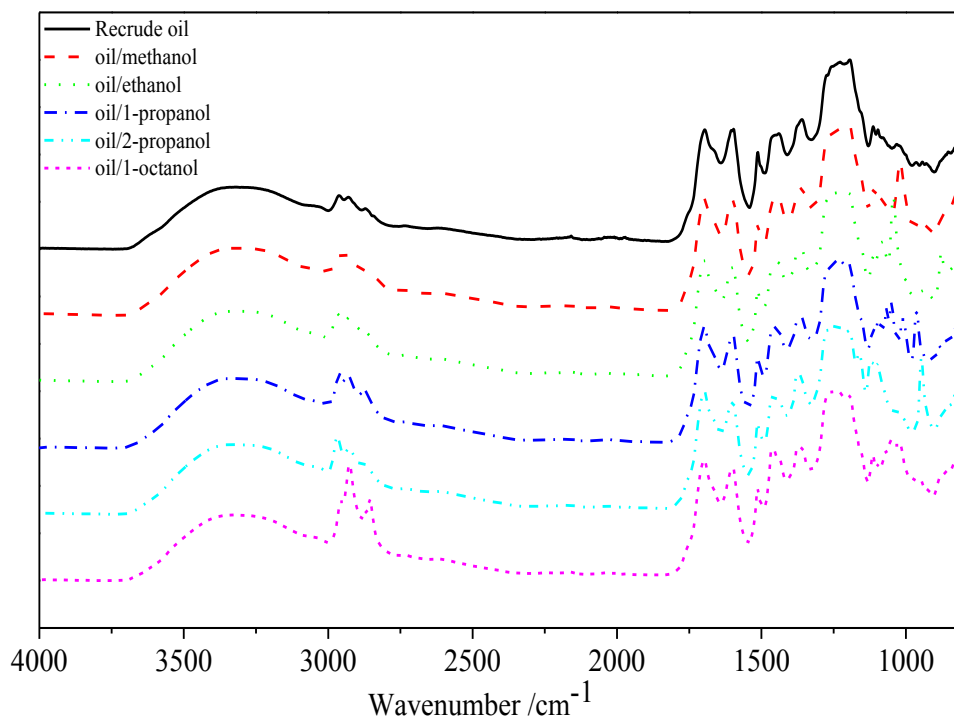


Figure 4.2 FTIR spectra for the ReCrude oil and pyrolysis oil/alcohol mixtures.

The introduction of alcohols resulted many spectral changes, as expected, including the appearance of new peaks and increase in intensity for existing peaks. Table 4.2 lists the newly formed peaks and peaks with obvious changes in their heights. The C=O peak at 1600 cm^{-1} assigned to carboxylic acid decreased due to acids were

consumed by esterification with added alcohols. The unconjugated C=O peak at 1700 showed very slight change (~2%). The newly formed peaks were mainly in the range from 1500 cm⁻¹ to 810 cm⁻¹. The significant increases in intensity for C-O deformation indicating alcohols were also reacted with aromatic compounds.

Table 4.1 Percent band height change due to the introduction of alcohols.

Wavenumber /cm ⁻¹	Band	Peak height change %				
		Oil /methanol	Oil /ethanol	Oil /1-propanol	Oil /2-propanol	Oil /1-octanol
813	C-H deformation in plane	23.03	27.84	22.22	51.38	26.32
815		--	--	--	49.91	--
855		--	--	16.70	--	--
880	O-H out-of-plane bending	--	44.99	--	--	--
885		--	--	19.51	--	--
947		--	--	--	82.54	--
962		--	--	64.12	--	--
1010		--	--	37.69	--	--
1020		49.21	--	--	--	--
1042	-CH ₂ -wagging in RO-CO, -O-	--	79.81	--	--	--
1050	CH ₂ -C,C-O	--	--	43.99	--	39.61
1062	deformation in	--	--	29.14	--	--
1080	alcohol	--	25.45	--	--	--
1097		--	--	7.14	25.79	--
1123		--	--	--	40.96	--
1163		--	--	--	13.98	--
1368	C-H rock for	--	--	--	9.53	--
1373	alkanes	--	--	--	--	6.35
1460	C-H bend for	--	--	7.00	6.55	--
1468	alkanes	--	--	--	--	16.97
1595	C=O stretch, aromatic skeletal vibration	--	--	--	--	-7.39
1600		-3.50	-4.02	-6.76	-5.60	-6.85
2866	C-H vibration in	11.85	24.23	35.18	21.33	73.01
2924	methyl and	18.96	25.98	37.86	28.28	125.70
2960	methylene	12.12	22.11	42.13	32.85	42.99
3300	O-H stretch	8.57	13.70	12.20	12.25	5.72

Figure 4.3 shows the proposed reaction mechanism. The esterification equilibrium was shifted toward the right side by the excess use of alcohols and continuous removal of water. The alkylation of phenols/alkyl substituted phenol may also occur.

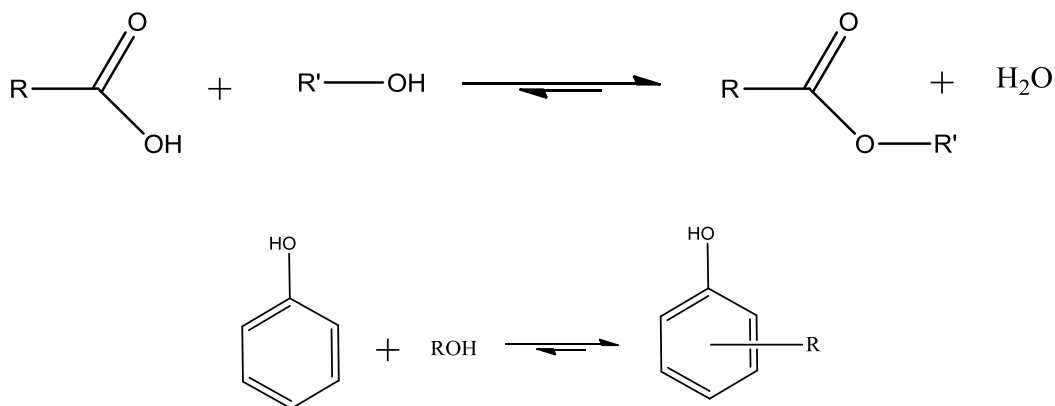


Figure 4.3 Reaction mechanism for pyrolysis oil/alcohol mixtures.

4.3.2 Effect of alcohol on viscosity of pyrolysis oil

Viscosity is an important criterion for the practical usage of pyrolysis oil. The viscosity of pyrolysis oil was immediately reduced by the introduction of alcohols. As shown in Figure 4.4, all samples exhibited typical non-Newtonian fluid behaviors. The pyrolysis oil/ethanol mixture showed similar viscosity with the ReCrude oil at low shear rates. Shear thinning phenomena were observed for all oils. The adding of 1-propanol and 2-propanol showed a very similar effect in reducing the viscosity of pyrolysis oil. 1-octanol was more effective than other alcohols for its longer hydrocarbon chains enhanced the solubility of pyrolysis oil. The limited effect for the introduction of methanol and ethanol was partly assigned to the poor solubility of the ReCrude oil in these alcohols (Yu, Deng et al. 2007).

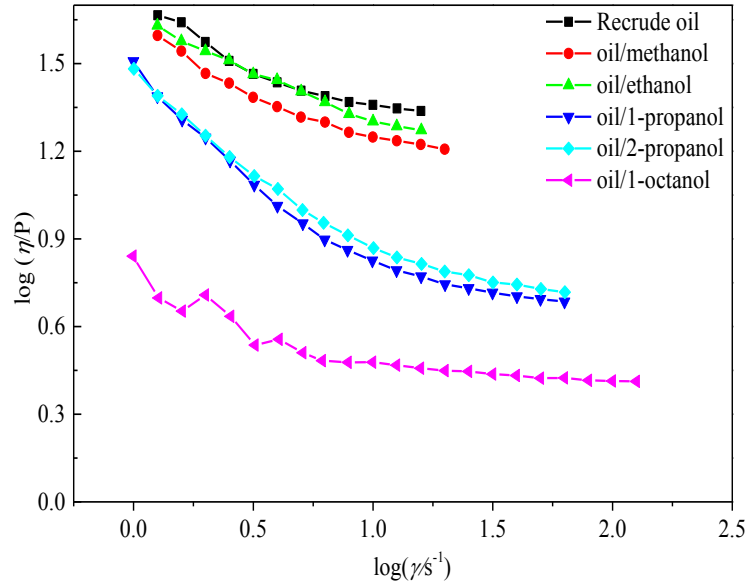


Figure 4.4 Logarithmic plots of apparent viscosity vs. shear rate for pyrolysis oil and pyrolysis oil/alcohol mixtures.

Non-Newtonian fluids can generally be described by some common models. Three models were tested for the pyrolysis oil/alcohol mixtures, including the Power Law (Eqn. 4.1), Bingham Plastic (Eqn. 4.2), and Herschel-Bulkley (Eqn. 4.3) models:

$$\tau = k \dot{\gamma}^m \quad (4.1)$$

$$\tau = \tau_B + \eta_B \dot{\gamma} \quad (4.2)$$

$$\tau = \tau_H + K \dot{\gamma}^n \quad (4.3)$$

where τ is the shear stress; η_B is the apparent viscosity; $\dot{\gamma}$ is the shear rate; m and n are the Power law model index and the Herschel–Bulkley model flow index, respectively, which indicate the degree of deviation from Newtonian flow character ($n < 1$ for

pseudoplastic behavior and $n > 1$ for dilatant behavior); k and K are consistency indexes, which reflect the viscous nature of the sample; and τ_B and τ_H are yield stress. In this study, the Power Law model shows the poorest correlation ($R^2 < 0.98$) while the Bingham Plastic model gave negative values for τ_B . The rheological behavior of all test samples was found to be best described by the Herschel-Bulkley model which had been successfully used to model the pyrolysis oil/coal slurries (Feng, Hao et al. 2014). Table 4.3 summarizes the fitted rheological parameters for the pyrolysis oil/alcohol mixtures. The flow index was close to 1 for all of the samples, with the exception of the pyrolysis oil/ethanol mixture. The much lower yield stress value for the pyrolysis oil/1-octanol mixture indicates that it was more soluble in the pyrolysis oil than other alcohols.

Table 4.2 Herschel-Bulkley rheology model fit results for pyrolysis oil and pyrolysis oil/alcohol mixtures.

Sample	Variable			R ²
	τ_H	K	n	
ReCrude oil	3.99545	1.577722	1.073109	0.99967
Oil/methanol	3.20645	1.442156	1.003894	0.999626
Oil/ethanol	2.37029	2.540011	0.854297	0.998665
Oil/1-propanol	2.61257	0.380053	1.038147	0.999797
Oil/2-propanol	2.53266	0.512316	0.985869	0.999888
Oil/1-octanol	0.10872	0.308686	0.998106	0.999994

4.3.3 Effect of alcohol on thermal properties of pyrolysis oil

4.3.3.1 TGA

TGA was used to study the thermal degradation behavior of samples. Figure 4.5 shows the TG and DTG curves for the ReCrude oil and pyrolysis oil/alcohol mixtures. The curves for pyrolysis oil/methanol and pyrolysis oil/ethanol were similar with those

for pyrolysis oil and pyrolysis oil/1-propanol, respectively. The weight loss process consisted of four steps. The loss in mass began at a low temperature for all samples, with DTG_{max} shifting from 40 to 117 °C as the chain length of esters increased. The peaks at ~50-70 °C in the derivative temperature analysis (DTA) curves (Figure 4.6) were due to the quick vaporization of volatile compounds. In the second stage, a quick weight loss at ~180 °C was observed due to the decomposition of thermally unstable compounds e.g. glucose. (Melligan, Dussan et al. 2012). The weight loss rate decreased significantly after 200 °C. In the third region broad peaks between 200 and 460 °C with DTG_{max} around 317 °C were found due to the breakup of inter-unit linkages of HMM lignin (Ba, Chaala et al. 2004) and evaporation of monomeric phenol units (Wörmeyer, Ingram et al. 2011). Although 1-octanol was less volatile, the residue for pyrolysis oil/1-octanol was obviously lower than other mixtures. DTA curves confirmed the pyrolysis process was complex—several broad negative peaks appeared indicating some exothermic reactions occurred.

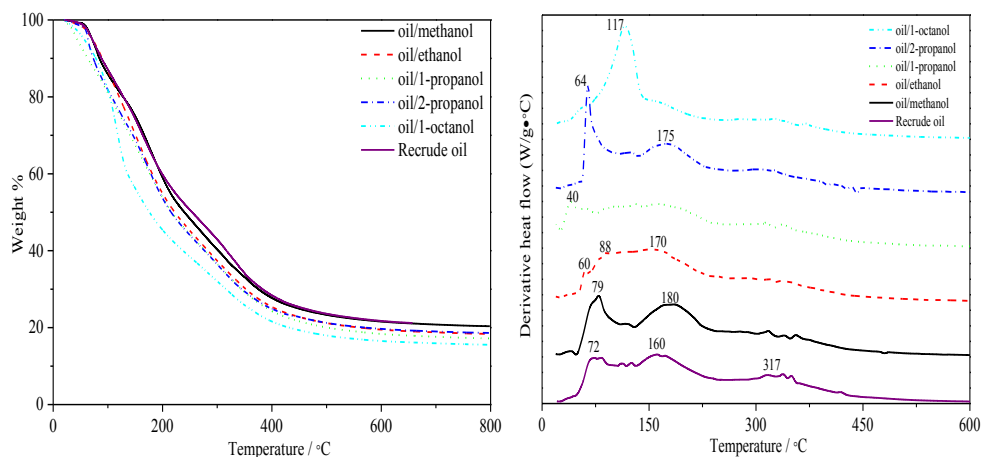


Figure 4.5 Residual weight and derived weight temperature vs. temperature plots for pyrolysis oil and pyrolysis oil/alcohol mixtures in N_2 atmosphere.

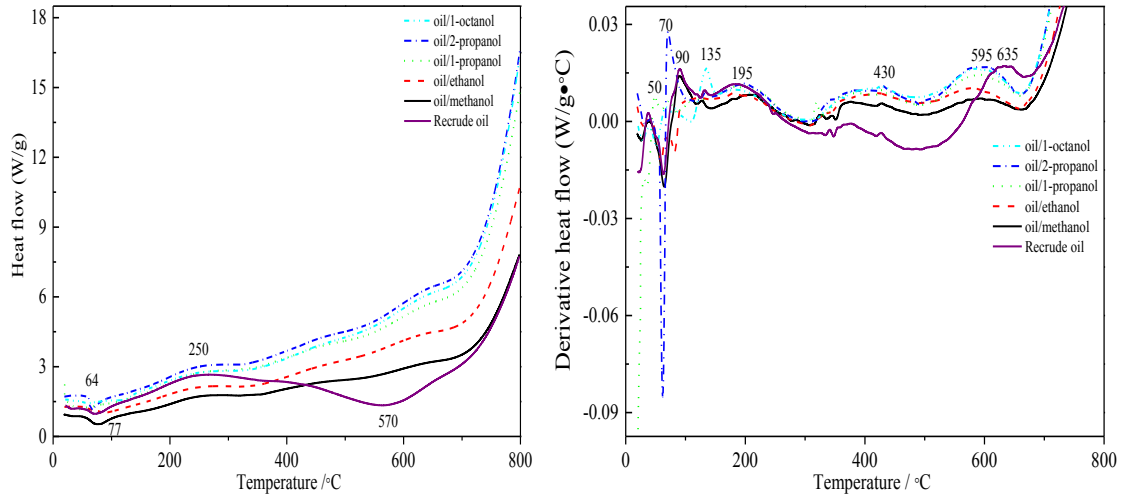


Figure 4.6 Heat flow and derivative heat flow vs. temperature plots for pyrolysis oil and pyrolysis oil/alcohol mixtures in N₂ atmosphere.

The kinetic parameters for different stage can be measured by Coats-Redfern method (Coats and Redfern 1964). The kinetic model function $f(\alpha)$ was assumed to be a function of the decomposition and the reaction rate, and the kinetic equation can be described as

$$d\alpha / dt = kf(\alpha) \quad (4.4)$$

$$K = A \exp\left(-\frac{E_a}{RT}\right) \quad (4.5)$$

$$\alpha = \frac{W_0 - W}{W_0 - W_\infty} \quad (4.6)$$

$$T = T_0 + \beta t \quad (4.7)$$

where α is the fraction of sample decomposed at time t ; W_0 and W_∞ represent the initial and final residual weight of the oil, respectively; K is the Arrhenius constant; E_a is the

activation energy (J/mol); A is the frequency factor (s^{-1}); R is the universal gas constant; β is the ramp rate; and T is the absolute temperature. By assuming the decomposition to be a simple reaction and the reaction order n ,

$$f(\alpha) = (1 - \alpha)^n \quad (4.8)$$

$$\frac{d\alpha}{dt} = \frac{A}{\beta} \exp\left(-\frac{E_a}{RT}\right) (1 - \alpha)^n \quad (4.9)$$

Combining the above equations, rearranging and integrating, we get

$$\int_0^\alpha \frac{d\alpha}{(1 - \alpha)^n} = \frac{A}{\beta} \int_0^T e^{\left(-\frac{E_a}{RT}\right)} dT \quad (4.10)$$

Taking the natural log with $n=1$

$$\ln\left(\frac{-\ln(1 - \alpha)}{T^2}\right) = \ln\left[\frac{AR}{\beta E_a} \left(1 - \frac{2RT}{E_a}\right)\right] - \frac{E_a}{RT} \quad (4.11)$$

And if $n \neq 1$

$$\ln\left[\frac{1 - (1 - \alpha)^{(1-n)}}{T^2(1-n)}\right] = \ln\left[\frac{AR}{\beta E_a} \left(1 - \frac{2RT}{E_a}\right)\right] - \frac{E_a}{RT} \quad (4.12)$$

Thus the plot of $\ln\left(\frac{-\ln(1 - \alpha)}{T^2}\right)$ or $\ln\left[\frac{1 - (1 - \alpha)^{(1-n)}}{T^2(1-n)}\right]$ against $1/T$ should result in a

straight line for the correct value of n , since for most values of E_a and for the general

reaction temperature range the expression $\ln\left[\frac{AR}{\beta E_a}\left(1 - \frac{2RT}{E_a}\right)\right]$ is sensibly constant (Coats and Redfern 1964).

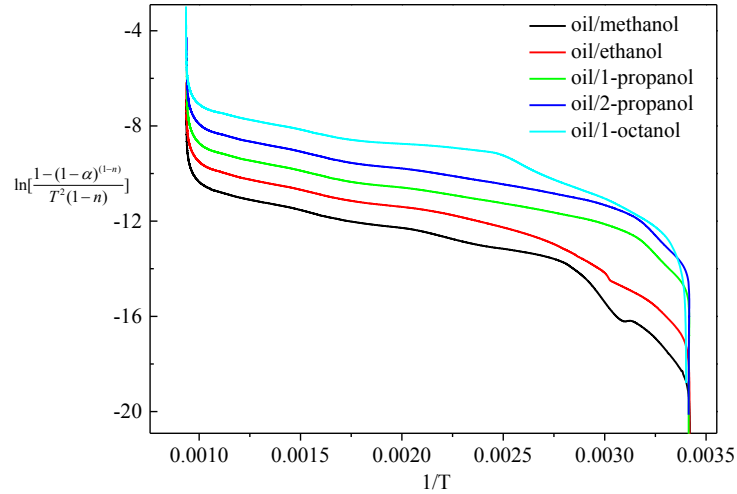


Figure 4.7 Decomposition kinetics plots for pyrolysis oil/alcohol mixtures ($n=1.5$ except for oil/2-propanol, $n=2$)

The equations were applied by a simple graphical technique. By substituting the assumed value of n , the plots of $\ln\left(\frac{-\ln(1-\alpha)}{T^2}\right)$ or $\ln\left[\frac{1-(1-\alpha)^{(1-n)}}{T^2(1-n)}\right]$ against $1/T$ were fitted to calculate the correlation coefficient of linear regression. The procedure was repeated until all high the correlation coefficients were close to a value of 1. Figure 4.7 shows the processed plots. Obvious transitions were observed for all samples indicating the dominant reaction mechanism was different in different temperatures range. Table 4.4 shows that it was reasonable to describe the pyrolysis process by the kinetic model into several stages. The Pearson correlation coefficients were lower than (-0.99), which

confirmed that the equations were suitable for the temperature region. The ReCrude oil followed two stage first order reaction with a transition temperature at 79 °C. The introduction of alcohol made the pyrolysis more complex—the apparent reaction order increased to be 1.5 or 2. Pyrolysis oil/methanol and pyrolysis oil/ethanol showed similar pyrolysis behaviors. Though the apparent reaction orders were different, pyrolysis oil/1-propanol and pyrolysis oil/2-propanol had close transition temperature. The much higher transition temperatures (133 °C and 300 °C) for pyrolysis oil/1-octanol were due to the unreacted 1-octanol continue to form esters in high temperature range.

Table 4.3 Kinetics parameters for pyrolysis oil and pyrolysis oil/alcohol mixtures

Sample	Temperature Range/°C	Reaction order	Slope	Intercept	Pearson R	E_a kJ/mol	A /min ⁻¹
ReCrude oil	79-747	1	-2255	-7.319	-0.99766	18.74807	7.4733
	22-79	1	-9022.2	11.648	-0.99539	75.010571	5E+09
Oil/methanol	80-700	1.5	-1691.3	-8.9657	-0.99753	14.061468	1.08
	51-80	1.5	-9671.6	13.6232	-0.9962	80.409682	4E+10
Oil/ethanol	105-703	1.5	-1634.2	-8.9841	-0.99509	13.586739	1.0245
	59-105	1.5	-4364	-1.7921	-0.99624	36.282296	3635.4
Oil/1-propanol	46-700	1.5	-1519.1	-9.1459	-0.99537	12.629797	0.8101
	20-46	1.5	-8612.2	12.9562	0.99682	71.601831	2E+10
Oil/2-propanol	55-678	2	-1508.3	-9.1716	-0.99575	12.540006	0.7839
	21-55	2	-8670.2	13.1562	-0.99823	72.084043	2E+10
Oil/1-octanol	300-717	1.5	-1817.2	-8.6419	-0.998	15.108201	1.6041
	133-300	1.5	-681.1	-10.595	-0.991	5.6626654	0.0853
	30-133	1.5	-3807.6	-2.9392	-0.99684	31.656386	1007.3

From the perspective of activation energy, the activation energy E_a of the second or the third stage should be higher than that of the first stage, because the latter stages involved in the decomposition of HMM lignin, and the energy required to overcome it apparently increases with molecular weight (Garcia-Perez, Wang et al. 2008). However,

the E_a calculated by Coats-Redfern method was the apparent activation energy for complex reactions: decomposition, vaporization, condensation, esterification, etc. The DTA curves confirmed exothermic reactions occurred in the temperature range 200-700 °C which reduced the average value for E_a .

Combustion characteristics of pyrolysis oil/alcohol mixture as detected by TGA were displayed in Figure 4.8. Pyrolysis oil/alcohol mixtures showed three-stage combustion behaviors. In the first stage the volatile were released and burned from 20 °C to 260 °C. In the second stage the formation of fixed carbon took place between 260 °C and 430 °C. The third stage was between 430 °C and 550 °C, at which the char combustion and minerals decomposition occurred. These three regions were also observed from the DTA curves in Figure 4.9. The DTA curves in air atmosphere were smoother than those in N₂ atmosphere for oxidation reaction were in dominant. For char combustion, both ReCrude oil and pyrolysis oil/alcohol mixtures char gave nearly the same wide range of combustion peak centered at 510 °C.

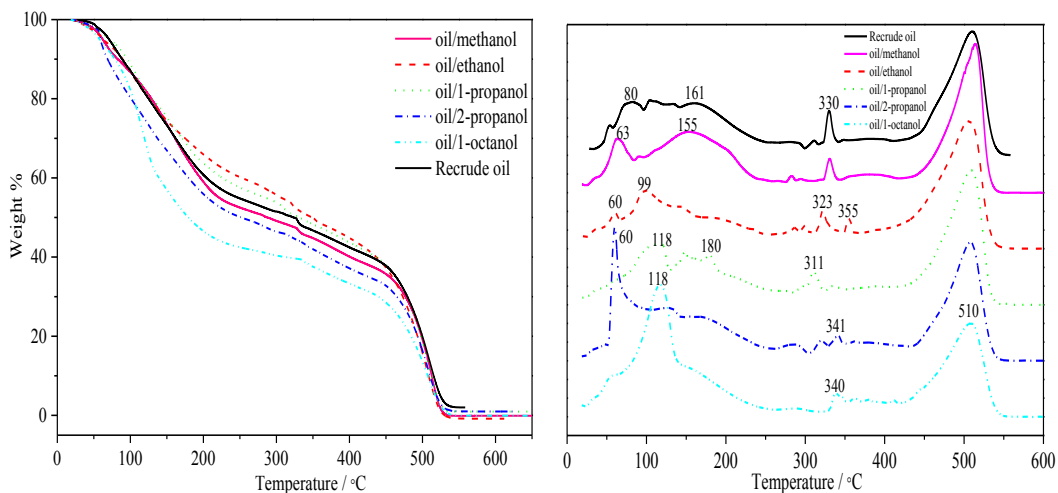


Figure 4.8 Residual weight and derived weight temperature plots for pyrolysis oil and pyrolysis oil/alcohol mixtures during combustion in air.

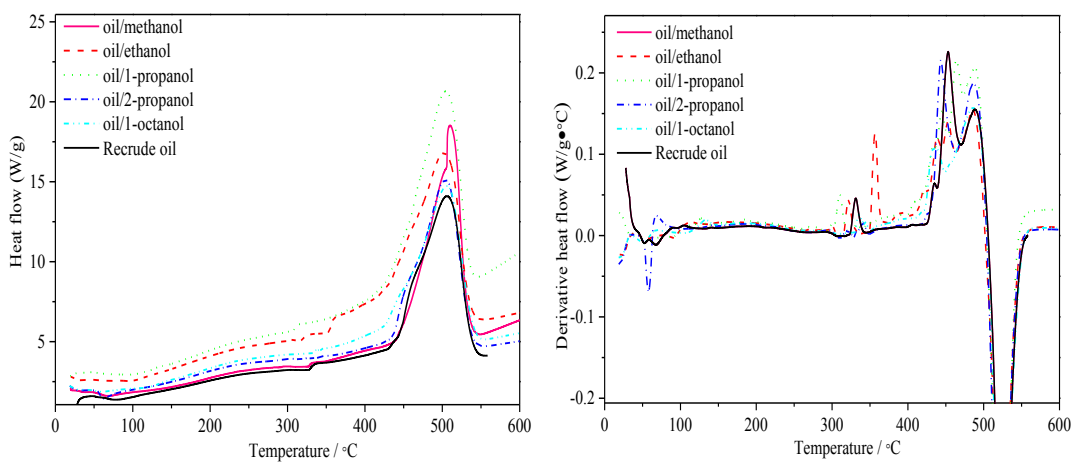


Figure 4.9 Heat flow and derivative heat flow vs. temperature plots for pyrolysis oil and pyrolysis oil/alcohol mixtures in air atmosphere.

The ignition temperature and burnout temperatures were important parameters used to describe the combustion behavior of fuels. Both the air flow rate and nitrogen flow rate were kept 50 mL/min to avoid fluctuation in ignition and burnout performances caused by oxygen concentration. There are different methods to determine the ignition

temperature (Tognotti, Malotti et al. 1985, Crelling, Hippo et al. 1992). In this research, T_i was regarded as the temperature at which TG curves in air and nitrogen diverge. The lower the ignition temperature the easier to ignite the fuel. Figure 4.10 shows the plots to determine T_i . From the diverging point, the T_i for pyrolysis oil and pyrolysis oil/alcohol mixtures were as follows: 175 °C for the ReCrude oil, 205 °C for oil/methanol, 100 °C for oil/ethanol, 20 °C for oil/1-propanol, 173 °C for oil/2-propanol, 125 °C for oil/1-octanol. The introduction of methanol increased the value of T_i while the other alcohols decreased the T_i value. 1-propanol was the most efficient in reducing T_i . The burnout temperature, T_h , was determined as the temperature at which the weight of a sample kept constant. A low burnout temperature usually indicated a short burnout time and a low ash content. The ash content for ReCrude oil was 2 wt%. The ash content increased with increasing molecular weight of alcohol while T_h showed slight change.

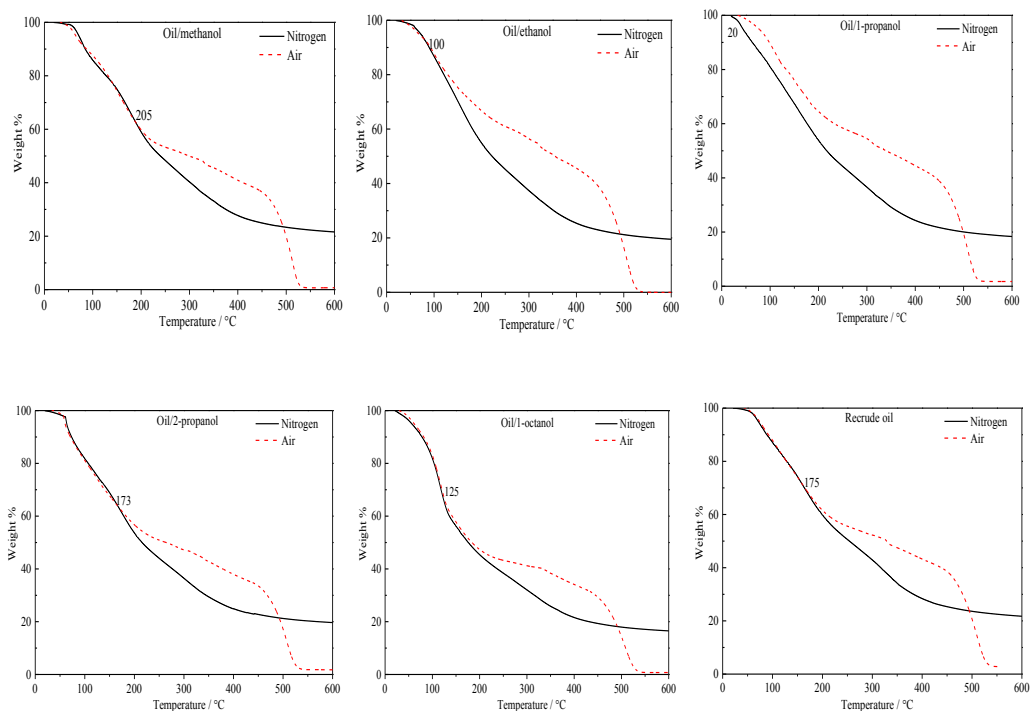


Figure 4.10 TG curves in nitrogen and air atmosphere for ignition temperature determination.

4.3.3.2 DSC

To better understand the effect of alcohol on the thermal properties of pyrolysis oil, DSC was performed on the pyrolysis oil and pyrolysis oil/alcohol mixtures. As shown in Figure 4.11, two endothermic peaks were observed in the first heating process for all samples except pyrolysis oil/1-octanol. No peaks were observed during the cooling process. The peaks at 98-134 °C might be assigned to dehydration of sugar derivatives (Borde and Cesàro 2001, Yamaguchi, Sato et al. 2014). The dehydration temperature decreased with increase in chain length of added alcohols. The peaks observed at 144-170 °C were assigned to decomposition of sugar compounds (Wörmeyer, Ingram et al. 2011).

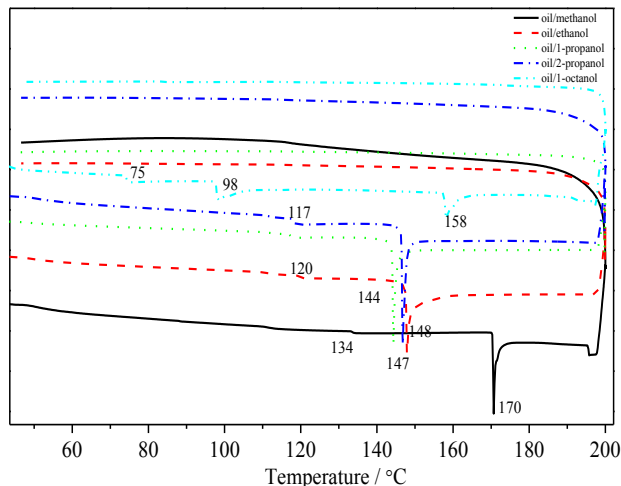


Figure 4.11 DSC plots for pyrolysis oil/alcohol mixtures.

The isothermal DSC technique can be used to monitor the net heat flows in and out of sample with an empty pan as inert reference. Etherification, esterification, condensation or polymerization, decomposition of sugars (fermentable and cross-linked) can also be classified as exothermic and endothermic according to whether energy released or absorbed via chemical reactions during the heating. Figure 4.12 shows the isothermal plot for the ReCrude oil and pyrolysis oil/alcohol mixtures. No signals were observed for the ReCrude oil aged at 80 °C for 270 min while a broad exothermic peak assigned to condensation reaction was observed at 150 °C. The pressure increase caused by vaporization of volatile compounds formed through etherification or condensation led to an explosion of the hermetic pan after 300 minutes. Many endothermic peaks assigned to decomposition of sugar derivatives and lignin were observed at 200 °C. The hydrolysis of levoglucosan to produce glucose occurred rapidly at higher temperature (Hu, Wang et al. 2013). The formed glucose played an important role in polymer formation upon heating up. Glucose can further undergo dehydration or decomposition into various

reactive compounds in return facilitate the decomposition of glucose and the condensation reactions. However, no peaks were observed for all pyrolysis oil/alcohol mixtures aged at 150 and 200 °C (except the pyrolysis oil/1-octanol mixture) indicating pyrolysis oil/alcohol mixtures had better thermal stability than the ReCrude oil.

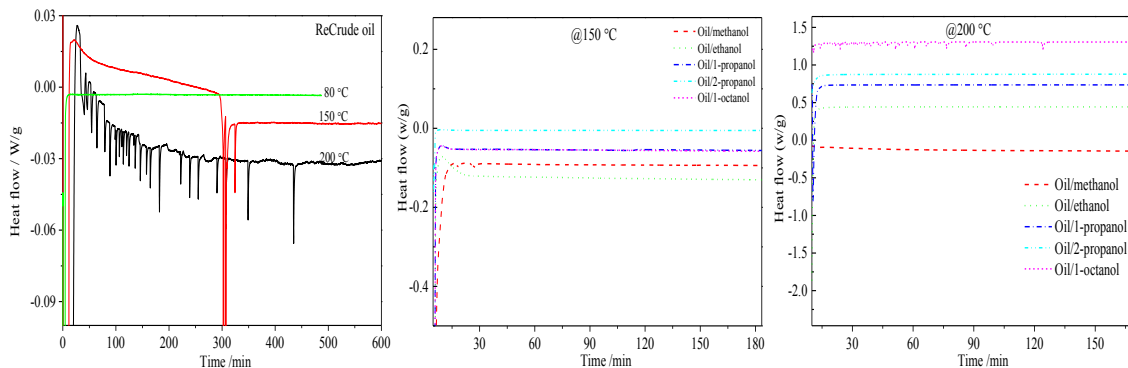


Figure 4.12 Isothermal DSC plots for pyrolysis oil and pyrolysis oil/alcohol.

4.3.4 Effect of alcohol on properties of pyrolysis oil after high temperature treatment

4.3.4.1 Water content

The ReCrude oil is the organic rich part and showed poor solubility in water. Both the ReCrude oil and pyrolysis oil/alcohol mixtures were firstly dissolved into hydralal solvent before the K-F titration process to reduce the error caused by slow response of the electrolyte. The ReCrude oil showed no phase separation during the aging process. However, all the pyrolysis oil/alcohols mixtures showed 2-5 vol% water formation in the top phase, which might because of alcohol extraction or reactions between alcohols and aldehyde/acids in pyrolysis oil. The water was poured out and the remaining homogenous part were performed water content measurement. Figure 4.13 displays the water content

change with increasing aging time for different pyrolysis oil/alcohol mixtures. The water concentration in the oil generally increased with aging time during 15 hours and then decreased. Water contents for pyrolysis oil/alcohol mixtures were generally lower than the ReCrude oil throughout the aging process.

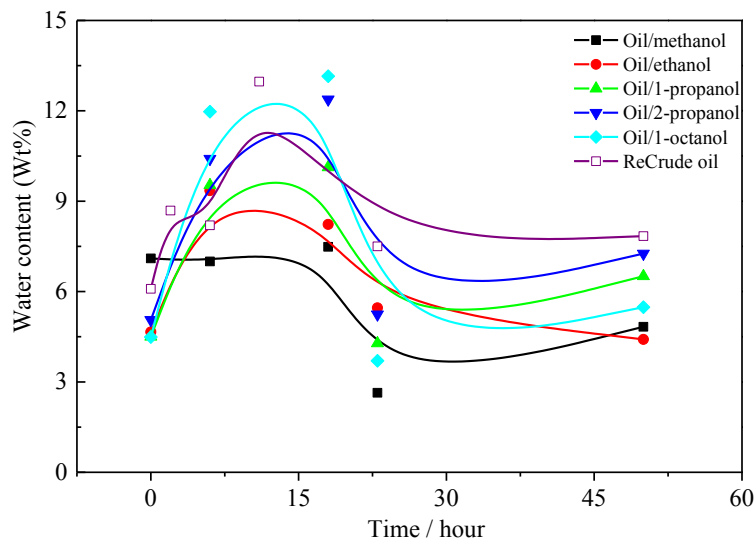


Figure 4.13 Water content vs aging time plots for pyrolysis oil and pyrolysis oil/alcohol mixtures aged at 200 °C.

4.3.4.2 HMM lignin content

Pyrolytic lignin has a peculiar structure compared to native and industrial lignin in its unsaturated structures, which often leads to instability problems during storage (Scholze and Meier 2001, Eide, Zahlsen et al. 2006). The high viscosity and poor distillability of high molecular mass (HMM) lignin makes it not suitable for combustion in gasoline engines. HMM lignin was also reported as a major cause for the instability of pyrolysis oil during storage (Scholze and Meier 2001). The HMM lignin content for the ReCrude oil increased rapidly from 33 wt% to 69 wt% after 50 hours. Similar trend was

observed for pyrolysis oil/methanol while slight increase were observed for the other bio/alcohol mixtures. The presence of alcohols lowered the formation rate of HMM lignin.

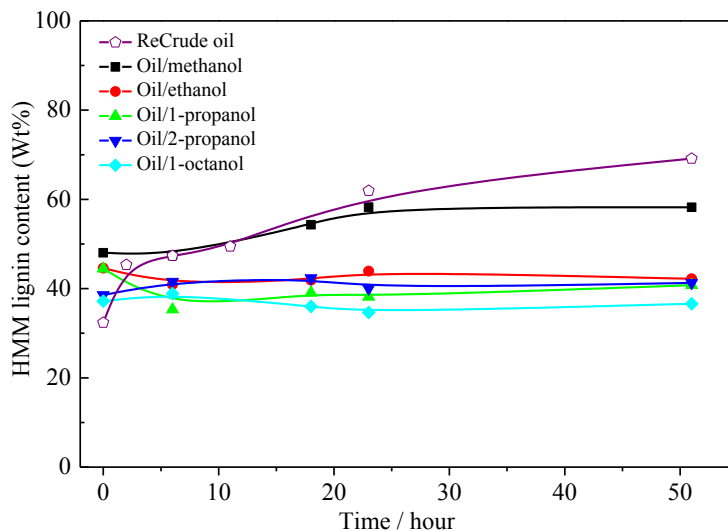


Figure 4.14 HMM lignin content vs aging time plots for pyrolysis oil and pyrolysis oil/alcohol mixtures aged at 200 °C.

4.3.4.3 Rheology

The viscosity increase with time is not desired because this increases the difficulty and cost of atomization when the oil is used for combustion. The high temperature aging was performed in sealed tubes and then cooled to room temperature after specific reaction time. The weight loss was negligible by measuring the oil weight before and after aging. Thus, the increase of viscosity with time would only be related to an increase in molecular weight and therefore viscosity measurements are an indirect measurement of the polymerization reactions that occur in the oil. The aged ReCrude oils and pyrolysis oil/methanol, pyrolysis oil/ethanol mixtures were sticky and their viscosity were out of

the rheometer test limit. The pyrolysis oil/1-propanol and pyrolysis oil/2-propanol aged for 50 hours were also not tested for the same reason. Figure 4.15 shows the viscosity of ReCrude oil and pyrolysis oil/alcohol mixtures as a function of shear rate at 40 °C. The pyrolysis oil/1-propanol and pyrolysis oil/2-propanol showed very similar behavior after aging—rapidly increased in 6 hours and then increased slightly during the next 45 hours. The viscosity for pyrolysis oil/1-octanol increased with aging time and was lower than the ReCrude oil even after aged for 50 hours.

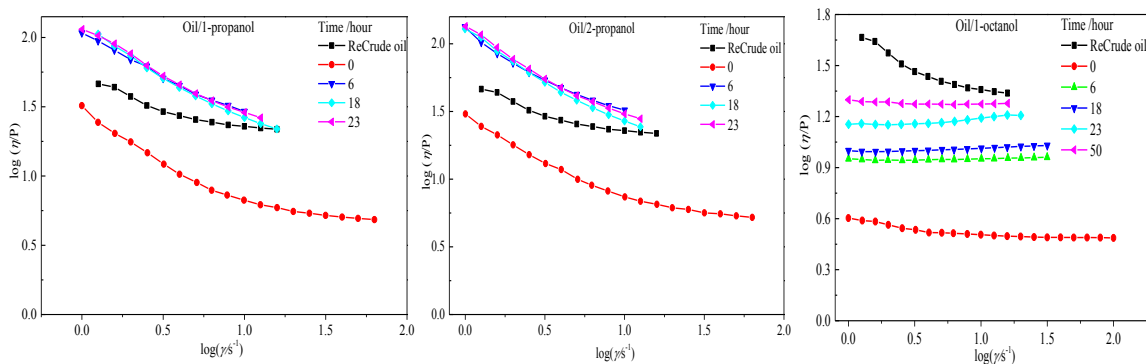


Figure 4.15 Logarithmic plots of apparent viscosity vs. shear rate for pyrolysis oil and pyrolysis oil/alcohol mixtures.

The non-Newtonian behavior could be generally described by Herschel–Bulkley model. Table 4.5 shows the calculated value for all the parameters. Both the flow index n and yield stress τ_B generally increased with increase aging time. The increase of n indicated the change from pseudoplastic flow behavior to dilatant or shear-thickening behavior. Alcohols can form hydrogen bond with many oxygen containing compounds in pyrolysis oil. However, hydrogen bonding formation was a very quick process, it was less likely the viscosity change during aging was assigned to hydrogen bonding formation

(Diebold and Czernik 1997). Since the dilatancy effect is generally associated with highly concentrated suspensions where particles are densely packed (Brown and Jaeger 2014), it was probable that the observed dilatant flow behavior could be connected to the higher content of HMM lignin in aged oils.

Table 4.4 Herschel-Bulkley rheology model fit results for pyrolysis oil and pyrolysis oil/alcohol mixtures

Sample	Time/ hour	Variable			R ²
		τ_H	K	n	
ReCrude oil	/	3.99545	1.57772	1.07311	0.99967
Oil/1-propanol	0 (control)	2.61257	0.38005	1.03815	0.9998
	6	8.15583	3.08682	0.8322	0.99658
	18	10.3197	2.20653	0.92099	0.9952
	23	11.6716	1.45529	1.0006	0.999
Oil/2-propanol	0 (control)	2.53266	0.51232	0.98587	0.99989
	6	10.0105	2.18978	1.00916	0.9999
	18	11.7225	1.47118	1.01019	0.99895
	23	12.1647	1.60345	1.05445	0.99907
Oil/1-octanol	0 (control)	0.10872	0.30869	0.99811	0.99999
	6	0.02896	0.95077	1.03475	1
	18	0.03854	0.84833	1.02106	1
	23	0.05494	1.31906	1.06851	0.9998
	50	0.28645	1.7265	1.02995	0.99999

4.3.4.4 GPC

The molecular weight distribution of both pyrolysis oil and pyrolysis oil/alcohol mixtures exhibited polydisperse behavior. The introduction of alcohol lowered the molecular weight of pyrolysis oil. Figure 4.16 showed the typical GPC plots for pyrolysis

oil/alcohol mixtures. The peaks assigned to the low molecular weight compounds shifted to high molecular weight direction with the increasing molecular weight of alcohols.

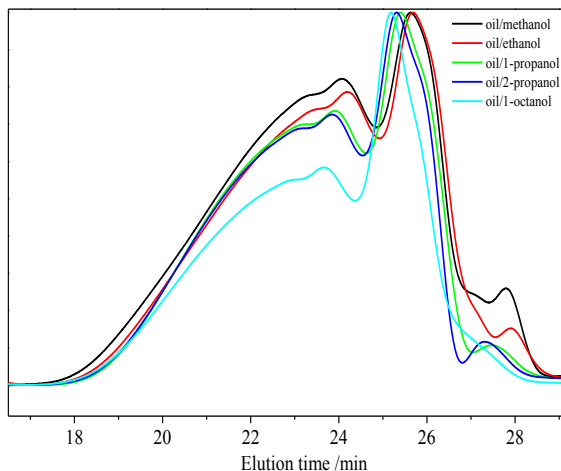


Figure 4.16 GPC plots for pyrolysis oils/alcohol mixtures aged for 6 hours.

Figure 4.17 shows the GPC curves for pyrolysis oil/alcohol mixtures. The proportion of high molecular fraction increased with the progress of storage time. This effect was more distinctive for the pyrolysis oil aged in the absence of alcohols. The increase was faster over the initial period. The results confirmed that polymerization/condensation occurred during storage.

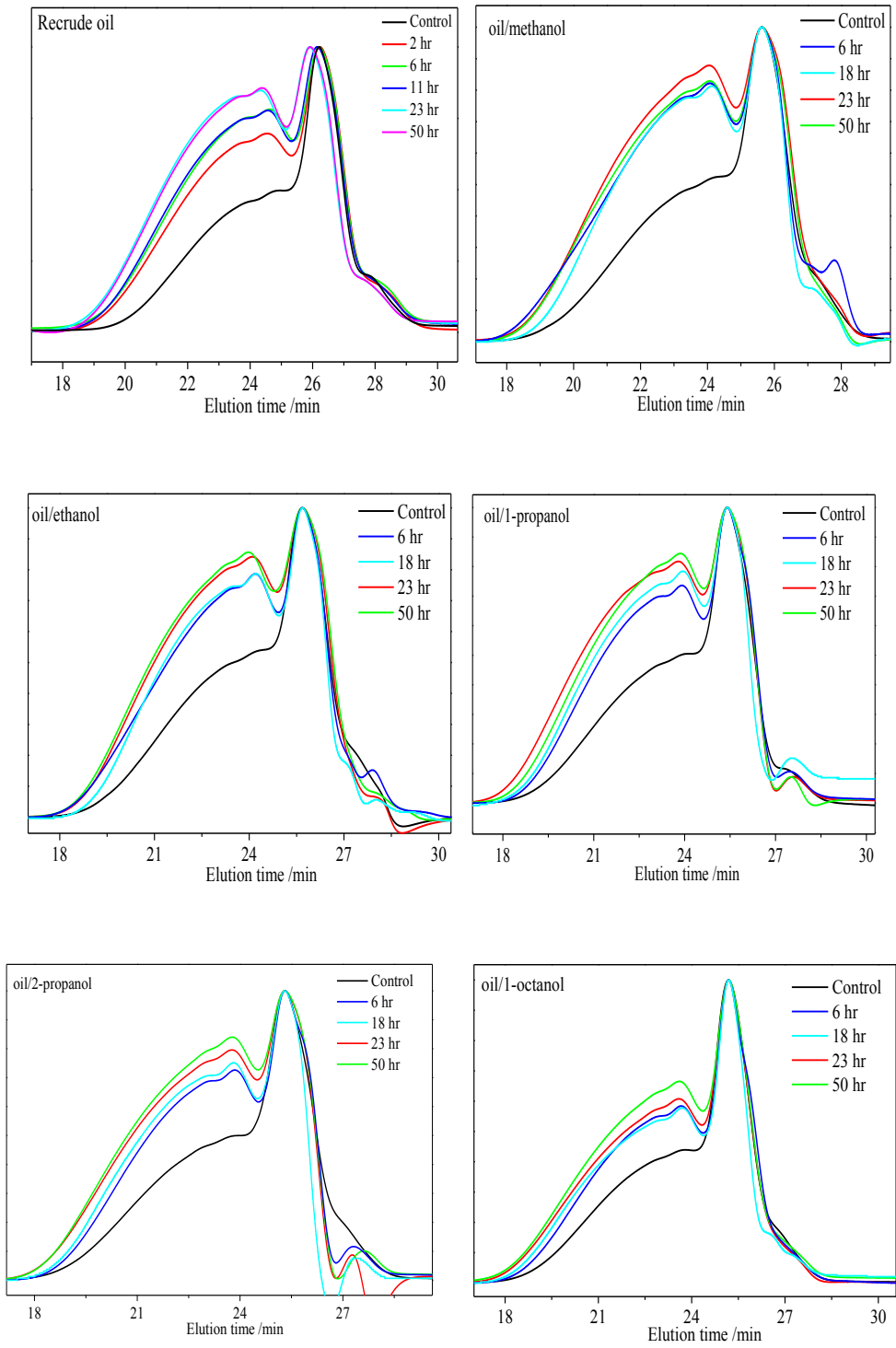


Figure 4.17 GPC curves for the ReCrude oil and pyrolysis oil/alcohol mixtures.

The number average molecular weight, M_n provided information about the molecular weight which was present at the greatest frequency in the sample. The weight average molecular weight, M_w was a weighted average which favors higher molecular weight molecules and always had a higher value than M_n . Table 4.6 lists M_n , M_w and PDI for the fresh and aged ReCrude oil and pyrolysis oil/alcohol mixtures. Both M_n and M_w generally increased with aging time. The fluctuation indicated complex reactions occurred and the proportion for the resulting polymers with different molecular weight kept changing throughout the aging process. Overall, the introduction of alcohols reduced the increasing rate for molecular weight.

Table 4.5 Molecular weight and molecular weight distributions for pyrolysis oil and pyrolysis oil/alcohol mixtures.

Temperature	Time /hour	M_n	M_w	PDI
ReCrude oil	Control	620	2196	3.04
	2	712	2103	2.96
	6	741	2213	2.99
	11	758	2179	2.88
	23	877	2432	2.77
	50	919	2649	2.88
Oil/methanol	Control	591	2130	3.60
	6	852	2922	3.43
	18	746	2020	2.71
	23	834	2767	3.32
	50	841	2629	3.13
Oil/ethanol	Control	589	1907	3.24
	6	792	2510	3.17
	18	732	1877	2.56
	23	824	2463	2.99
	50	833	2552	3.06
Oil /1-propanol	Control	552	1723	3.12
	6	792	2238	2.83
	18	885	2650	2.99
	23	765	2343	3.06
	50	752	2428	3.23
Oil /2-propanol	Control	515	1737	3.37
	6	651	1924	2.96
	18	739	1934	2.62
	23	688	2010	2.92
	50	819	2359	2.88
Oil/ 1-octanol	Control	492	1632	3.32
	6	652	2054	3.15
	18	673	2277	3.38
	23	793	2394	3.02
	50	853	2563	3.0

4.3.4.5 ATR-FTIR Spectroscopy

The chemical composition change can be monitored by detecting the change of specific functional groups with aging time. The percentage of transmittance intensities of all peaks were normalized to the highest peak. Then the peak height ratio was used to represent the relative concentrations of the functional group. The bands assignment for the ReCrude oil were performed in Chapter 2 and Table 4.2. Figure 4.18 showed the FTIR spectra for the ReCrude oil aged at 200 °C in the absence of alcohols. A decrease in intensities of carbonyl bands (1700 cm^{-1}) can mostly be related to decarboxylation of esters or acids (Scholze and Meier 2001). Peaks at 1500 cm^{-1} correspond to aromatic skeletal vibrations showed slight change indicating no detectable benzene ring formation reactions occurred. The peak intensities for O-H increased with aging time due to the formation of water. The FTIR spectra confirmed the condensation/polymerization occurred during aging.

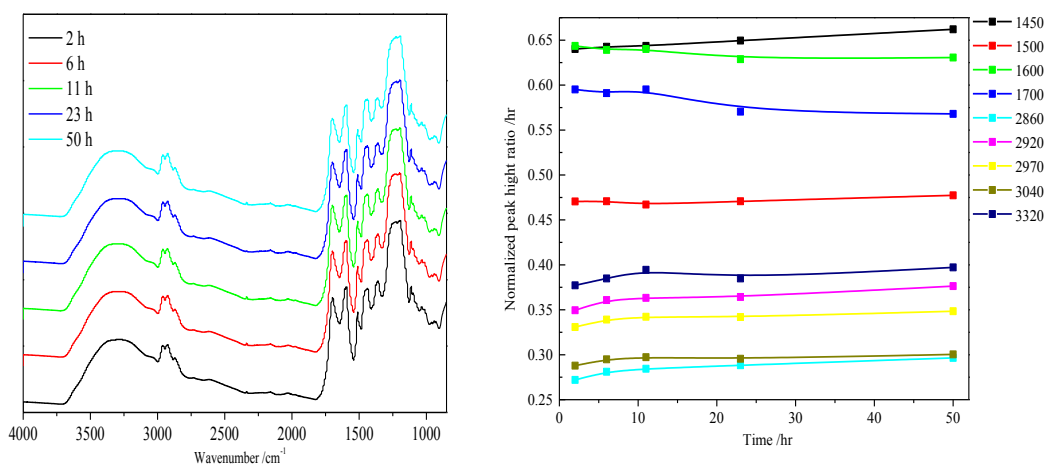


Figure 4.18 FTIR spectra and peak intensities change with aging time for the ReCrude oil aged at 200 °C.

Figure 4.19 presents the FTIR spectra for the fresh and aged pyrolysis oil/alcohol mixtures. All samples showed increases in 3300 cm^{-1} indicating the formation of water during aging. The carboxyl ester groups and protonated carboxyl acid groups in solution were reported to absorb at $\sim 1740\text{ cm}^{-1}$ (Bociek and Welti 1975, Venyaminov and Kalnin 1990) while the corresponding carboxylate groups absorb at $\sim 1600\text{ cm}^{-1}$. In the pyrolysis oil/alcohols FTIR spectra, the peaks at 1740 cm^{-1} merged into the broad strong peak centered at 1695 cm^{-1} . The obvious decreases in intensities for the bands at 1695 cm^{-1} and 1600 cm^{-1} indicated decarboxylation occurred for both esters and acids. However, the decarboxylation for esters were more severe. The fingerprint region below 1500 cm^{-1} changed significantly which confirmed heavy decomposition of esters occurred. Unfortunately, these bands were originated by complex interacting vibrational modes, and consequently less plausible to assign a band to a specific atom group vibration. For all samples, the highest peaks became narrower and shifted to the high wavenumber direction indicating C-O proportion increased after the heat treatment. Overall, the introduction of alcohols accelerated the decarboxylation which helped to reduce the oxygen content.

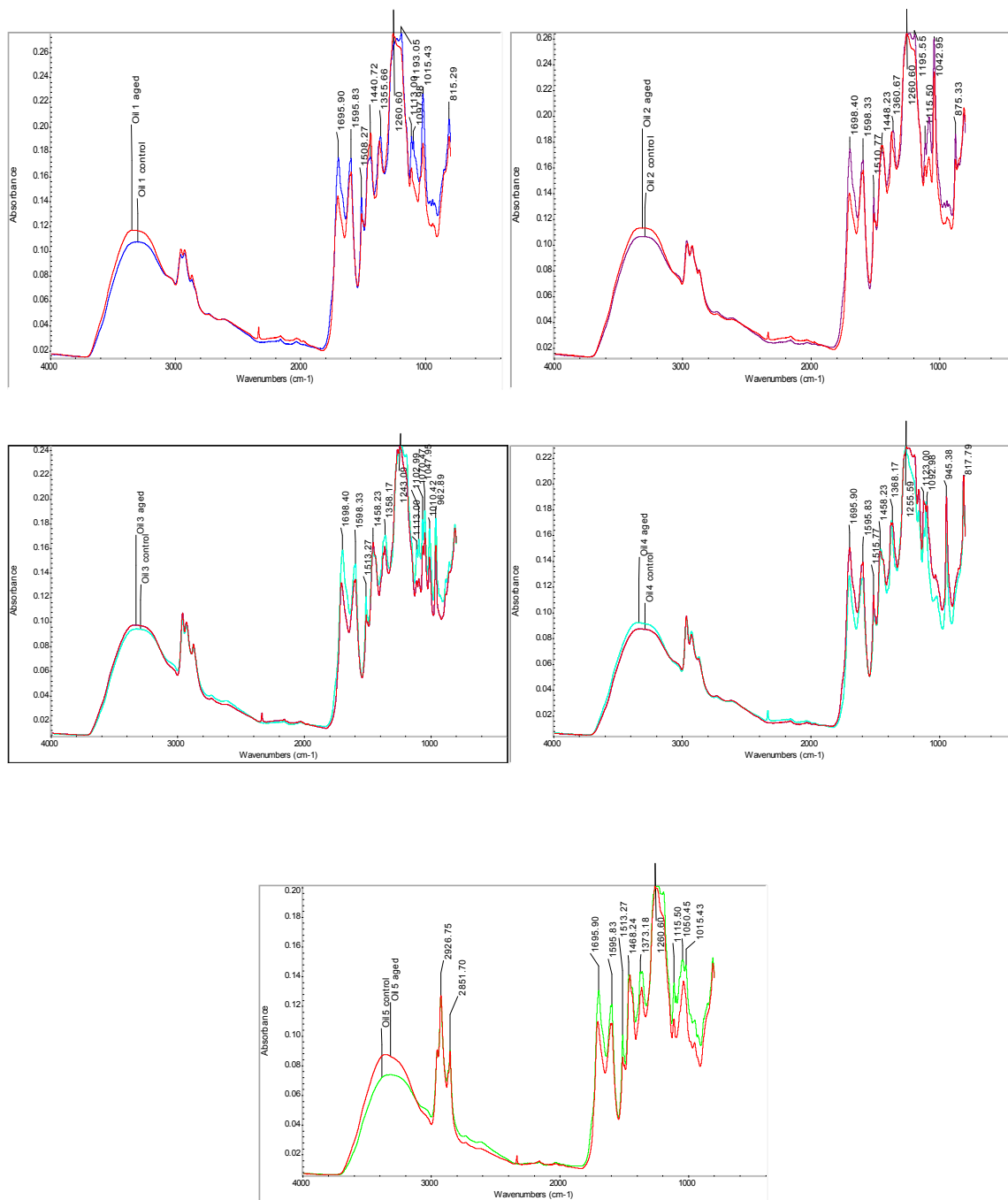


Figure 4.19 FTIR spectra for control and aged pyrolysis oil/alcohol mixtures.

4.3.4.6 GC-MS

Compositions of the fresh and aged pyrolysis oil/alcohol mixtures were investigated by GC-MS. The aim of the study is to determine the change of reactive compounds on dependence of the structure of alcohols during high temperature treatment, in the view of formulating detailed reaction mechanism. The pyrolysis oil/alcohol mixtures were dissolved into CH₂Cl₂ and then filtrated with 0.45 PVDF membrane to remove the HMM lignin fraction. Chlorobenzene was used as the internal standard. The chromatogram were listed in Appendix A.

The major peaks after aging match qualitatively with those of pyrolysis oils without heat treatment. By normalizing the spectra based on the area of the internal standard, chlorobenzene, comparisons could be made regarding the relative concentration of compounds before and after heat treatment. Figure 4.20 compared the normalized area for the major peaks in the GC spectra for fresh and aged pyrolysis oil/alcohol mixtures at 200 °C for 50 hours. The added alcohols were not detected in the pyrolysis oil/alcohol mixtures except pyrolysis oil/1-octanol. The larger sterically hindered group of 1-octanol reduced its reaction rate with other active compounds in pyrolysis oil. Peak areas for 2-cyclopenten-1-one, 1,2-benzenediol, 3-methyl-1,2-benzenediol, 4-methyl-1,2-benzenediol, 4-ethyl-1,3-benzenediol, 4-ethyl-2-methoxy-phenol, 4-propyl-1,3-benzenediol reduced with aging time. As the temperature was increased, a weak thermal stability of 2-cyclopenten-1-one may cause its decrease (Branca, Giudicianni et al. 2003). Conversely, phenanthrene content increased after aging. The main composition for CH₂Cl₂ soluble fraction of ReCrude oil— phenols and methyl substituted phenols, did not show obvious decrease while the abundance of benzenediol decreased significantly.

Similar great decreases in phenolic -OH contents in the pyrolytic lignin samples were reported for longer storage periods (Kim, Kim et al. 2012).

Table 4.6 Esters detected in aged pyrolysis oil/alcohol mixtures.

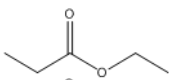
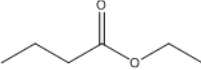
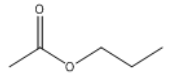
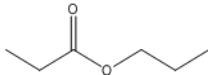
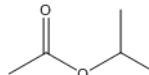
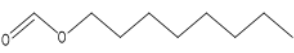
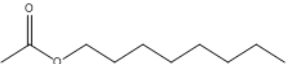
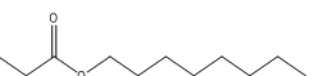
Sample	Time/min	Compound	Structure
Oil/ethanol	5.14	propanoic acid, ethyl ester	
	8.61	butanoic acid, ethyl ester	
Oil/1-propanol	5.24	<i>n</i> -propyl, acetate	
	8.96	propanoic acid, propyl ester	
Oil/2-propanol	3.66	acetic acid, 1-methylethyl ester	
Oil/1-octanol	20.65	formic acid, octyl ester	
	25.67	acetic acid, octyl ester	
	28.97	propanoic acid, octyl ester	

Table 4.6 lists esters detected after heat treatment. For the pyrolysis oil/1-propanol mixture, the content of *n*-propyl acetate increased significantly and two new esters—butanoic acid, pentyl ester and propanoic acid, propyl ester were observed after reaction. For the pyrolysis oil/2-propanol mixture, acetic acid, 1-methylethyl ester appeared after heat treatment. For the pyrolysis oil /1-octanol mixture, 1-octanol completely disappeared while propanoic acid, octyl ester newly formed and peak intensity for acetic acid, octyl ester significantly increased. The formation of new esters suggested acids formed by degradation of susceptible components (Alsbou and Helleur

2014). Furfural was reported to have a strong tendency to polymerize because of the high reactivity of carbonyl group (Hu, Wang et al. 2013). With high temperature aging, the sugar derivatives decomposed to form anhydrosugars, such as levoglucosan, could participate in the polymerization reactions or undergo hydrolysis to glucose. Glucose could undergo dehydration reactions to form potentially reactive intermediates. The dehydration and elimination reactions leading to formation of other components, such as furans, acetic and formic acids, and hydroxypropanone.

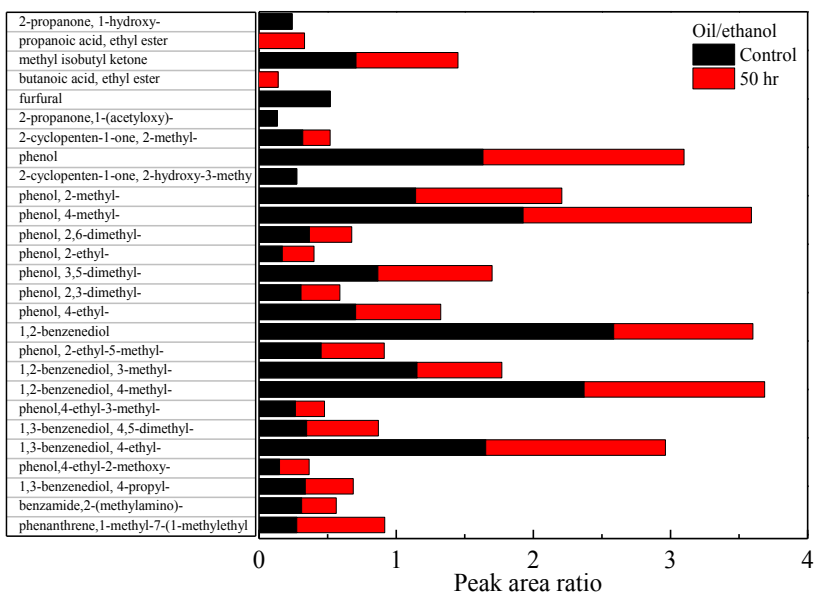
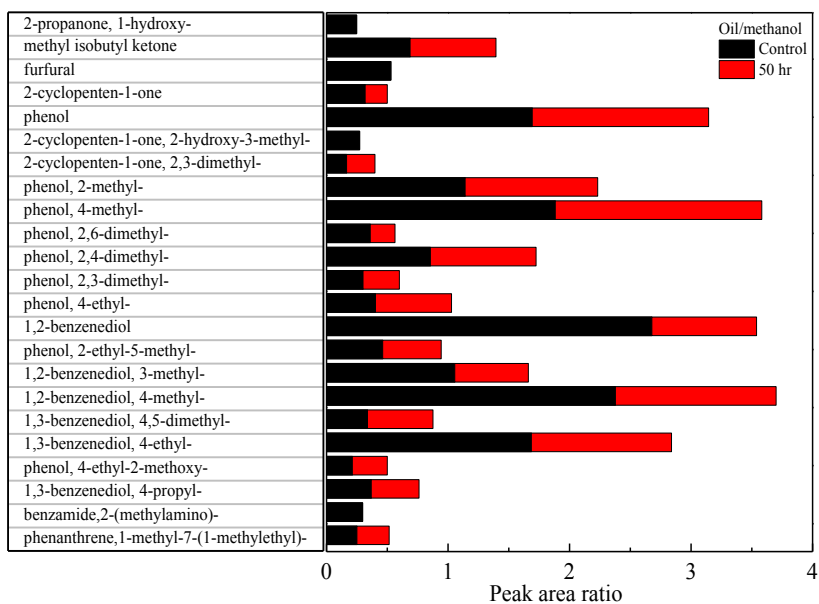


Figure 4.20 Peak area ratio for major compounds evident in control and aged pyrolysis oil/alcohol mixtures.

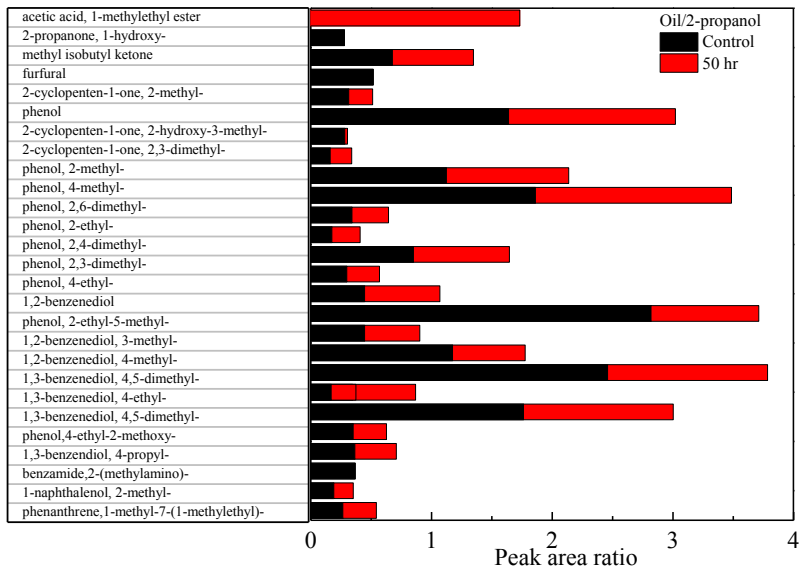
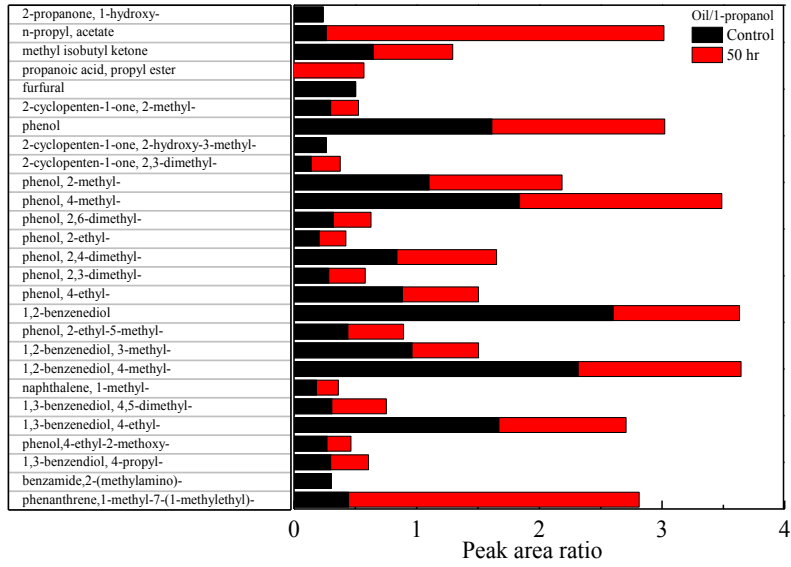


Figure 4.20 (Continued)

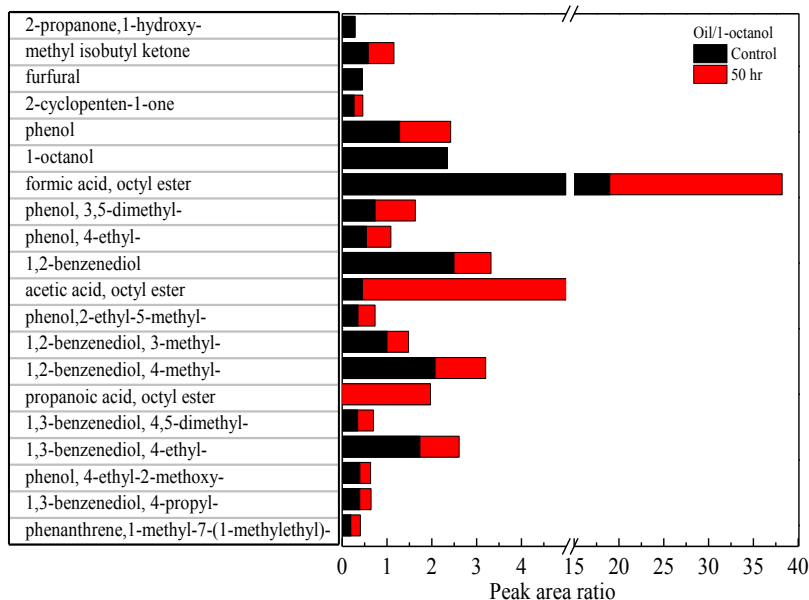


Figure 4.20 (Continued)

4.4 Conclusions

The time-dependent rheology of pyrolysis oil/alcohol mixtures were found to be well fitted by the Herschel–Bulkley model. The aged pyrolysis oil/1-propanol, pyrolysis oil/2-propanol and pyrolysis oil/1-octanol were also successfully expressed with Herschel–Bulkley model with yield stress increased with aging time. The rheological characteristics of aged oils showed a change from pseudo plastic or shear-thinning to dilatant or shear-thickening with increasing in aging time. GC-MS and FTIR proved esterification was the major reactions caused by the introduction of alcohols to the ReCrude oil. DSC results indicated all alcohols except 1-octanol significantly improved the thermal stability of pyrolysis oil. TG results proved 1-propanol significantly changed the pyrolysis behavior and made the pyrolysis oil easily to ignite. The high temperature aging process lead to increase in water content for all pyrolysis oil/alcohol mixtures. Methanol was found less efficient in reducing the increase rate of high molecular mass

lignin with increasing aging time. FTIR confirmed the introduction of alcohols accelerated the decarboxylation during high temperature treatment which helped to reduce the oxygen content. Benzenediol and alkyl-substituted benzenediol played an important role in increasing the molecular weight and viscosity for both the ReCrude oil and pyrolysis oil/alcohol mixtures. The added alcohols reduced the molecular weight increase by reaction with the newly formed acids during high temperature treatment. Overall, fuel properties of pyrolysis oil/alcohols improved over the ReCrude oil.

4.5 References

- Agblevor, F. A., O. Mante, N. Abdoulmoumine and R. McClung (2010). "Production of Stable Biomass Pyrolysis Oils Using Fractional Catalytic Pyrolysis." Energy & Fuels **24**(7): 4087-4089.
- Al-Sabawi, M., J. Chen and S. Ng (2012). "Fluid Catalytic Cracking of Biomass-Derived Oils and Their Blends with Petroleum Feedstocks: A Review." Energy & Fuels **26**(9): 5355-5372.
- Alsbou, E. and B. Helleur (2014). "Accelerated Aging of Bio-oil from Fast Pyrolysis of Hardwood." Energy & Fuels **28**(5): 3224-3235.
- Ba, T., A. Chaala, M. Garcia-Perez, D. Rodrigue and C. Roy (2004). "Colloidal Properties of Bio-oils Obtained by Vacuum Pyrolysis of Softwood Bark. Characterization of Water-Soluble and Water-Insoluble Fractions." Energy & Fuels **18**(3): 704-712.
- Bociek, S. M. and D. Welti (1975). "The quantitative analysis of uronic acid polymers by infrared spectroscopy." Carbohydrate Research **42**(2): 217-226.
- Borde, B. and A. Cesàro (2001). "A DSC Study of Hydrated Sugar Alcohols. Isomalt." Journal of Thermal Analysis and Calorimetry **66**(1): 179-195.
- Boucher, M. E., A. Chaala, H. Pakdel and C. Roy (2000). "Bio-oils obtained by vacuum pyrolysis of softwood bark as a liquid fuel for gas turbines. Part II: Stability and ageing of bio-oil and its blends with methanol and a pyrolytic aqueous phase." Biomass and Bioenergy **19**(5): 351-361.
- Branca, C., P. Giudicianni and C. Di Blasi (2003). "GC/MS Characterization of Liquids Generated from Low-Temperature Pyrolysis of Wood." Industrial & Engineering Chemistry Research **42**(14): 3190-3202.
- Bridgwater, A. V. (2012). "Review of fast pyrolysis of biomass and product upgrading." Biomass and Bioenergy **38**(0): 68-94.
- Brown, E. and H. M. Jaeger (2014). "Shear thickening in concentrated suspensions: phenomenology, mechanisms and relations to jamming." Reports on Progress in Physics **77**(4): 046602.
- Brozena, A. (2013). "Vapor pressure of 1-octanol below 5 kPa using DSC." Thermochimica Acta **561**(0): 72-76.
- Butler, E., G. Devlin, D. Meier and K. McDonnell (2011). "A review of recent laboratory research and commercial developments in fast pyrolysis and upgrading." Renewable and Sustainable Energy Reviews **15**(8): 4171-4186.

- Coats, A. W. and J. P. Redfern (1964). "Kinetic Parameters from Thermogravimetric Data." Nature **201**(4914): 68-69.
- Crelling, J. C., E. J. Hippo, B. A. Woerner and D. P. West Jr (1992). "Combustion characteristics of selected whole coals and macerals." Fuel **71**(2): 151-158.
- Diebold, J. P. (2000). A Review of the Chemical and Physical Mechanisms of the Storage Stability of Fast Pyrolysis Bio-Oils, National Renewable Energy Laboratory.
- Diebold, J. P. and S. Czernik (1997). "Additives To Lower and Stabilize the Viscosity of Pyrolysis Oils during Storage." Energy & Fuels **11**(5): 1081-1091.
- Doerr, R. C., A. E. Wasserman and W. Fiddler (1966). "Composition of Hickory Sawdust Smoke. Low-Boiling Constituents." Journal of Agricultural and Food Chemistry **14**(6): 662-665.
- Eide, I., K. Zahlse, H. Kummernes and G. Neverdal (2006). "Identification and Quantification of Surfactants in Oil Using the Novel Method for Chemical Fingerprinting Based on Electrospray Mass Spectrometry and Chemometrics." Energy & Fuels **20**(3): 1161-1164.
- Elliott, D. C. (2007). "Historical Developments in Hydroprocessing Bio-oils." Energy & Fuels **21**(3): 1792-1815.
- Feng, P., L. Hao, C. Huo, Z. Wang, W. Lin and W. Song (2014). "Rheological behavior of coal bio-oil slurries." Energy **66**(0): 744-749.
- Garcia-Perez, M., S. Wang, J. Shen, M. Rhodes, W. J. Lee and C.-Z. Li (2008). "Effects of Temperature on the Formation of Lignin-Derived Oligomers during the Fast Pyrolysis of Mallee Woody Biomass." Energy & Fuels **22**(3): 2022-2032.
- Hu, X., Y. Wang, D. Mourant, R. Gunawan, C. Lievens, W. Chaiwat, M. Gholizadeh, L. Wu, X. Li and C.-Z. Li (2013). "Polymerization on heating up of bio-oil: A model compound study." AIChE Journal **59**(3): 888-900.
- Kim, T.-S., J.-Y. Kim, K.-H. Kim, S. Lee, D. Choi, I.-G. Choi and J. W. Choi (2012). "The effect of storage duration on bio-oil properties." Journal of Analytical and Applied Pyrolysis **95**(0): 118-125.
- Mante, O. D. and F. A. Agblevor (2012). "Storage stability of biocrude oils from fast pyrolysis of poultry litter." Waste Management **32**(1): 67-76.
- Melligan, F., K. Dussan, R. Auccaise, E. H. Novotny, J. J. Leahy, M. H. B. Hayes and W. Kwapinski (2012). "Characterisation of the products from pyrolysis of residues after acid hydrolysis of Miscanthus." Bioresource Technology **108**(0): 258-263.

- Mortensen, P. M., J. D. Grunwaldt, P. A. Jensen, K. G. Knudsen and A. D. Jensen (2011). "A review of catalytic upgrading of bio-oil to engine fuels." *Applied Catalysis A: General* 407(1-2): 1-19.
- Oasmaa, A., E. Kuoppala, J.-F. Selin, S. Gust and Y. Solantausta (2004). "Fast Pyrolysis of Forestry Residue and Pine. 4. Improvement of the Product Quality by Solvent Addition." *Energy & Fuels* 18(5): 1578-1583.
- Scholze, B. and D. Meier (2001). "Characterization of the water-insoluble fraction from pyrolysis oil (pyrolytic lignin). Part I. PY-GC/MS, FTIR, and functional groups." *Journal of Analytical and Applied Pyrolysis* 60(1): 41-54.
- Tognotti, L., A. Malotti, L. Petarca and S. Zanelli (1985). "Measurement of Ignition Temperature of Coal Particles Using a Thermogravimetric Technique." *Combustion Science and Technology* 44(1-2): 15-28.
- Venjaminov, S. Y. and N. N. Kalnin (1990). "Quantitative IR spectrophotometry of peptide compounds in water (H₂O) solutions. I. Spectral parameters of amino acid residue absorption bands." *Biopolymers* 30(13-14): 1243-1257.
- Weerachanchai, P., C. Tangsathitkulchai and M. Tangsathitkulchai (2009). "Phase behaviors and fuel properties of bio-oil-diesel-alcohol blends." *World Academy of Science, Engineering and Technology* 32: 355 - 361.
- Wörmeyer, K., T. Ingram, B. Saake, G. Brunner and I. Smirnova (2011). "Comparison of different pretreatment methods for lignocellulosic materials. Part II: Influence of pretreatment on the properties of rye straw lignin." *Bioresource Technology* 102(5): 4157-4164.
- Yamaguchi, A., O. Sato, N. Mimura and M. Shirai (2014). "Intramolecular dehydration of mannitol in high-temperature liquid water without acid catalysts." *RSC Advances* 4(85): 45575-45578.
- Yu, F., S. Deng, P. Chen, Y. Liu, Y. Wan, A. Olson, D. Kittelson and R. Ruan (2007). "Physical and chemical properties of bio-oils from microwave pyrolysis of corn stover." *Applied Biochemistry and Biotechnology* 137-140(1-12): 957-970.

CHAPTER V

CONCLUSIONS AND FUTURE WORK

5.1 Conclusion

A combination of techniques was used to characterize the properties of the ReCrude oil. The ReCrude oil was water insoluble. The water content was 4.77 wt%. The solids content was 3.32 wt% in CH₃OH/CH₂Cl₂ (v/v = 50/50). The high molecular mass (HMM) lignin content was ~33 wt%. The ash content was 0.12 wt%. The low molecular mass (LMM) fraction of the ReCrude oil was mainly composed of phenols, benzenediols and their derivatives. The LMM fraction also contained more aldehydes, ketones, carboxylic acids, and esters than the HMM lignin. Three stages were observed in both the pyrolysis process and combustion process for the ReCrude oil. The activation energy increased with increasing fractional conversion. The T_g for HMM lignin was 110 °C.

Generally, The ReCrude oil was not thermodynamically and chemically stable. Major physicochemical changes of the ReCrude oil took place during storage at temperatures over 60 °C. The water content, HMM lignin content, molecular weight and viscosity increased with increasing aging time and temperature. The higher temperature results in higher increasing rate. Decomposition of sugars for heat-treatment above 200 °C significantly affects the water content. Concentrations of phenol, methyl/ethyl substituted phenols, furfural, 1,2-benzenediol and benzamide decreased with aging time. The applicable temperature range for the accelerated aging should be below 150 °C.

The current research suggested when pyrolysis oil is processed in a low temperature (>200 °C) hydrotreating reactor, decomposition of sugar compounds resulted in the formation of acids which accelerated the aging reactions. The addition of alcohols reduced the increase rate for viscosity and molecular weight by esterification with acids. GC-MS confirmed the alkylation reactions reduced the reactivity of phenol compounds during high temperature treatment. Benzenediol and alkyl-substituted benzenediol played an important role in increasing the molecular weight and viscosity for both the ReCrude oil and pyrolysis oil/alcohol mixtures. The time-dependent rheology for fresh and aged pyrolysis oil/alcohol mixtures were found to be well fitted by the Herschel–Bulkley model. The yield stress increased with aging time. The rheological characteristics of aged oils showed a change from pseudo plastic to dilatant with increasing in aging time. 1-octanol showed the highest solubility toward the pyrolysis oil while oil/1-octanol showed the lowest thermal stability.

1-propanol significantly changed the pyrolysis behavior and made the pyrolysis oil easily to ignite. Methanol was found less efficient in reducing the increase of HMM lignin with increasing time. The added alcohols reduced the molecular weight increase by reaction with the newly formed acids during high temperature treatment. The introduction of alcohols accelerated the decarboxylation during high temperature treatment which helped to reduce the oxygen content. Overall, the introduction of alcohols improved the thermal and chemical stability of the ReCrude oil.

5.2 Future work

The increase in HMM lignin content plays an important role in the poor quality of aged pyrolysis oil. Decomposition of HMM lignin and re-polymerization occurred during

high temperature treatment. CH_2Cl_2 can separate most of the HMM lignin. The combustion properties indicated most of the solids were concentrated in HMM lignin. By removing the HMM lignin can make the further upgrading more feasible. HMM lignin can be used to produce phenolic resin. However, CH_2Cl_2 is toxic and expensive. More research needs to be done to develop low cost and economical friendly separation techniques.

Though 1-octanol showed limited stability toward the ReCrude oil, it significantly reduced the viscosity and molecular weight for the oil. The introduction of long chain alcohols also increased the C/O ratio and heating value. A combination of different alcohols may contribute to improve the overall properties for pyrolysis oil. More investigations are needed for the hydrotreating of these stabilized the pyrolysis oil.

APPENDIX A
CHROMATOGRAM FOR PYROLYSIS OIL/ALCOHOL MIXTURES

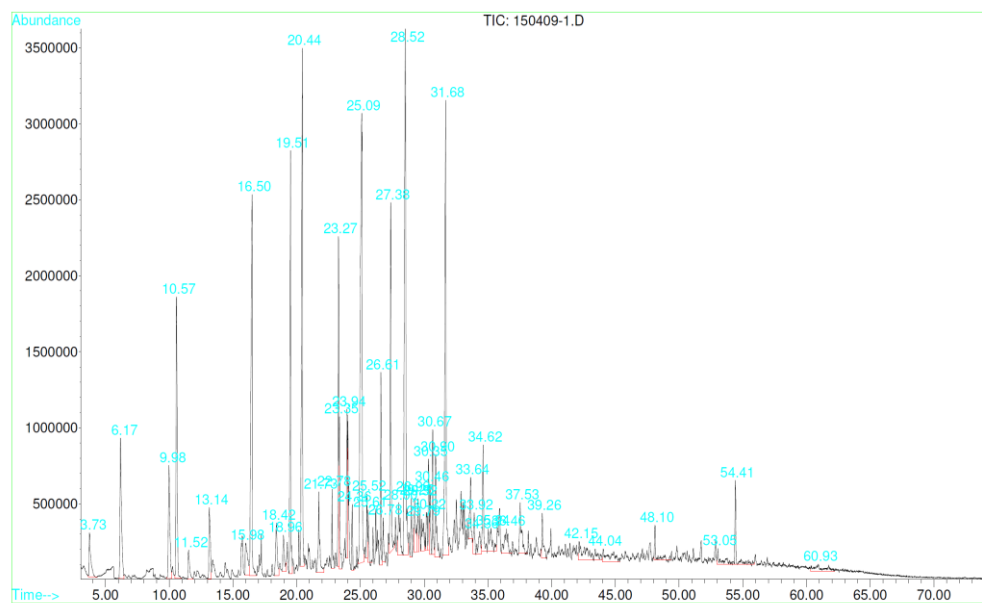


Figure A.1 Chromatogram for pyrolysis oil/methanol

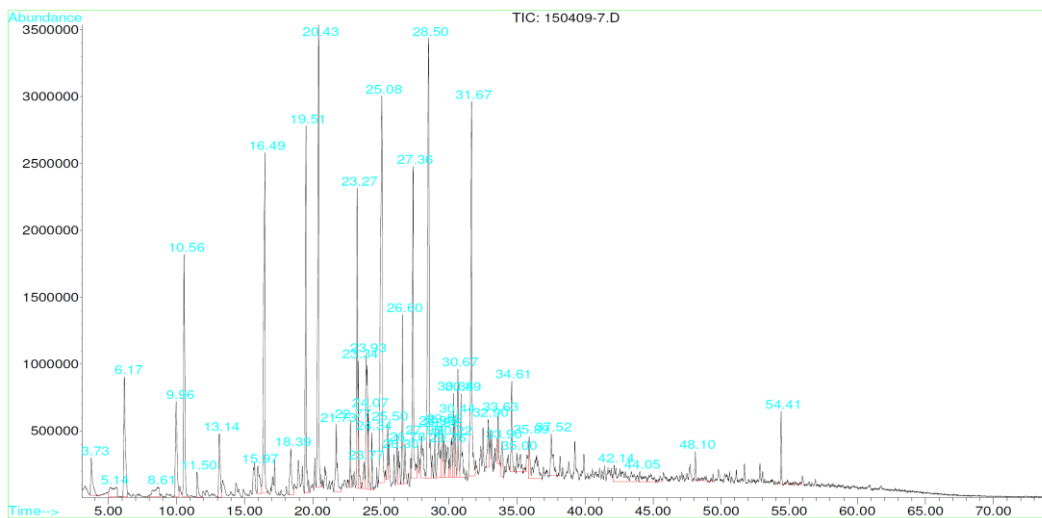


Figure A.2 Chromatogram for pyrolysis oil/ethanol

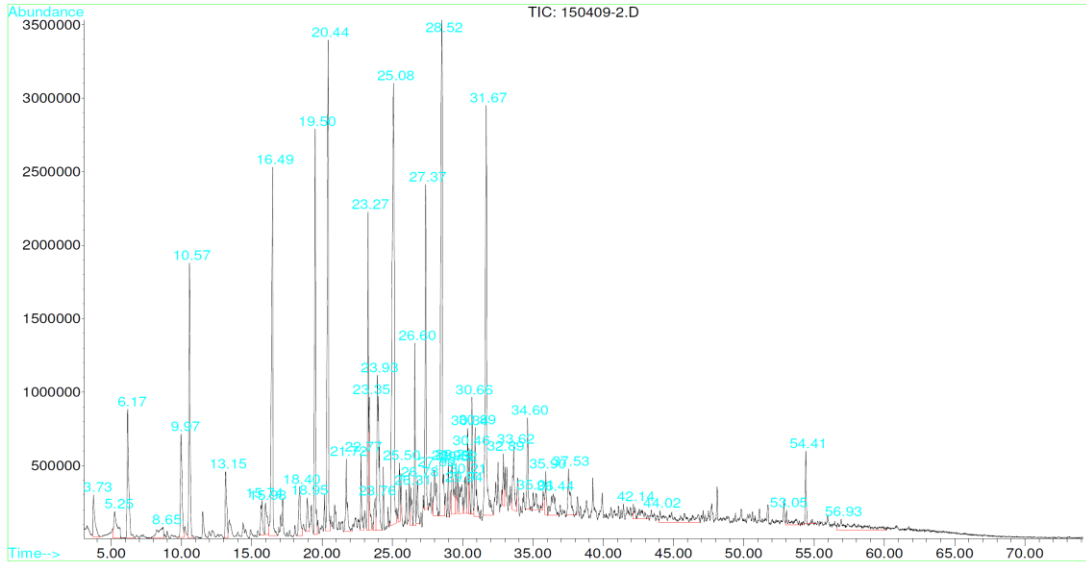


Figure A.3 Chromatogram for pyrolysis oil/1-propanol

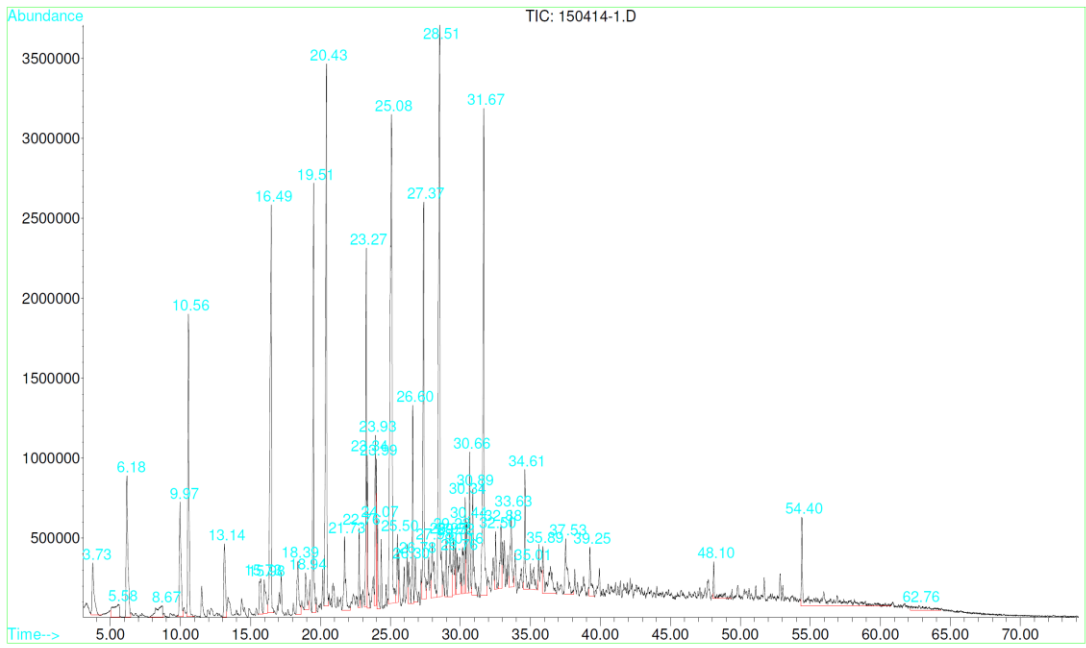


Figure A.4 Chromatogram for pyrolysis oil/2-propanol

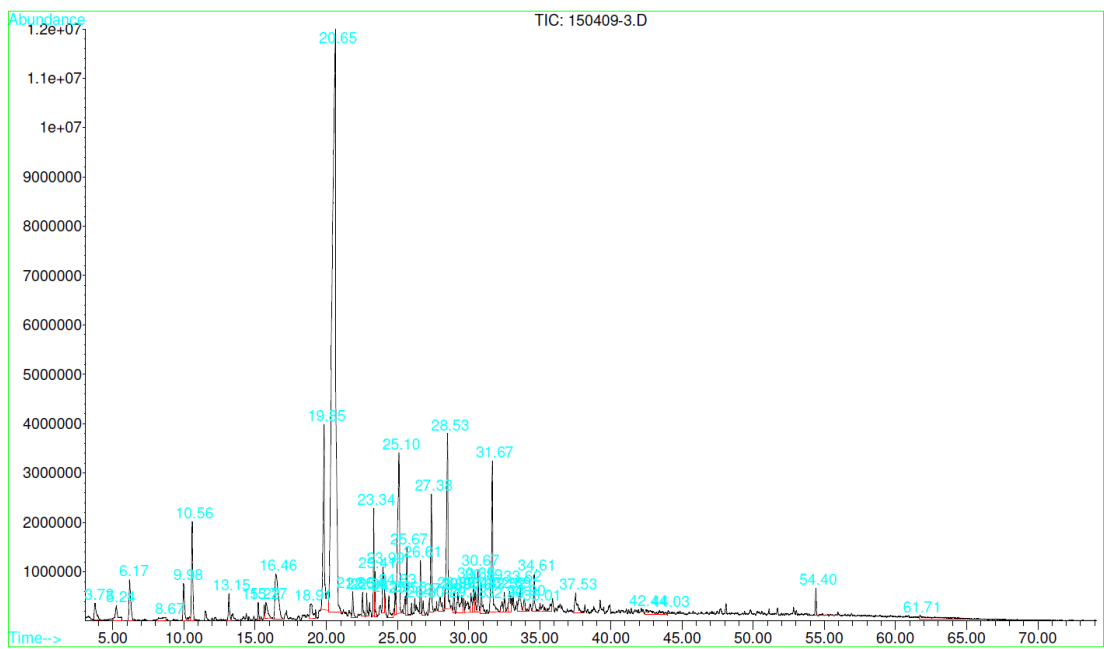


Figure A.5 Chromatogram for pyrolysis oil/1-octanol